THE THEORY OF FLUXGATE SENSOR SYSTEMS

by

ZU-CHENG GAO

B.Sc. (Honours), ChangChun College of Geology, 1964

A THESIS SUBMITTED IN PARTIAL FULFILMENT OF

THE REQUIREMENTS FOR THE DEGREE OF

DOCTOR OF PHILOSOPHY

in

THE FACULTY OF GRADUATE STUDIES

Department of Geophysics and Astronomy

We accept this thesis as conforming

to the required standard

THE UNIVERSITY OF BRITISH COLUMBIA

November 1985

In presenting this thesis in partial fulfilment of the requirements for an advanced degree at the University of British Columbia, I agree that the Library shall make it freely available for reference and study. I further agree that permission for extensive copying of this thesis for scholarly purposes may be granted by the head of my department or by his or her representatives. It is understood that copying or publication of this thesis for financial gain shall not be allowed without my written permission.

Zu-Cheng GAO

Department of Geophysics & Astronomy

The University of British Columbia
1956 Main Mall
Vancouver, Canada
V6T 1Y3

Date Jan. 24, 86

Dedicated to

my parents, Zun-Li Gao and Mary Yung Gao

and my sister, Rose Zu-Juan Gao

ABSTRACT

In recent years, the fluxgate sensor system has become increasingly important for the measurement of magnetic fields. It has become the instrument of choice for some aeronomy research programs, for ocean bottom deployment and for vessel detection by seafloor sensors. It has considerable potential for airborne magnetometry and gradient measurements. This renewed interest arises because the capabilities of the instrument are now known to be much superior to those achieved by earlier designs, and because there is a continued need for sensors with a vector capability. Added practical advantages accrue because it is a rugged instrument, economical to manufacture and has low power requirements.

The advances in technology have not been accompanied by corresponding advances in the theoretical understanding of the fluxgate. Prior to publications from the University of British Columbia, most representations were cumbersome, incomplete and sometimes incorrect.

The approach presented for the first time in this thesis introduces a gating function which straightforwardly represents the fluxgate mechanism separately from the complications of hysteresis and demagnetization. The characteristics of the gating function are easily measurable and can be regarded as the performance indices of the sensor. The approach also presents a general state equation which is valid not only for single sensors, but also for symmetric multiple sensors (e.g. gradiometers). Then the complete solution set (the monodromy, the general solution and periodic solution) is solved for the state equation.

Based on the theories of Floquet-Lyapunov and of Hsu, the instability criterion and the method of calculation are investigated. The generalized instability map, illustrated in a

parameter plane, is useful for the design of stable fluxgate sensor systems. The instability has been also checked in the phase space. The sensitivity map presented through this approach can be used to calculate the real signal for a fluxgate sensor with any value of parameters. Moreover, this approach not only formulates an integrated fluxgate theory, but also provides a guide to the selection of operating parameters and components for a practical design.

TABLE OF CONTENTS

LIST OF FIGURES

ACKNOWLEDGMENT

I wish to express my sincere thanks to Dr. R. D. Russell for his enthusiastic encouragement and guidance throughout my research. I should also thank to him for valuable advice and comments on the presentation of my theory.

I am most grateful to Dr. B. B. Narod and Dr. G. Bluman for their helpful suggestions, careful reviewing of the manuscript, especially patient by making many improvements to the English. I appreciate the help of Dr. T. Watanabe and Dr. M. S. Davies through their comments and discussion.

I am indebted to my friends J. R. Bennest and P. Whaite and to Dr. F. Kollar of the Earth Physics Branch, DEMR, for their help during the building and testing of the portable fluxgate ring core gradiometer, and for their fruitful discussions on the fluxgate technology.

Thanks are due to other professors, staff members and colleagues in our Department for their encouragement and friendship.

This work was financed entirely by grants from NSERC Canada and by research agreements between the Department of Energy, Mines and Resources, Earth Physics Branch, and R. D. Russell.

CHAPTER 1

INTRODUCTION

Since 1935, when H. Aschenbrenner and G. Goubeau applied a second harmonic fluxgate magnetometer to measure the geomagnetic field [1.1], fluxgate sensor systems have been evolving in geoscience. Due to their high reliability, robustness, compact size, low power consumption, vector capabilities, high sensitivity and economy, geophysicists in many parts of the world still study and develop new variants of fluxgate magnetic sensor systems. For instance, in the last two years, H. T. Dong in the People's Republic of China (1984 [1.2]), M. Kono *et al* in Japan (1984 [1.3]), C. H. Lühr *et al* in the Federal Republic of Germany (1985 [1.4]), D. J. Southwood *et al* in the U. K. (1985 [1.5]) and the Geophysical Instrumentation Group of UBC in Canada (1984 [1.6]), all have reported on their new fluxgate sensor systems. Of course, in the U. S. A., which is credited with the development of the most advanced fluxgate technology, geophysicists have been continuously interested in the development of fluxgate sensor systems, e.g. the fluxgate sensor system of the CCE spacecraft launched in August, 1984 [1.7]. Also, fluxgate magnetometer systems have been suggested as the next generation of magnetic array variometers in the U.S. (1984 [1.8]).

In contrast, the theoretical study of the fluxgate mechanism seems to lag well behind its application. Probably the approach of Williams and Nobel (1950 [1.9]) has been most influential on fluxgate theory in the last three decades. This approach was employed in many textbooks to explain the principle of second harmonic fluxgate (rod) magnetometers. It used three straight lines instead of the full $B-H$ hysteresis loop of the core material, and then from Faraday's law derived the output voltage for a fluxgate sensor. Because Williams and Nobel used the effective permeability as a basic variable, they did not require

the complicated calculation of the demagnetization factor. Geyger in his book " Nonlinear-Magnetic Control Devices " (1964 [1.10]) gave more than 50 pages to a review of fluxgate magnetometers and also summarized his studies of fluxgate ring-core sensors. His analysis was based on the work of Williams and Noble, but extended to the ring core which was treated as a superposition of two half cores.

Since then, many papers have been published to elaborate and extend their theory. Gordon *et al* (1965 [1.11]) extended Geyger's work on ring-core sensors and proposed that the dominant factor affecting the sensitivity would be the product of the demagnetization factor and the initial d.c. permeability. Marshall (1967 [1.12]) suggested using an exponential approximation for dB/dH and using a Maclaurin series to simplify the calculation of output voltage. The approach of Primdahl (1969 [1.13]) depended on calculating the gating characteristics from real $B-H$ curves measured for a ferrite material. Burger (1972 [1.14]) believed that to estimate the demagnetization of the ring core, the ellipsoidal shell model is better than the two halfcore model of Marshall [1.12] or of Gordon *et al* [1.11]. Also he suggested using six linear segments as an accurate hysteresis loop model.

In contrast to using more and more complicated models, Qiu considered the use of measurable results to obtain a simplified output voltage expression with engineering accuracy. In his paper (1978 [1.15]), after simplifying the demagnetization expression, Qiu introduced an experimental series formula for various fluxgate sensors. His latest paper (1979 [1.16]) discussed the ring-core magnetometer with a load where an arctangent is used to approximate the $B(H)$ function. According to my observations of a ring-core magnetometer, the real sensitivity is far from the one calculated by Qiu's formula. One of the reasons may be that his formula regards the self inductance of the sensor winding to be a constant, which is wrong!

In summary, these approaches are similar to the analysis of Williams and Nobel , but use either a more sophisticated description of hysteresis for the calculation of output voltage, or more complicated core models for the calculation of demagnetization. However, as one author said with deep feeling: " it is complex, too complex,. . ." [1.14].

Unfortunately, it is my contention that the demagnetization factor might be more complicated than considered in the approaches mentioned above. For instance, Zolotova (1977 [1.17]) proved that the demagnetization factor of a toroidal-tape ring core is not a constant quantity which depends only on the core's geometric parameters, but that it also depends on the permeability of the core material and the number of wound turns. She believes that this is a reason why the measured results disagree with the calculations using previous formulas.

Although such studies of the $B(H)$ function and demagnetization factor have been contributing to practical improvements of the performance of the fluxgate sensor, such approaches involve too many parameters which not only blur the nature of the fluxgate mechanism but also are difficult to test for practical design. Can we find some better variables that are easily measurable and that can represent the fluxgate mechanism without such complications?

The analysis of Serson and Hannaford (1956 [1.18]) utilized a time-dependent permeability $\mu(t)$. This was an impressive attempt to clarify the fluxgate theory. The paper of Russell, Narod and Kollar (1983 [1.19]) regarded the fluxgate magnetometer sensor to be a modulated inductor. They derived an equation based on Lagrange's equation, and gave an instability map for the magnetometer. This approach shows that the fluxgate mechanism is linear and easily understandable. It marked a major step. In a subsequent paper, Narod and Russell (1984 [1.20]) extended their approach to a study of sensitivity. The method of Russell and Narod, based on the work of Nayfeh and Mook (1979 [1.21]),

cannot easily deal with the complications of multiple sensors and mutual inductances, that lead to coupled high-order differential equations. But multiple sensor gradiometers have been applied in several areas, in particular to magneto-telluric studies. Also the physical principle of the gated inductance should be clearly developed in the most general case.

We need a fluxgate theory that is intuitive and complete, i.e. based on straightforward physical principles and unique mathematical expressions with essential rigour; that is valid not only for single fluxgate sensors, but also for multiple sensors; that is applicable for engineering purposes, i.e. the parameters are easily measurable and the results can be employed for practical design.

During the past two years I have approached the theory of fluxgate sensor systems from many points of view. This thesis gathers together most of my work in an attempt to formulate an integrated fluxgate theory. The thesis consists of 10 chapters. Chapter 1, the present one, gives a brief review of the preexisting studies of fluxgate theory and introduces the objectives of the thesis. The purpose of Chapter 2 is to describe the fluxgate mechanism in a straightforward manner utilizing basic principles of physics. There, the important concept of the gating function is introduced, which conveniently represents the effects of drive current and most details of construction and physical properties of the fluxgate materials. In Chapter 3, I extend the state equation approach, which is popular in the modern theory of time-invariant control systems, to time-variant fluxgate sensor systems. The state equation set up here is a generalized one, not only for the gradiometer but also for the magnetometer and other symmetric combinations of fluxgate sensors. Based on the Floquet-Lyapunov theorem and on the Liouville-Jacobi formula [1.22], a stability analysis of the transient solution for the state equation without forcing term is given in Chapter 4. Also the method of calculation is discussed in detail.

In Chapter 5, the parameter mapping approach is applied to time-variant fluxgate sensor systems. Generalized parameter coordinates are determined. Chapter 6 develops the instability maps on the parameter plane, which gives a complete portrayal of both the unstable and stable regions in the parameter domain. This information is useful for the practical design of stable fluxgate sensor systems.

Chapter 7 deals with the fluxgate state equation with a forcing term. The expression and waveforms of the general solution are also given there. In Chapter 8, the solutions of fluxgate state equations are studied in detail in phase space and the global or local stabilities are checked in the time domain again. Chapter 9 starts from the periodic solution for the fluxgate sensor system, and then the important concept of sensitivity is defined and studied. The general sensitivity map and the analysis of the influence of each parameter will help the designer to develop stable and sensitive fluxgate system configurations.

Chapter 10 is the conclusion.

I have attempted to keep the thesis logical and concise. So the text of this thesis includes only my original work, except for the review in Chapter 1. If there was any stimulation from others, the source is indicated by a footnote or in the reference index. For the sake of clarity I have made efforts to provide an intuitive presentation of my theory with essential strictness in mathematics. Moreover, the reader familiar with the topic will find that some theorems or principles that were based on tedious derivations in the reference monographs have been rederived or explained in a new, intuitive and concise way.

Since the present approach crosses several fields, geophysical instrumentation, modern control theory and mathematics; and mixes such various special techniques as fluxgate theory, linear time-variant systems, state equations, parameter mapping, phase space, stability theory and linear differential equations with periodic coefficients, the reader may

meet subjects with which he is unfamiliar. When specialized terminology appears for the first time in the text, it is emphasized by italic font with a brief description attached. If the terminology is defined by this approach, I will declare this either by the words "name", "call", and "define", or by expressions with the symbol $\stackrel{\triangle}{=}$.

Matrices are in boldface, capital Roman characters, e.g. $\mathbf{X}$, and vectors in boldface, lower case Roman characters, e.g. $\mathbf{x}$. To help the reader trace the main development without interruption, most derivations are moved to Appendix A. In addition, a notation list and some specialized theorems are attached for reference as Appendix B.

CHAPTER 2

THE GATING FUNCTION AND THE FLUXGATE MECHANISM

It is well known that the self inductance of a winding around a core which is made of magnetically soft material, can be expressed globally as

$$L(H) = K_{Fe} \cdot N^2 \cdot \mu_d(H) + L_0, \tag{2.1}$$

where K_{Fe} is a constant determined by the geometry of the core and the winding, N is the number of turns in the winding, L_0 is the self inductance of the winding without the core and $\mu_d(H)$ is the effective differential permeability which is equal to dB/dH, the slope of the dynamic hysteresis loop at the applied magnetic field H.

Except at very small H, no matter what hysteresis the core has, the value of μ_d monotonically decreases as the magnitude of the exerting magnetic field H increases, and has its minimum value when H drives the core into saturation. According to (2.1), $L(H)$ has the same characteristics as $\mu_d(H)$: decreasing with increasing H from an original value L. When the core is saturated the $L(H)$ remains at the value $\sim L_0$. In Fig. 2.1, the experimental value of $L(H)$ is plotted for a fluxgate sensor with a ring core while a magnetic field H is exerted along the axis of the sensor winding.

When the sensor, as in Fig. 2.1 and without external field, is excited by a drive winding wound on the ring core and carrying the drive current I_d, the effect of the excited magnetic field on μ_d is similar to that of an external field. A large amplitude of I_d will correspond to a low value of μ_d or low self inductance of the sensor winding. The experimental result of $L(I_d)$ as a function of I_d for the same sensor is illustrated in Fig. 2.2, where the effect of hysteresis shows as a twin-line in $L(I_d)$. We define the drive current value at the point,

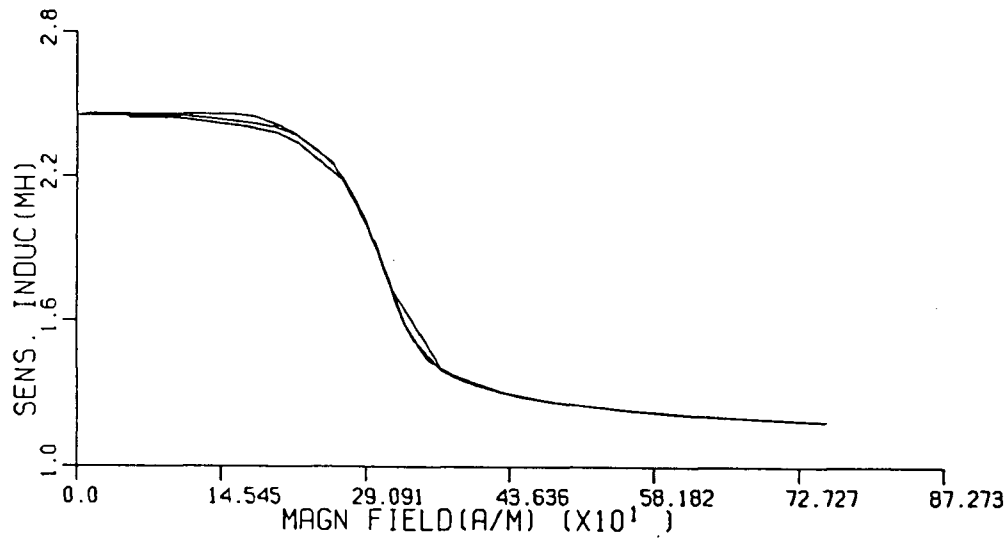

Fig. 2.1 The experimental result of self inductance $L(H)$ for a fluxgate sensor winding with a ring core while a magnetic field H is exerted on the axis of sensor winding. The bifurcation of $L(H)$ results from the effect of hysteresis when H is increasing or decreasing.

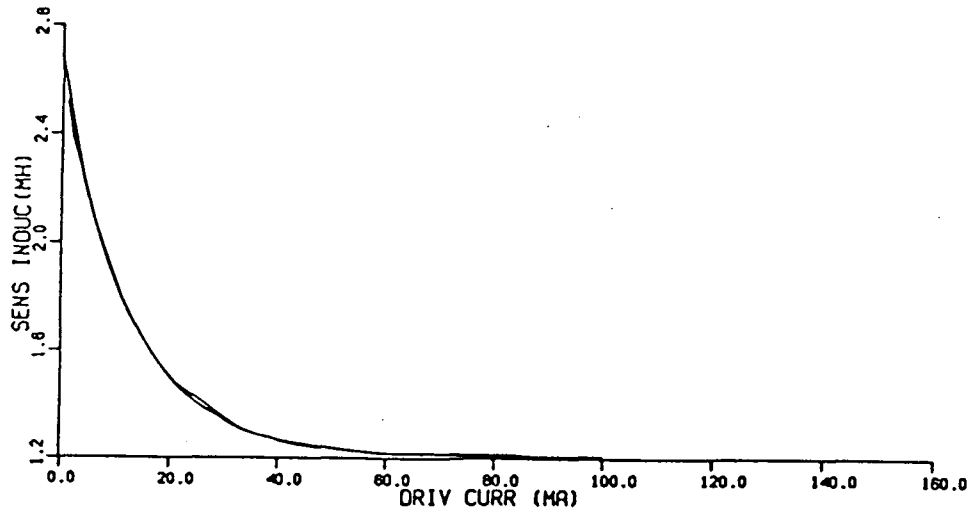

Fig. 2.2 The experimental result of $L(I_d)$ as a function of the drive current I_d which excites a magnetic field in the core where the fluxgate sensor is the as same as in Fig. 2.1. The effect of hysteresis shows as a twin-line in $L(I_d)$.

where the self inductance reduces to $10\% \cdot (L - L_0) + L_0$, as the *threshold of drive current* I_{dt}. For example, in Fig. 2.2 the threshold of the drive current is around $35ma$. For a ring core, we can define the *gate threshold* H_G as

$$H_G \triangleq \frac{I_{dt} \cdot N_c}{\pi \cdot d_{rc}}, \tag{2.2}$$

where N_c is the number of turns and d_{rc} is the diameter of the ring core. The H_G is a useful characteristic parameter for the ring core fluxgate sensor.

Let us now consider the drive current to be a periodic impulsive sequence $I_d(t)$ with alternating positive and negative pulses which are large enough to drive the core into deep saturation. Fig. 2.3 gives several typical $I_d(t)$ wave forms where the amplitudes are much larger than I_{dt}.

We can regard the time-variant self inductance of the sensor winding $L(t)$ as a constant self inductance L, gated by a periodic, dimensionless function named the *gating function* $\theta(t)$, as is illustrated in Fig. 2.4. The negative impulses represent saturation of the core when the magnitude of the drive current is greater than I_{dt}. The *gate period* T is equal to half the drive period. In Fig. 2.4 the rise times and fall times of the impulses are assumed to be equal to Δ. If the amplitude of the drive current impulses is much larger than the threshold current I_{dt}, as in most practical fluxgate sensor systems, we can assume $\Delta/T \rightarrow 0$ and the gating function $\theta(t)$ can be thought of as the square-wave shown in Fig. 2.5. We call the ratio of the original inductance L to the saturated inductance L_0 as the *gate ratio* p, and the *duty cycle* η is defined as the ratio of the impulse duration time to the period T. The gating function is uniquely determined by the parameters η, T and p. In Fig. 2.5 the gate ratio p is about 2.2 for this sensor. Thus, we can express $L(t)$ as $L \cdot \theta(t)$.

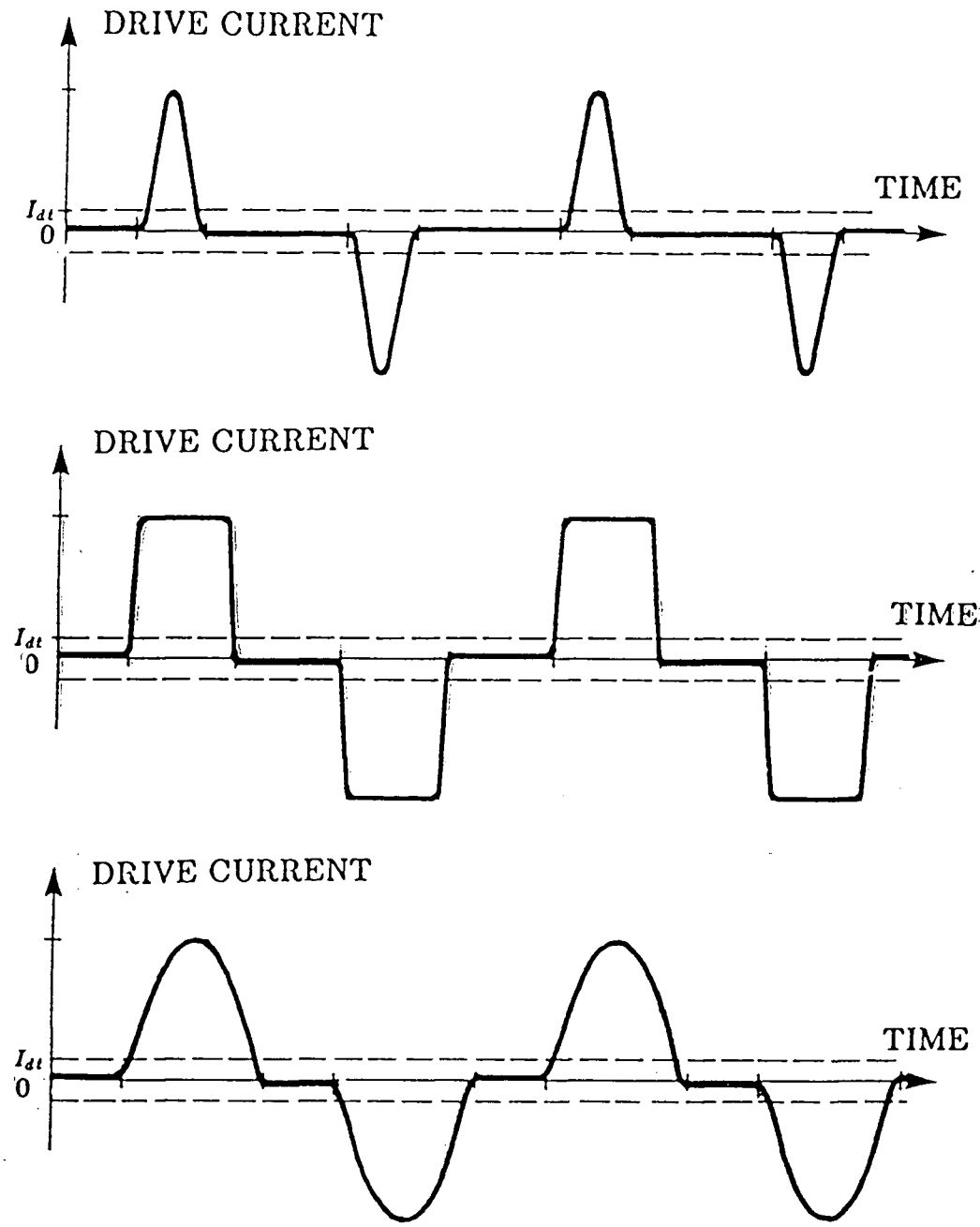

Fig. 2.3 Several typical drive current waveforms where I_{dt} is the threshold of the drive current.

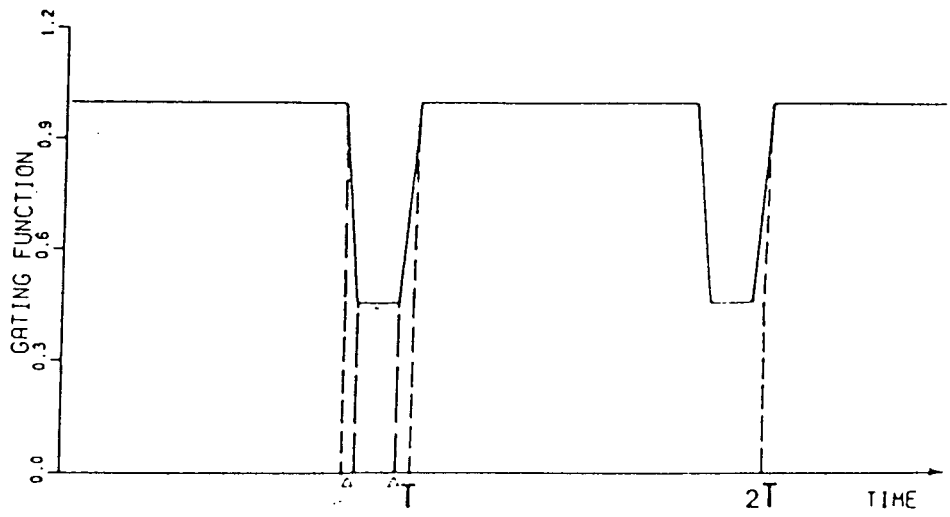

Fig. 2.4 The gating function considering the times of falling and rising edges to be equal to Δ. The gating period T is equal to half the drive period.

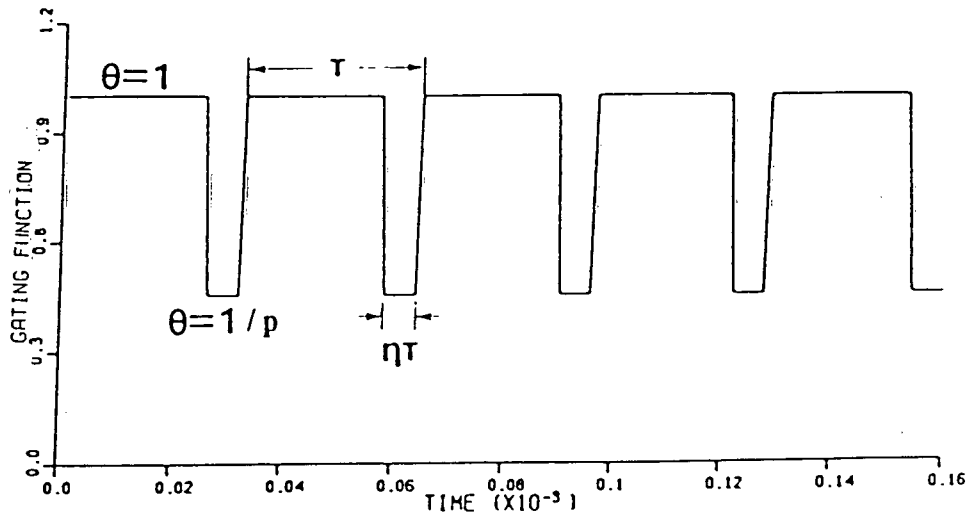

Fig. 2.5 The gating function is a rectangular ripple when the amplitude of the drive current impulses is much larger than threshold I_{dt}. T is the gate period, η is the duty cycle and p is the gate ratio, i.e. the ratio of the original to saturated inductance.

It is well known that for two tightly coupled windings, the maximum mutual inductance is equal to the square root of the product of the self inductances in each winding. Thus we may consider that if a sensor has two similar sensor windings, the mutual inductance as a function of the drive current has characteristics similar to the self inductance of each winding. For simplification, we might also treat the gated mutual inductance $M(t)$ between two tightly coupled sensor windings as the product of a constant M multipied by $\theta(t)$, where M is the original mutual inductance between the two windings around the same core without drive current.

As will be seen subsequently, the gating function plays a key role in the present approach to fluxgate theory. Its characteristic parameters, i.e. the gate period T, the duty cycle η and gate ratio p, are major indices of the performance of a fluxgate sensor system [cf: chapter 9].

The foregoing discussion leads to an important conclusion: the fluxgate mechanism is based on the fact that the inductances of the sensors are gated by a periodic gating function; and the gating function can be regarded approximately as a rectangular ripple with half the drive period.

Russell *et al* [2.1], Narod and Russell [2.2] and Narod *et al* [2.3] utilized the concept of modulation of $L(t)$ and emphasized that: " the detailed shape of the hysteresis curve is of little direct importance, provided only that $L(t)$ is well-defined and periodic "[2.2].

The contribution of my description above is that, based on basic physical principles and experimental results, the mechanism of the gated inductances is straightforwardly explained and sets up a complete description of the gating function and its characteristic parameters. In addition, I believe that by defining the gating function, one can concentrate on the interaction between time-variant inductances and other elements in the

fluxgate sensor system, and ignore not only the exact hysteresis, but also the drive current waveform.

The gating function includes the effects of drive current and most geometric factors of construction and materials in the sensor. As a straightforward demonstration, I can interpret the time dependent permeability, $\mu(t)$, of Serson and Hannaford [2.4] in the form of (2.1). Then we observe that the $L(t)$ is a rectangular ripple similar to the gating function in Fig. 2.5, though the drive current $I_d(t)$ was assumed to be a sinusoid in [2.4].

Thus, in the following chapters, I will use the gating function to set up the generalized fluxgate equation and mathematical solution. I will also study the stability and sensitivity of fluxgate sensor systems and discuss the influences of characteristic parameters η, T, p of the gating function and of elements in sensor loops without involving the $I_d(t)$ wave form, demagnetization, hysteresis, etc.

Finally, since these characteristic parameters η, p, etc., of the gating function and the gate threshold H_G are easily measured, they constitute convenient performance indices which will help investigators' studies of the drive current wave form, studies of optimal construction and tests of materials for the improvement of fluxgate sensor sysems.

CHAPTER 3

GENERALIZED STATE EQUATION

Recently a portable fluxgate ring core gradiometer has been constructed [3.1]. The principle of the gradiometer is shown in Fig. 3.1 (a). It consists of two sensors A and B which are located in magnetic fields $\mathbf{H}_1$ and $\mathbf{H}_2$, respectively.

Since sensor A(1) has the opposite polarity of sensor B(1), we can measure the gradient of the magnetic field for the distance between A and B. Meanwhile the sensors A(2) and B(2) measure the sum of the projections of $\mathbf{H}_1$ and $\mathbf{H}_2$ on the direction of the magnetic axle of their respective sensors.

Fig. 3.1 (b) illustrates the equivalent circuit of Fig. 3.1 (a), where C represents the series capacitance, r represents the combined resistance of the sensor and load in the A(1)-B(1) loop, and R is for the A(2)-B(2) loop. The symbols l_1, L_1, l_2 and L_2 denote the self-inductances for A(1), A(2), B(1) and B(2), respectively. Also M_1 denotes the mutual inductance between A(1) and A(2), and M_2, the mutual inductance between B(1) and B(2). Ideally, M_1 and M_2 are proportional to square roots of the products of l_1, L_1 and of l_2, L_2, respectively.

As we demonstrated in the previous chapter, we can express the time-variant self inductances as $l_1 \cdot \theta(t), l_2 \cdot \theta(t)$, $L_1 \cdot \theta(t)$, $L_2 \cdot \theta(t)$ and the time-variant mutual inductances as $M_1 \cdot \theta(t)$ and $M_2 \cdot \theta(t)$, where $\theta(t)$ is the gating function as shown in Fig. 2.5.

Applying the Lagrange equation to the gradiometer [cf: Appendix A-1], we obtain

$$2l\left(\theta q'\right)' + \left(M_1 - M_2\right)\left(\theta Q'\right)' + \frac{q}{C} + rq' = a_1\theta', \tag{3.1}$$

$$2L\left(\theta Q'\right)' + \left(M_1 - M_2\right)\left(\theta q'\right)' + \frac{Q}{C} + RQ' = a_2\theta', \tag{3.2}$$

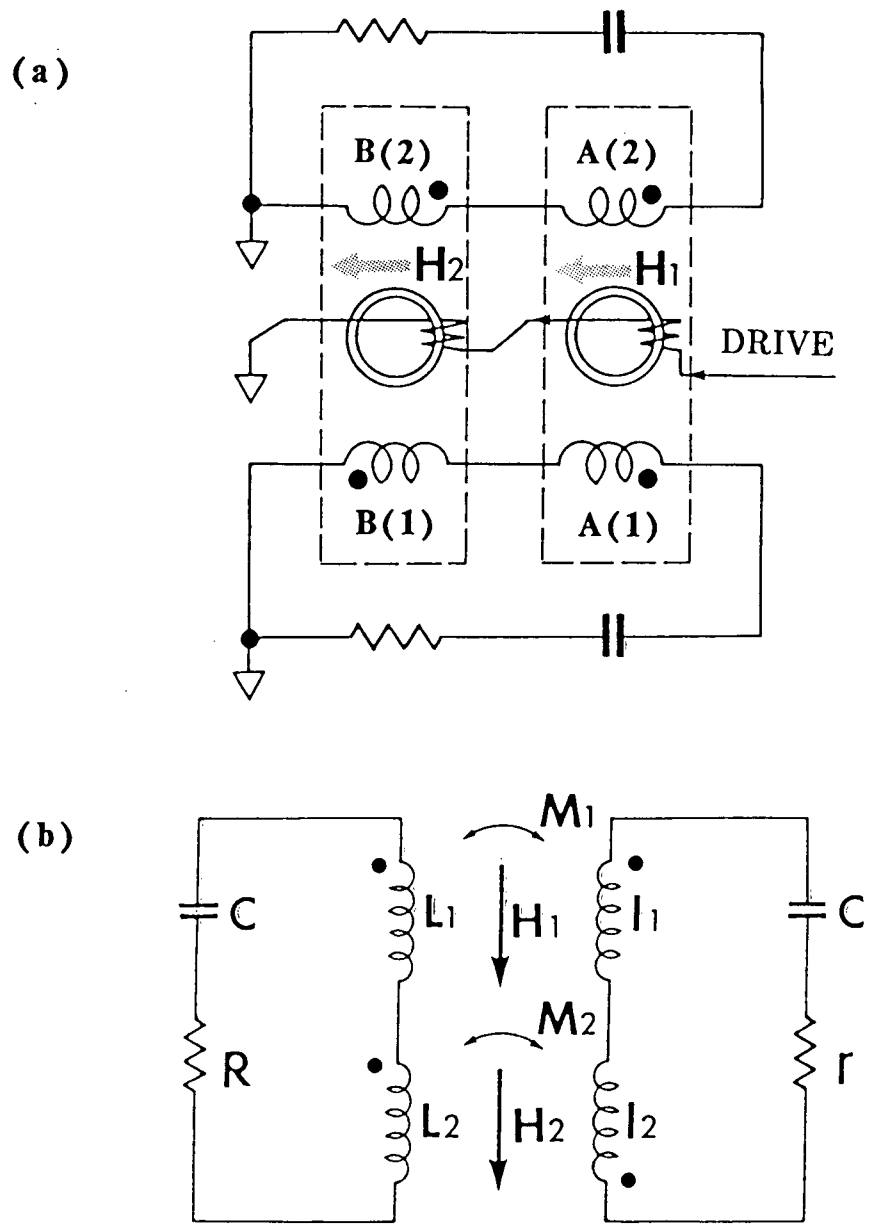

Fig. 3.1 (a) Principle of the fluxgate ring core gradiometer. The sensor A is located in magnetic field $\mathbf{H}_1$, sensor B in $\mathbf{H}_2$. (b) Equivalent circuit of (a). l_1, l_2, L_1 and L_2 denote the self inductances for A(1), B(1), A(2) and B(2); M_1 or M_2 represents the mutual inductance between A(1), A(2) or B(1), B(2); C is the serial capacitance; R or r is the resistance in A(2)-B(2) loop or in A(1)-B(1) loop, respectively.

where q and Q are the charges on the capacitors C of the A(1)-B(1) loop and the A(2)-B(2) loop, respectively; and if we use k_1, k_2, K_1, K_2 as sensor constants for A(1), A(2), B(1), B(2), respectively, we can also define the following constants:

$$a_1 \triangleq (\mathbf{H}_2 \cdot \mathbf{k}_2) l_2 - (\mathbf{H}_1 \cdot \mathbf{k}_1) l_1;$$

$$a_2 \triangleq -(\mathbf{H}_2 \cdot \mathbf{K}_2) L_2 - (\mathbf{H}_1 \cdot \mathbf{K}_1) L_1;$$

$$2l \triangleq l_1 + l_2;$$

$$2L \triangleq L_1 + L_2;$$

$$b \triangleq M_1 - M_2.$$

We can rearrange (3.1) and (3.2) as

$$2l\,(\theta q'' + \theta' q') + b\,(\theta Q'' + \theta' Q') + \frac{q}{C} + r q' = \theta' a_1, \tag{3.3}$$

$$2L\,(\theta Q'' + \theta' Q') + b\,(\theta q'' + \theta' q') + \frac{Q}{C} + R Q' = \theta' a_2. \tag{3.4}$$

Then we obtain

$$\theta \begin{pmatrix} 2l & b \\ b & 2L \end{pmatrix} \begin{pmatrix} q'' \\ Q'' \end{pmatrix} + \left(\theta' \begin{pmatrix} 2l & b \\ b & 2L \end{pmatrix} + \begin{pmatrix} r & 0 \\ 0 & R \end{pmatrix} \right) \begin{pmatrix} q' \\ Q' \end{pmatrix} + \frac{1}{C} \begin{pmatrix} q \\ Q \end{pmatrix} = \theta' \begin{pmatrix} a_1 \\ a_2 \end{pmatrix}. \tag{3.5}$$

We shall assume $r = R$ and use the following notation

$$\mathbf{D} \triangleq \begin{pmatrix} 2l & b \\ b & 2L \end{pmatrix}, \tag{3.6}$$

$$\mathbf{q} \triangleq \begin{pmatrix} q \\ Q \end{pmatrix},$$

$$\mathbf{a}_2 \stackrel{\triangle}{=} \begin{pmatrix} a_1 \\ a_2 \end{pmatrix}.$$

Thus (3.5) becomes in compact matrix form:

$$\theta \mathbf{D}\, \mathbf{q}'' + (\theta' \mathbf{D} + R\mathbf{I_2})\, \mathbf{q}' + \frac{1}{C}\, \mathbf{q} = \theta'\, \mathbf{a}_2, \tag{3.7}$$

where $\mathbf{I_n}$ is the $n \times n$ unit matrix.

We can obtain the state equation for the gradiometer by choosing the following state variables:

$$x_1 \stackrel{\triangle}{=} q,$$

$$x_2 \stackrel{\triangle}{=} Q,$$

$$x_3 \stackrel{\triangle}{=} q' = i,$$

$$x_4 \stackrel{\triangle}{=} Q' = I.$$

where i is the current in the A(1)-B(1) loop and I is the current in the A(2)-B(2) loop. This gives us two equations

$$x_1' - x_3 = 0,$$

$$x_2' - x_4 = 0.$$

Combining them with (3.7), yields the state equation as

$$\begin{pmatrix} \mathbf{I_2} & \mathbf{O_2} \\ \mathbf{O_2} & \theta \mathbf{D} \end{pmatrix} \mathbf{x}' + \begin{pmatrix} \mathbf{O_2} & -\mathbf{I_2} \\ \frac{1}{C}\mathbf{I_2} & \theta' \mathbf{D} + R\mathbf{I_2} \end{pmatrix} \mathbf{x} = \theta' \begin{pmatrix} \mathbf{o_2} \\ \mathbf{a_2} \end{pmatrix}. \tag{3.8}$$

where $\mathbf{O}_n$ is the $n \times n$ zero matrix and $\mathbf{o}_n$ is zero n-vector. Since $\mathbf{D}$ is a nonsingular symmetric matrix, $\mathbf{D}^{-1}$ exists and

$$\mathbf{D}^{-1} = \frac{1}{4Ll - b^2} \begin{pmatrix} 2L & -b \\ -b & 2l \end{pmatrix}. \tag{3.9}$$

Then we obtain

$$\begin{aligned} \mathbf{x}' &= \begin{pmatrix} \mathbf{O}_2 & \mathbf{I}_2 \\ -\frac{1}{C\theta}\mathbf{D}^{-1} & -(\frac{\theta'}{\theta}\mathbf{I}_2 + \frac{R}{\theta}\mathbf{D}^{-1}) \end{pmatrix} \mathbf{x} + \frac{\theta'}{\theta} \begin{pmatrix} \mathbf{o}_2 \\ \mathbf{D}^{-1}\mathbf{a}_2 \end{pmatrix} \\ &= \mathbf{A}(t)\,\mathbf{x} + \mathbf{f}(t), \end{aligned} \tag{3.10}$$

where $\mathbf{A}(t)$ is called the *time-variant coefficient matrix* which is nonsingular, piecewise-continuous, integrable and periodic, i.e. $\mathbf{A}(t+T) = \mathbf{A}(t)$. $\mathbf{f}(t)$ is called the *time-variant forcing term* and it is also periodic.

In a practical design, we shall keep $2l = 2L$. We will also use the notation

$$\begin{aligned} B &\triangleq \frac{b}{L}, \\ \mathbf{S}_2 &\triangleq \frac{1}{4 - B^2} \begin{pmatrix} 2 & -B \\ -B & 2 \end{pmatrix} \\ &= \mathbf{D}^{-1} L. \end{aligned} \tag{3.11}$$

Then,

$$\mathbf{A}(t) = \begin{pmatrix} \mathbf{0}_2 & \mathbf{I}_2 \\ -\frac{1}{\theta LC}\mathbf{S}_2 & -(\frac{\theta'}{\theta}\mathbf{I}_2 + \frac{R}{\theta L}\mathbf{S}_2) \end{pmatrix}, \tag{3.12}$$

$$\mathbf{f}(t) = \frac{\theta'}{\theta} \begin{pmatrix} \mathbf{o}_2 \\ \frac{1}{L}\mathbf{S}_2\,\mathbf{a}_2 \end{pmatrix}. \tag{3.13}$$

Proceeding similarly, we can obtain the state equation for the magnetometer in the same form as that for the gradiometer. That is

$$\mathbf{x}' = \mathbf{A}(t)\,\mathbf{x} + \mathbf{f}(t),$$

but where

$$\mathbf{x} = (x_1, x_2)^T = (q, i)^T,$$

$$\mathbf{A}(t) = \begin{pmatrix} 0 & 1 \\ -\frac{1}{\theta LC} & -(\frac{\theta'}{\theta} + \frac{R}{\theta L}) \end{pmatrix}, \tag{3.14}$$

$$\mathbf{f}(t) = \frac{\theta}{\theta'} \begin{pmatrix} 0 \\ \frac{1}{L}\mathbf{a}_1 \end{pmatrix}, \tag{3.15}$$

$$\mathbf{a}_1 = -(\mathbf{H}_1 \cdot \mathbf{K}_1)\, L. \tag{3.16}$$

The symbols are defined as for the gradiometer except that the subscripts all become 1 since there is only one loop.

In general, we can use a generalized state equation form to represent fluxgate sensor systems as

$$\mathbf{x}' = \mathbf{A}(t)\,\mathbf{x} + \mathbf{f}(t), \tag{3.17}$$

$$\mathbf{A}(t) = \begin{pmatrix} \mathbf{O_j} & \mathbf{I_j} \\ -\frac{1}{\theta LC}\mathbf{S_j} & -(\frac{\theta'}{\theta}\mathbf{I_j} + \frac{R}{\theta L}\mathbf{S_j}) \end{pmatrix}, \tag{3.18}$$

$$\mathbf{f}(t) = \frac{\theta'}{\theta\, L} \begin{pmatrix} \mathbf{o}_j \\ \mathbf{S_j}\,\mathbf{a}_j \end{pmatrix}, \tag{3.19}$$

where we define j to be the *order* of the fluxgate sensor system, e.g. for the gradiometer $j = 2$ and for the magnetometer $j = 1$; $\mathbf{I_j}, \mathbf{O_j}$ and $\mathbf{o}_j$ are the jth order unit matrix, zero

matrix and zero vector, respectively; $\mathbf{S_1} = 1$. When $j > 2$, the expressions are more complicated than above.

Substituting (3.18) into (3.17), setting $\mathbf{f}(t) = 0$ and expanding the product of matrix $\mathbf{A}(t)$ and vector $\mathbf{x}(t)$, we have for the magnetometer

$$\begin{aligned} x_1' &= x_2, \\ x_2' &= -\frac{1}{\theta LC}x_1 - \frac{\theta'}{\theta}x_2 - \frac{R}{\theta L}x_2. \end{aligned}$$

Noticing $x_1 = q, x_2 = i$, we get

$$q'' + \left(\frac{\theta'}{\theta} + \frac{R}{\theta L}\right) \cdot q' + \frac{1}{\theta LC} \cdot q = 0.$$

This is exactly comparable to (9) of Russell *et al* [3.2].

The generalized state equation form is significant. Its time-variant coefficients represent the inductances gated by a periodic gating function which depicts the fluxgate mechanism. If the forcing term in equation (3.17) is zero, the inhomogeneous equation reduces to the homogeneous case.

$$\mathbf{x}' = \mathbf{A}(t)\,\mathbf{x}. \tag{3.20}$$

The solution of (3.20) illustrates the transient behaviour of (3.17) and gives us a sufficient condition for instability for equation (3.17). In the next three chapters, we will study equation (3.20) and its instability in detail.

CHAPTER 4

THE TRANSIENT SOLUTION

In this chapter, I first study the transient solution for the state equation. Then the instability criterion is stated and the method of calculation of the instability is discussed. Also the concept of boundary matrices is defined and analysed in detail.

§4.1 Expression of solution and instability criterion

According to the Floquet-Lyapunov theorem [4.1], the *matrizant* or the *state transition matrix*, i.e. the unique solution $\mathbf{X}(t)$ of equation (3.20) with the initial value $\mathbf{X}(0) = \mathbf{I_{2j}}$, may be expressed as

$$\mathbf{X}(t) = \mathbf{V}(t)\exp(t\mathbf{K}) \tag{4.1}$$

where the $2j \times 2j$ matrix $\mathbf{V}(t+T) = \mathbf{V}(t)$ and $\mathbf{V}(0) = \mathbf{I}_{2j}$. $\mathbf{K}$ is a constant matrix which is related to the *monodromy* matrix $\mathbf{X}(T)$ (i.e. the value of the matrizant after one period), by

$$\mathbf{X}(T) = \exp(T\mathbf{K}) \tag{4.2}$$

The expression (4.2) is easily verified. Take the equation (4.1) at time T,

$$\begin{aligned}\mathbf{X}(T) &= \mathbf{V}(T)\exp[T\mathbf{K}] \\ &= \mathbf{V}(0)\cdot\exp(T\mathbf{K}) \\ &= \exp(T\mathbf{K}).\end{aligned} \tag{4.3}$$

Let us take (4.1) at the time $(t+T)$ and use (4.2), then

$$\mathbf{X}(t+T) = \mathbf{X}(t) \cdot \mathbf{X}(T) \tag{4.4}$$

The equation (4.4) shows that the monodromy $\mathbf{X}(T)$ is a multiplicative factor advancing the state variables by one period. In other words, $\mathbf{X}(T)$ determines how the state variables increase or decrease with increasing time.

Let us denote by $\mathbf{\Lambda}$ the diagonal matrix containing the *multipliers*, i.e. the eigenvalues of $\mathbf{X}(T)$. Then there is a nonsingular constant matrix $\mathbf{Q}$ such that

$$\mathbf{\Lambda} \triangleq \mathbf{Q}\,\mathbf{X}(T)\,\mathbf{Q}^{-1} \tag{4.5}$$

Consequently, we take the transform

$$\mathbf{Z}(t) \triangleq \mathbf{X}(t)\,\mathbf{Q}^{-1}, \tag{4.6}$$

and substitute (4.6) into (3.20), yielding

$$\mathbf{Z}' = \mathbf{A}(t)\,\mathbf{Z}, \tag{4.7}$$

$$\mathbf{Z}(0) = \mathbf{X}(0)\,\mathbf{Q}^{-1} = \mathbf{Q}^{-1} \tag{4.8}$$

Hence, $\mathbf{Z}(t)$ is also a fundamental solution of (3.20) with initial condition (4.8).

Let us examine the relationship between $\mathbf{Z}(t+T)$ and $\mathbf{\Lambda}$. Using (4.4) and (4.6), we obtain

$$\mathbf{Z}(t+T) = \mathbf{Z}(t)\,\mathbf{Q}\,\mathbf{X}(T)\,\mathbf{Q}^{-1} = \mathbf{Z}(t) \cdot \mathbf{\Lambda} \tag{4.9}$$

The expression (4.9) demonstrates the fact that when the argument of $\mathbf{Z}$ increases by one period, its value increases by a factor $\mathbf{\Lambda}$.

Keep in mind, that $\mathbf{Z}(0)$ is not equal to either $\mathbf{I_{2j}}$, or $\mathbf{O_{2j}}$. Thus, $\mathbf{Z}(t+T)$ is always related to the **total** matrix $\mathbf{\Lambda}$, not a particular multiplier.

Meanwhile, linear system theory tells us that a solution of equation (3.20) related to the matrizant $\mathbf{X}(t,\tau)$ with arbitrary initial condition $\mathbf{x}(\tau)$ is [cf: Appendix A-2]

$$\mathbf{x}(t) = \mathbf{X}(t,\tau)\cdot\mathbf{x}(\tau), \tag{4.10}$$

where $\mathbf{X}(t,\tau)$ means the matrizant started at time τ.

From (4.4), (4.9) and (4.10), we know that using either the monodromy or the constant matrix $\mathbf{K}$ it is possible to determine the boundedness of the matrizant or solutions with arbitrary initial condition as time goes to infinity.

So we can state that if the multipliers of the system described by equation (3.20) are inside the unit circle, the system is stable. This statement agrees with the discussion in [4.1], [4.2]. We will use this criterion to determine the transient instability of fluxgate sensor systems.

Our next task is to find the monodromy matrix or the multipliers of (3.20) for fluxgate sensor systems.

§4.2 The determinant of $\mathbf{X}(T)$

Now we apply the Liouville-Jacobi formula [4.1] to equation (3.20) for fluxgate sensor systems to get the determinant of $\mathbf{X}(T)$.

The Liouville-Jacobi formula states that for any fundamental solution $\mathbf{\Phi}(t)$ of (3.20), the following relation is true

$$\det[\mathbf{\Phi}(t)] = \det[\mathbf{\Phi}(\tau)] \exp\left[\int_{\tau}^{t} \mathrm{tr}[\mathbf{A}(s)]\, ds\right], \tag{4.11}$$

where $\mathrm{tr}[\mathbf{A}]$ is the trace of the matrix $\mathbf{A}$. We apply (4.11) to the matrizant at $\tau = 0$, $t = T$, yielding

$$\begin{aligned}\det[\mathbf{X}(T)] &= \det[\mathbf{X}(0)] \exp\left[\int_{0}^{T} \mathrm{tr}[\mathbf{A}(s)]\, ds\right] \\ &= \exp\left[\int_{0}^{T} \mathrm{tr}[\mathbf{A}(s)]\, ds\right].\end{aligned} \tag{4.12}$$

From the general expression for $\mathbf{A}(t)$, i.e. (3.18), we obtain

$$\begin{aligned}\int_{0}^{T} \mathrm{tr}[\mathbf{A}(s)]\, ds &= -\int_{0}^{T} \left(\frac{j\theta'(s)}{\theta(s)} + \frac{R}{\theta(s)\, L} \cdot \mathrm{tr}[\mathbf{S_j}]\right) ds \\ &= -j \ln[\theta(s)]\Big|_{0}^{T} - R \cdot \mathrm{tr}[\mathbf{S_j}] \int_{0}^{T} \frac{ds}{\theta(s)\, L} \\ &= -RT \cdot \mathrm{tr}[\mathbf{S_j}] \cdot \frac{1}{T} \int_{0}^{T} \frac{ds}{\theta(s)\, L} \\ &= -\frac{RT}{L_E} \cdot \mathrm{tr}[\mathbf{S_j}],\end{aligned} \tag{4.13}$$

where, for convenience, we define the *average self inductance* L_E, over one period as

$$\frac{1}{L_E} \triangleq \frac{1}{T} \int_{0}^{T} \frac{ds}{\theta(s)\, L}. \tag{4.14}$$

If the gating function with falling or rising time Δ is as shown in Fig. 2.4, we have

$$L_E = \frac{L}{1 + (p-1)\,\eta - \frac{2\Delta}{T} + \frac{2\Delta p}{(p-1)T} \ln p}, \tag{4.15}$$

If $\Delta/T \to 0$, i.e. the case in Fig. 2.5, then

$$L_E = \frac{L}{1 + (p-1)\,\eta}, \tag{4.16}$$

For derivations of (4.15) and (4.16), please refer to Appendix A-3.

Hence, the determinant of the monodromy is

$$\det[\mathbf{X}(T)] = \exp\left[-\frac{RT}{L_E} \cdot tr[\mathbf{S_j}]\right]. \tag{4.17}$$

This result shows that RT/L_E is a determinative factor for fluxgate sensor systems. In later chapters, this will be discussed in detail.

RT/L_E is a dimensionless quantity, which can be rewritten as

$$\frac{RT}{L_E} = j \cdot 2\pi \cdot \frac{\omega_R}{\omega}, \tag{4.18}$$

where we define

$$\omega_R \triangleq \frac{R}{jL_E}, \tag{4.19}$$

$$\omega \triangleq \frac{2\pi}{T}. \tag{4.20}$$

So, for the magnetometer $(j = 1)$

$$\det[\mathbf{X}(T)] = \exp\left[-\frac{RT}{L_E}\right] = \exp\left[-2\pi\frac{\omega_R}{\omega}\right], \tag{4.21}$$

and for the gradiometer $(j = 2)$

$$\det[\mathbf{X}(T)] = \exp\left[-\frac{4}{4-B^2}\frac{RT}{L_E}\right] = \exp\left[-\frac{16\pi}{4-B^2}\cdot\frac{\omega_R}{\omega}\right]. \tag{4.22}$$

Since $B = (M_1 - M_2)/L < 1$, we have

$$0 < \det[\mathbf{X}(T)] < 1. \tag{4.23}$$

This means that the products of multipliers of (3.20), for fluxgate sensor systems are real and less than unity.

In practical engineering, we are always able to keep the B less than 5 percent. We may assume $B = 0$, then (4.22) becomes the same as (4.21), i.e.

$$\det[\mathbf{X}(T)] = \exp[-\frac{RT}{L_E}]. \tag{4.24}$$

Now let us examine the constant matrix $\mathbf{K}$. Recall (4.2) and take its determinant, then

$$\det[\mathbf{X}(T)] = \det[\exp(T\mathbf{K})]. \tag{4.25}$$

Comparing this with (4.17), we obtain

$$\mathrm{tr}[\mathbf{K}] = \sum_{i=1}^{2j} \lambda_{ki} = -\mathrm{tr}[\mathbf{S_j}] \cdot \frac{R}{L_E}, \tag{4.26}$$

where $\{\lambda_{ki}\}$ are the *characteristic exponents* of (3.20), i.e. the eigenvalues of $\mathbf{K}$.

In passing, we may point out that $\det[\mathbf{X}(T)]$ depends on the parameters R, T, L, p and η, no matter what value of C is taken. We select the optimal capacitance only in order to rearrange the ratio among (or between) the multipliers in order that we may increase the second harmonic of the signal current [cf: chapter 9].

§4.3 Methods to calculate the monodromy

Next let us calculate the monodromy $\mathbf{X}(T)$. In 1973, Hsu [4.3] developed a method to determine the approximate value of the monodromy, which he called the *growth matrix* $\mathbf{H}(m)$. The method is: divide one period into m equal intervals, with $t_0 = 0 < t_1 < \ldots < t_m = T$. The time interval is $\Delta = t_n - t_{n-1}$. In the nth interval, a constant matrix $\mathbf{C_n}$ replaces the matrix $\mathbf{A}(t)$. The $\mathbf{C_n}$ is defined by Hsu to be

$$\mathbf{C_n} \triangleq \frac{1}{\Delta} \int_{t_{n-1}}^{t_n} \mathbf{A}(s)\, ds, \qquad s \in (t_{n-1}, t_n).$$

Then the growth matrix is

$$\mathbf{H}(m) \triangleq \exp(\Delta \cdot \mathbf{C_m}) \exp(\Delta \cdot \mathbf{C_{m-1}}) \ldots \exp(\Delta \cdot \mathbf{C_1}). \tag{4.27}$$

In 1974, Hsu [4.4] proved that the growth matrix $\mathbf{H}$ will converge to $\mathbf{X}(T)$, when $m \to \infty$ or $\Delta \to 0$, i.e.

$$\mathbf{X}(T) = \lim_{m \to \infty} \mathbf{H}(m). \tag{4.28}$$

We used this convergence to derive the precise expression of $\mathbf{X}(T)$ for the fluxgate sensor equation (3.20) with gating function as shown in Fig. 2.5.

Applying Hsu's method to the gating function $\theta(t)$, we obtain the precise expression for the monodromy $\mathbf{X}(T)$ as

$$\mathbf{X}(T) = \mathbf{P}^{-1} \cdot \exp[\eta T \mathbf{P} \mathbf{W}] \cdot \mathbf{P} \cdot \exp[(1-\eta) T \mathbf{W}], \tag{4.29}$$

or

$$\mathbf{X}(T) = \exp[\eta T \mathbf{W} \mathbf{P}] \exp[(1-\eta) T \mathbf{W}], \tag{4.30}$$

$$\mathbf{W} \triangleq \begin{pmatrix} \mathbf{O_j} & \mathbf{I_j} \\ -\frac{1}{LC}\mathbf{S_j} & -\frac{R}{L}\mathbf{S_j} \end{pmatrix}, \tag{4.31}$$

$$\mathbf{P} \triangleq \begin{pmatrix} \mathbf{I_j} & \mathbf{O_j} \\ \mathbf{O_j} & p\mathbf{I_j} \end{pmatrix}. \tag{4.32}$$

The detailed derivation of (4.29)–(4.32) can be seen in Appendix A-4. The constant matrix $\mathbf{W}$ may be called the *loop matrix*, since it contains the loop elements R, L, C. We call the constant matrices $\mathbf{P}$ and $\mathbf{P}^{-1}$ the *boundary matrices*, for reasons which will be explained in the next section.

Expressions (4.29)–(4.32) can be used to calculate $\mathbf{X}(T)$ for various values of the parameters R, L, C, p, η and T. Then suitable values of parameters can be determined.

Let us check the results of (4.29)-(4.32) by comparing with the results obtained from the Liouville-Jacobi formula. Taking the determinant of (4.30), yields

$$\det[\mathbf{X}(T)] = \det\left[\exp[\eta T \mathbf{WP}]\right] \det\left[\exp[(1-\eta)T\mathbf{W}]\right].$$

Then

$$\det[\mathbf{X}(T)] = \exp\left[\eta T \sum_{1}^{2j} \lambda_{2i}\right] \exp\left[(1-\eta)T \sum_{1}^{2j} \lambda_{1i}\right],$$

where $\{\lambda_{2i}\}$ are the eigenvalues of $\mathbf{WP}$ and $\{\lambda_{1i}\}$ are the eigenvalues of $\mathbf{W}$.

Note that,

$$\sum_{1}^{2j} \lambda_{2i} = \mathrm{tr}[\mathbf{WP}] = -\frac{pR}{L} \cdot \mathrm{tr}[\mathbf{S_j}],$$

$$\sum_{1}^{2j} \lambda_{1i} = \mathrm{tr}[\mathbf{W}] = -\frac{R}{L} \cdot \mathrm{tr}[\mathbf{S_j}].$$

Consequently,

$$\begin{aligned}\det[\mathbf{X}(T)] &= \exp\left[-\eta T \frac{pR}{L} \cdot \mathrm{tr}[\mathbf{S_j}] - (1-\eta)T\frac{R}{L} \cdot \mathrm{tr}[\mathbf{S_j}]\right] \\ &= \exp\left[-\frac{RT}{L_E} \cdot \mathrm{tr}[\mathbf{S_j}]\right]. \end{aligned} \tag{4.33}$$

The result (4.33) coincides with the result (4.13) obtained from the Liouville-Jacobi formula.

In addition, I have developed two other derivations which straightforwardly lead to expressions for the monodromy which are the same as (4.29)-(4.32), for the gating function of Fig. 2.5. The merit of Hsu's method is that it can deal with a more complicated case, e.g. the gating function shown in Fig. 2.4 where the edge time Δ cannot be ignored. As

pointed out before, most modern practical fluxgate sensor systems have gating functions as shown in Fig. 2.5. Moreover, the expression, for the gating function as shown in Fig. 2.4, is more complicated than (4.29), so I did not include the complicated results in this thesis.

§4.4 Boundary matrix

The reason for describing $\mathbf{P}$ and its inverse $\mathbf{P}^{-1}$ as boundary matrices, is that $\mathbf{P}$ and $\mathbf{P}^{-1}$ play the role of connecting the state variables at the boundaries where $\theta(t)$ has a jump.

A good deal of insight into the physical nature of the boundary matrix can be obtained by studying the expression for the monodromy from the matrizant point of view.

Recall expression (4.10)

$$\mathbf{x}(t) = \mathbf{X}(t,\tau)\cdot\mathbf{x}(\tau). \tag{4.10}$$

Applying (4.10) to the interval $(0, t_1^-)$ where t_1^- is the time before the falling jump of $\theta(t)$, we have

$$\mathbf{x}(t) = \mathbf{X}(t,0)\cdot\mathbf{x}(0).$$

If $\theta(t)$ = constant, $\theta'(t) = 0$ in the time-interval, then the time-variant coefficient $\mathbf{A}(t)$ becomes a constant matrix $\mathbf{A}$ and (3.20) becomes

$$\mathbf{X}'(t) = \mathbf{A}\cdot\mathbf{X}(t), \tag{4.34}$$

where

$$\mathbf{A} = \begin{pmatrix} \mathbf{O_j} & \mathbf{I_j} \\ -\frac{1}{LC\theta}\mathbf{S_j} & -\frac{R}{L\theta}\mathbf{S_j} \end{pmatrix}. \tag{4.35}$$

The matrizant of (4.34) has a standard solution in system theory and can be expressed in the equation

$$\mathbf{X}(t,\tau) = \exp\left[(t-\tau)\mathbf{A}\right]. \tag{4.36}$$

For the interval of $\theta(t)$ =1, $\mathbf{A} = \mathbf{W}$, and thus (4.10) becomes

$$\mathbf{x}(t) = \exp\left[(t-\tau)\mathbf{W}\right] \cdot \mathbf{x}(\tau). \tag{4.37}$$

Noting that at $\tau = 0$, the initial values $\mathbf{X}(0) = \mathbf{I_{2j}}$ for the matrizant, we have

$$\begin{aligned} \mathbf{X}(t) &= \exp\left[(t-0)\mathbf{W}\right] \cdot \mathbf{X}(0) \\ &= \exp\left[(t-0)\mathbf{W}\right]. \end{aligned} \tag{4.38}$$

At $t = t_1^-$, we obtain

$$\begin{aligned} \mathbf{X}(t_1^-) &= \exp\left[(t_1^- - 0)\mathbf{W}\right] \\ &= \exp\left[(1-\eta)T\mathbf{W}\right]. \end{aligned} \tag{4.39}$$

where t_1^- is the time before the falling jump.

Similarly, for $\theta(t) = 1/p$, $\mathbf{A} = \mathbf{PW}$, and we have

$$\mathbf{X}(t) = \exp\left[(t-\tau)\mathbf{PW}\right] \cdot \mathbf{X}(\tau). \tag{4.40}$$

In the interval (t_1^+, T^-), where t_1^+ is the time after the falling jump and T^- is the time before the rising jump of $\theta(t)$, we have

$$\mathbf{X}(t) = \exp\left[(t - t_1^+)\mathbf{PW}\right] \cdot \mathbf{X}(t_1^+).$$

At $t = T^-$,

$$\mathbf{X}(T^-) = \exp\left[\eta T \mathbf{PW}\right] \cdot \mathbf{X}(t_1^+). \tag{4.41}$$

It is difficult to solve for the matrizant during jumps of $\theta(t)$, e.g. on the interval (t_1^-, t_1^+), however, according to the property of the matrizant we can express the solution as

$$\begin{aligned} \mathbf{X}(t) &= \mathbf{X}(t, t_1^-) \cdot \mathbf{X}(t_1^-), \\ \mathbf{X}(t_1^+) &= \mathbf{X}(t_1^+, t_1^-) \cdot \mathbf{X}(t_1^-), \end{aligned} \tag{4.42}$$

where $\mathbf{X}(t_1^+, t_1^-)$ represents the matrizant of equation (3.20) in the falling jump (t_1^-, t_1^+). In same way, at T, we have

$$\mathbf{X}(T) = \mathbf{X}(T^+) = \mathbf{X}(T^+, T^-) \cdot \mathbf{X}(T^-). \tag{4.43}$$

Combining these expressions (4.39), (4.41), (4.42) and (4.43) together, we obtain

$$\mathbf{X}(T) = \mathbf{X}(T^+, T^-) \cdot \exp[\eta T \mathbf{PW}] \cdot \mathbf{X}(t_1^+, t_1^-) \cdot \exp[(1 - \eta)\, T\mathbf{W}]. \tag{4.44}$$

But we have already shown the monodromy $\mathbf{X}(T)$ as (4.29), namely,

$$\mathbf{X}(T) = \mathbf{P}^{-1} \cdot \exp[\eta T \mathbf{P}\mathbf{W}] \cdot \mathbf{P} \cdot \exp[(1-\eta) T \mathbf{W}]. \tag{4.45}$$

Comparing (4.44) to (4.45) and noticing $\mathbf{P} \neq 0$, we obtain that

$$\mathbf{X}(t_1^+, t_1^-) = \mathbf{P}, \tag{4.46}$$

$$\mathbf{X}(T^+, T^-) = \mathbf{P}^{-1}. \tag{4.47}$$

Thus, (4.43) and (4.44) become

$$\mathbf{X}(t_1^+) = \mathbf{P} \cdot \mathbf{X}(t_1^-), \tag{4.48}$$

$$\mathbf{X}(T^+) = \mathbf{P}^{-1} \cdot \mathbf{X}(T^-). \tag{4.49}$$

These expressions imply that $\mathbf{P}$ or $\mathbf{P}^{-1}$ is the solution at the boundaries where the gating function has jumps. In other words, $\mathbf{P}$ and $\mathbf{P}^{-1}$ represent the transfer progress of state variables at the boundaries. For this reason, I have named $\mathbf{P}$ and $\mathbf{P}^{-1}$ as the boundary matrices.

Recalling the definition of $\mathbf{P}$, i.e. (4.32), and calculating the $\mathbf{P}^{-1}$, we have

$$\mathbf{P} \triangleq \begin{pmatrix} \mathbf{I_j} & \mathbf{O_j} \\ \mathbf{O_j} & p\mathbf{I_j} \end{pmatrix}, \tag{4.50}$$

$$\mathbf{P}^{-1} \triangleq \begin{pmatrix} \mathbf{I_j} & \mathbf{O_j} \\ \mathbf{O_j} & \frac{1}{p}\mathbf{I_j} \end{pmatrix}. \tag{4.51}$$

From expressions (4.48), (4.50) for the transfer progress of state variables, we find the following facts for equation (3.20) without a forcing term: the charges are continuous and

the currents have a jump, i.e.

$$q^+ = q^-, \qquad Q^+ = Q^-; \tag{4.52}$$

$$\theta^+ i^+ = \theta^- i^-, \qquad \theta^+ I^+ = \theta^- I^-. \tag{4.53}$$

For example, at time t_1 of falling jump, $i^+ = p\, i^-$.

The above conclusion agrees with the analysis of the fluxgate sensor from a physical point of view. We will extend these concepts to the case with a forcing term in the latter part of this thesis.

CHAPTER 5

PARAMETER MAPPING

To study the transient response and stability for a time-invariant system (linear or nonlinear) parameter mapping is a powerful tool [5.1]. Parameter mapping is the transformation of the points from the complex s plane, (i.e. the roots of the characteristic equation) into points in the parameter subspace. Here we make an attempt to use a similar idea for time-variant fluxgate sensor systems.

The key to parameter mapping is to determine the coordinates on the parameter plane by a mapping relation which is often represented by the characteristic equation. We want to illustrate the results of the monodromy $\mathbf{X}(T)$ on the parameter plane for stability analysis. But there is difficulty in developing a characteristic equation for $\mathbf{X}(T)$, because it relates to equation (3.20) with time-variant coefficients.

Since the constant matrix $\mathbf{K}$ is related to $\mathbf{X}(T)$ by expression (4.2), let us check $\mathbf{K}$, for fluxgate sensor systems, in detail.

§5.1 System matrix U

First we take the Lyapunov reducible transform [5.2],

$$\mathbf{x} = \mathbf{V}(t)\,\mathbf{y}. \tag{5.1}$$

Differentiate (4.1) and substitute the results into equation (3.20). After some manipulations, we obtain

$$\mathbf{A}(t)\,\mathbf{V}(t) = \mathbf{V}(t)' + \mathbf{V}(t)\,\mathbf{K}. \tag{5.2}$$

Then, the equation (3.20) becomes

$$\begin{aligned}\mathbf{x}' &= \mathbf{A}(t)\,\mathbf{x} = \mathbf{A}(t)\,\mathbf{V}(t)\,\mathbf{y} \\ &= \mathbf{V}(t)'\,\mathbf{y} + \mathbf{V}(t)\,\mathbf{K}\,\mathbf{y}. \end{aligned} \tag{5.3}$$

On the other hand, if we differentiate (5.1), we get

$$\mathbf{x}' = (\mathbf{V}(t)\,\mathbf{y})' = \mathbf{V}(t)'\,\mathbf{y} + \mathbf{V}(t)\,\mathbf{y}'. \tag{5.4}$$

Comparing (5.3) with (5.4) yields

$$\mathbf{y}' = \mathbf{K}\,\mathbf{y}. \tag{5.5}$$

The equation (5.5) has constant coefficients, and is similiar to the state equation, which is often dealt with in the modern control theory. Remember that in the last chapter we have the expression (4.26) for $\mathbf{K}$:

$$\mathrm{tr}[\mathbf{K}] = \sum_{i=1}^{2j} \lambda_{ki} = -\frac{R}{L_E} \cdot \mathrm{tr}[\mathbf{S_j}]. \tag{4.26}$$

To find the proper parameter plane which represents the parameters in the characteristic equation of $\mathbf{K}$ and $\mathbf{X}(T)$, $\mathrm{tr}[\mathbf{K}]$ is not enough.

Since the mean value over a period is a characteristic for the periodic function [5.3], as we treated L_E before, we define the *mean value* of $\mathbf{A}(t)$ over a period as the *system matrix* $\mathbf{U}$, i.e.

$$\mathbf{U} \triangleq \frac{1}{T}\int_0^T \mathbf{A}(t)\,dt$$

$$= \frac{1}{T}\int_0^T \mathbf{X}(t)' \cdot \mathbf{X}(t)^{-1}\, dt. \tag{5.6}$$

It is easily verified that

$$\mathbf{U} = \begin{pmatrix} \mathbf{O_j} & \mathbf{I_j} \\ -\frac{1}{L_E C}\mathbf{S_j} & -\frac{R}{L_E}\mathbf{S_j} \end{pmatrix}. \tag{5.7}$$

Note that $\mathbf{U}$ includes most of the parameters in fluxgate sensor systems, i.e. R, L, C, p and η to a certain degree. Nevertheless $\mathbf{U}$ is time-invariant and describes the behavour of the equation (3.20). The trace of $\mathbf{U}$ is

$$\mathrm{tr}[\mathbf{U}] = \sum_{i=1}^{2j} \lambda_{ui} = -\frac{R}{L_E} \cdot \mathrm{tr}[\mathbf{S_j}]. \tag{5.8}$$

which is the same as $\mathrm{tr}[\mathbf{K}]$, e.g. for the gradiometer, we have

$$\mathrm{tr}[\mathbf{U}] = \mathrm{tr}[\mathbf{K}] = -\frac{4}{4 - B^2} \cdot \frac{R}{L_E}. \tag{5.8}'$$

Moreover, if we substitute (4.2) into (4.29) and take $\eta = 0$, we will find $\mathbf{U}$ is equal to $\mathbf{K}$ with $\eta = 0$. Thus, we have a reasonable expectation that the characteristic equation for $\mathbf{U}$ will be useful in determining the coordinates on the parameter plane for the study of $\mathbf{X}(T)$ or $\mathbf{K}$.

§5.2 Characteristic equation and parameter coordinate

For the magnetometer case $j = 1$, the characteristic equation for $\mathbf{U}$ is

$$s^2 + \frac{R}{L_E}s + \frac{1}{L_E C} = 0, \tag{5.9}$$

or

$$s^2 + \omega_{RM} s + \omega_{CM}^2 = 0, \tag{5.10}$$

where s has the same dimension as ω,

$$\begin{aligned} \omega_{RM} &\triangleq \frac{R}{L_E}, \\ \omega_{CM}^2 &\triangleq \frac{1}{L_E C}. \end{aligned} \tag{5.11}$$

One can associate these results with the well known characteristic equation of a second order system:

$$s^2 + \alpha s + \beta = 0, \tag{5.12}$$

$$\alpha = 2\varsigma\, \omega_n, \tag{5.13}$$

$$\beta = \omega_n^2, \tag{5.14}$$

$$s = -\varsigma\omega_n \pm j\omega_n\sqrt{1-\varsigma^2}, \tag{5.15}$$

where ς is referred to as the *relative damping coefficient* ; ω_n is refered to as the *undamped natural frequency*; α and β are adjustable parameters which are commonly used as the ordinate and abscissa of the parameter plane for a time-invariant system when the mapping is taken with the characteristic equation.

Hence, we obtain

$$\alpha \sim \omega_{RM} \triangleq \frac{R}{L_E}, \tag{5.16}$$

$$\beta \sim \omega_{CM}^2 \triangleq \frac{1}{L_E C}, \tag{5.17}$$

$$\varsigma \sim \frac{\omega_{RM}}{2\omega_{CM}}, \tag{5.18}$$

$$\omega_n \sim \omega_{CM}. \tag{5.19}$$

However we must distinguish between the differences in the dimension of s in the characteristic equation and the multipliers λ. s has the dimension of sec^{-1}, but the multipliers are dimensionless. Since our task is to illustrate the multipliers of $\mathbf{X}(T)$ on the parameter plane, the coordinates must be dimensionless.

As we discussed before, the product of the multipliers, i.e. the determinant of $\mathbf{X}(T)$, depends on ω_R/ω [cf: (4.21) and (4.22)]. So a natural choice for the parameter ordinate α is ω_R/ω, and the abscissa β is chosen to be ω_C^2/ω^2.

For the gradiometer, the characteristic equation for U is [cf: Appendix A-5]:

$$s^4 + \left(\frac{8}{4-B^2}\omega_{RG}\right) s^3 + \left(\frac{4}{4-B^2}\omega_{RG}^2 + \frac{8}{4-B^2}\omega_{CG}^2\right) s^2 + \left(\frac{8}{4-B^2}\omega_{RG}\omega_{CG}^2\right) s + \frac{4}{4-B^2}\omega_{CG}^4 = 0, \tag{5.20}$$

where

$$\omega_{RG} \triangleq \frac{R}{2L_E},$$
$$\omega_{CG}^2 \triangleq \frac{1}{2L_E C}. \tag{5.21}$$

As mentioned before, in a practical gradiometer B is less than a few percent. If we assume $B = 0$, then (5.20) becomes

$$s^4 + (2\omega_{RG})\, s^3 + (\omega_{RG}^2 + 2\omega_{CG}^2) s^2 + (2\omega_{RG}\omega_{CG}^2)\, s + \omega_{CG}^4 = 0,$$

i.e.

$$(s^2 + \omega_{RG}s + \omega_{CG}^2)^2 = 0. \tag{5.22}$$

Comparing (5.22) to (5.10), we find that the forgoing discussion is also suitable for the gradiometer. If we use the generalized definition for ω_C^2 and recall (4.19) for ω_R

$$\omega_R \stackrel{\triangle}{=} \frac{R}{jL_E}, \tag{4.19}$$

$$\omega_C^2 \stackrel{\triangle}{=} \frac{1}{jL_EC}. \tag{5.23}$$

Thus,

$$\alpha = \frac{\omega_R}{\omega} = \frac{RT}{j \cdot 2\pi \cdot L_E}, \tag{5.24}$$

$$\beta = \frac{\omega_C^2}{\omega^2} = \frac{T^2}{j \cdot 4\pi^2 \cdot L_EC}. \tag{5.25}$$

Thus, we expect similar portraits for the gradiometer and the magnetometer in the generalized parameter plane.

CHAPTER 6

INSTABILITY MAP AND APPLICATION

Let us now illustrate the instability map in the parameter domain and compare instability maps of magnetometers with maps of gradiometers. Then we will find that the instability map is generalized and it is useful for practical design of stable fluxgate sensor systems.

§6.1 Instability map

Using equations (4.29)-(4.32), I have calculated the multipliers for a variety of parameter values in a real gradiometer sensor system, which has the configuration and the gating function shown in Fig. 3.1 and Fig. 2.5, respectively. For comparison, I also have calculated the multipliers for a corresponding magnetometer. Then I mapped the amplitude of the first multipliers, λ_M, to the parameter plane.

$$\lambda_M \stackrel{\triangle}{=} max\left(|\lambda_i| : 1 \leq i \leq 2j\right), \tag{6.1}$$

where λ_i is the multiplier.

As an example, I have plotted the contours for $\lambda_M = 0.05$, 0.1, 0.2, 0.4, 0.8 and 1.0 for the gradiometer with $\eta = 0.22$, $B = 0.0$ in Fig. 6.1 (a); and for the magnetometer with $\eta = 0.22$ in Fig. 6.1 (b). The contours are labeled with the amplitude multiplied by 100.

These plots show that the gradiometer and the magnetometer have exactly the same portraits in the parameter plane.

(a)

GRADIOMETER

$\eta = 0.22$

$$\alpha = \frac{\omega_R}{\omega} = \frac{RT}{4\pi L_E}$$

$$\beta = \frac{\omega_C^2}{\omega^2} = \frac{T^2}{8\pi^2 L_E C}$$

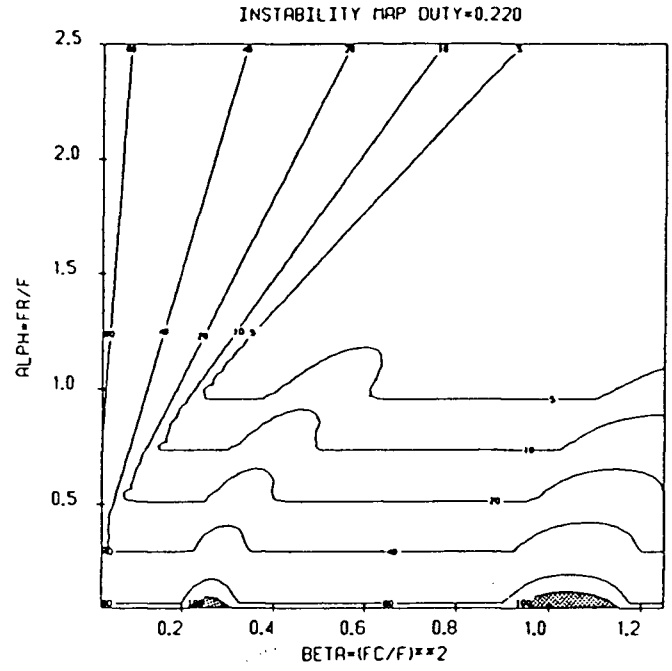

(b)

MAGNETOMETER

$\eta = 0.22$

$$\alpha = \frac{\omega_R}{\omega} = \frac{RT}{2\pi L_E}$$

$$\beta = \frac{\omega_C^2}{\omega^2} = \frac{T^2}{4\pi^2 L_E C}$$

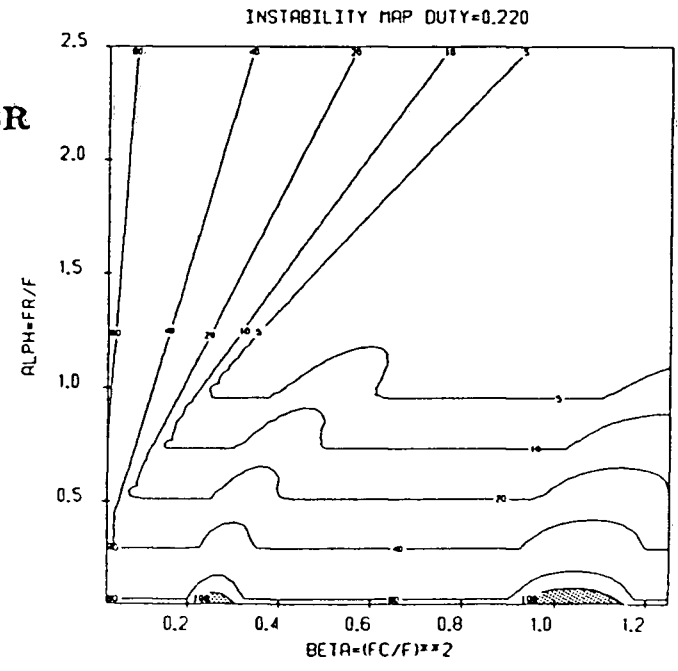

Fig. 6.1 The instability map, i.e. the amplitude contours of (λ_m = 0.05, 0.1, 0.2, 0.4, 0.8 and 1.0) on the parameter plane. The contours are labeled with the amplitude multiplied by 100. (a) for the gradiometer with $B = 0.00$ and $\eta = 0.22$; (b) for the magnetometer with $\eta = 0.22$. The unstable region is stippled and other regions are asymptotically stable.

The regions of $\lambda_M \geq 1$ are unstable. As mentioned in §**4.1**, if any multiplier has a magnitude larger than unity the system will be unstable, i.e. a fluxgate sensor system takes parameters on these regions which will produce an instability. In fact, if we do the *inverse-mapping*, the regions of $\lambda_M \geq 1$ in the parameter plane map onto the right half plane on the s plane. Obviously, it is unstable.

In contrast, the $\lambda_M < 1$ region in the parameter plane maps onto the left half of the s plane except for the imaginary axis. This represents the region for which the fluxgate system is asymptotically stable for the case without a forcing term.

To demonstrate the portraits, Fig. 6.2 illustrates the Q and I transient waveforms which were simulated by computer for a real magnetometer sensor in those regions discussed above. The operational parameters of these waveforms are: $\beta = 0.98$, but α is varied as labeled. These waveforms show that:

(1), in the unstable region, unbounded symmetrical resonant oscillations occur (see Fig. 6.2 (a));

(2), in the $\lambda_M < 1$ region, the transient response asymptotically approaches zero with increasing time (see Fig. 6.2 (b) and (c)).

Since there is a nonlinear limitation which prevents infinite output, the instabilities are observed as rapid changes of polarity of the output in the unstable region.

I should point out that the instability map for the magnetometers in references [6.1] and [6.2] correspond to the unstable region and a part of region $\lambda_M < 1$, i.e. approximately the part under $\varsigma = 0.78$, in my parameter plane diagrams.

However, some designers of fluxgate magnetometers, e.g. Serson and Hannaford (1956 [6.3]), had noted that when the resistance in the loop is too small, i.e. in the unstable

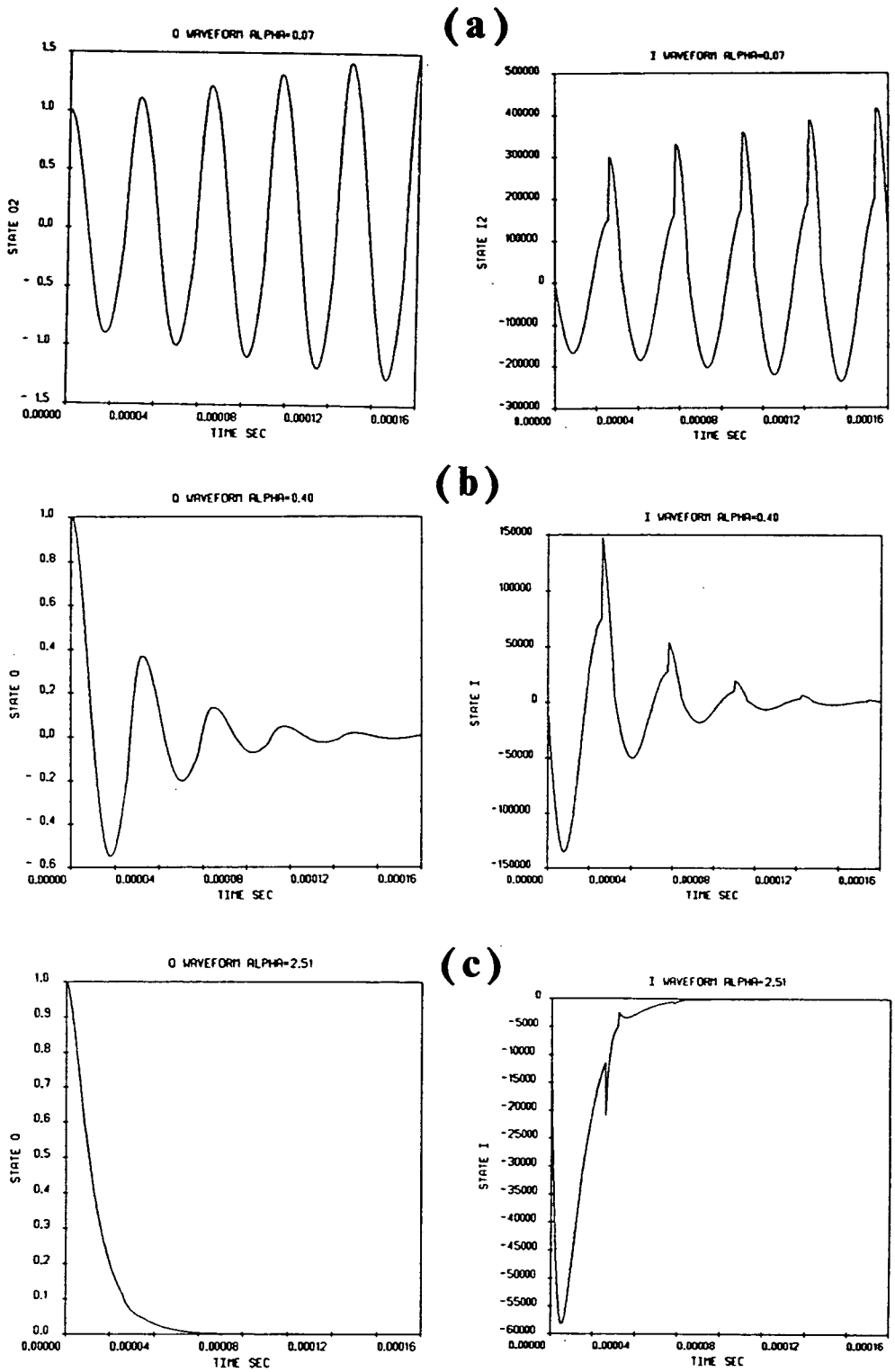

Fig. 6.2 The Q and I transient waveforms for a magnetometer with the same $\beta = 0.98$ and different α simulated by computer. In the unstable region, e.g. (a) $\alpha = 0.07$, the waveforms are unbounde d symmetrical resonant oscillations. In the region $\lambda_m < 1$, e.g. (b) $\alpha = 0.4$ and (c) $\alpha = 2.51$, the transient response asymptotically approaches zero.

region on my instability map, the fluxgate sensor will be unstable, though they explained it in a different way.

Fig. 6.3 (a) and (b) show more examples of the amplitude contours for the gradiometer and the magnetometer with the same $\eta = 0.46$. We find that they are also the same.

The unique instability map in the generalized parameter plane can represent any symmetric fluxgate sensor system. But it should be kept in mind that in order to get the same operating parameters, the value of the resistance in a loop for a gradiometer will be double of that for a magnetometer, since $j = 2$.

Fig 6.4 (a), (b), (c) and (d) illustrate the contours of multipliers corresponding to different values of the duty cycle $\eta = 0.18, 0.414, 0.50$ and 0.62, respectively. The diagrams show that when η is near 0.414, the contours parallel to the β axis are extended and straightened.

§6.2 An application

The part of the contours parallel to the β axis can be significant for the design of fluxgate sensor systems. These parts represent the cases where the multipliers are two repeated complex conjugate pairs, i.e.

$$\lambda_M = |\lambda_i| \qquad (i = 1, \ldots, 2j). \tag{6.2}$$

Substitute this into (4.33). Then

$$|\lambda|^{2j} = \exp\left[-\mathrm{tr}[\mathbf{S_j}]\frac{RT}{L_E}\right], \tag{6.3}$$

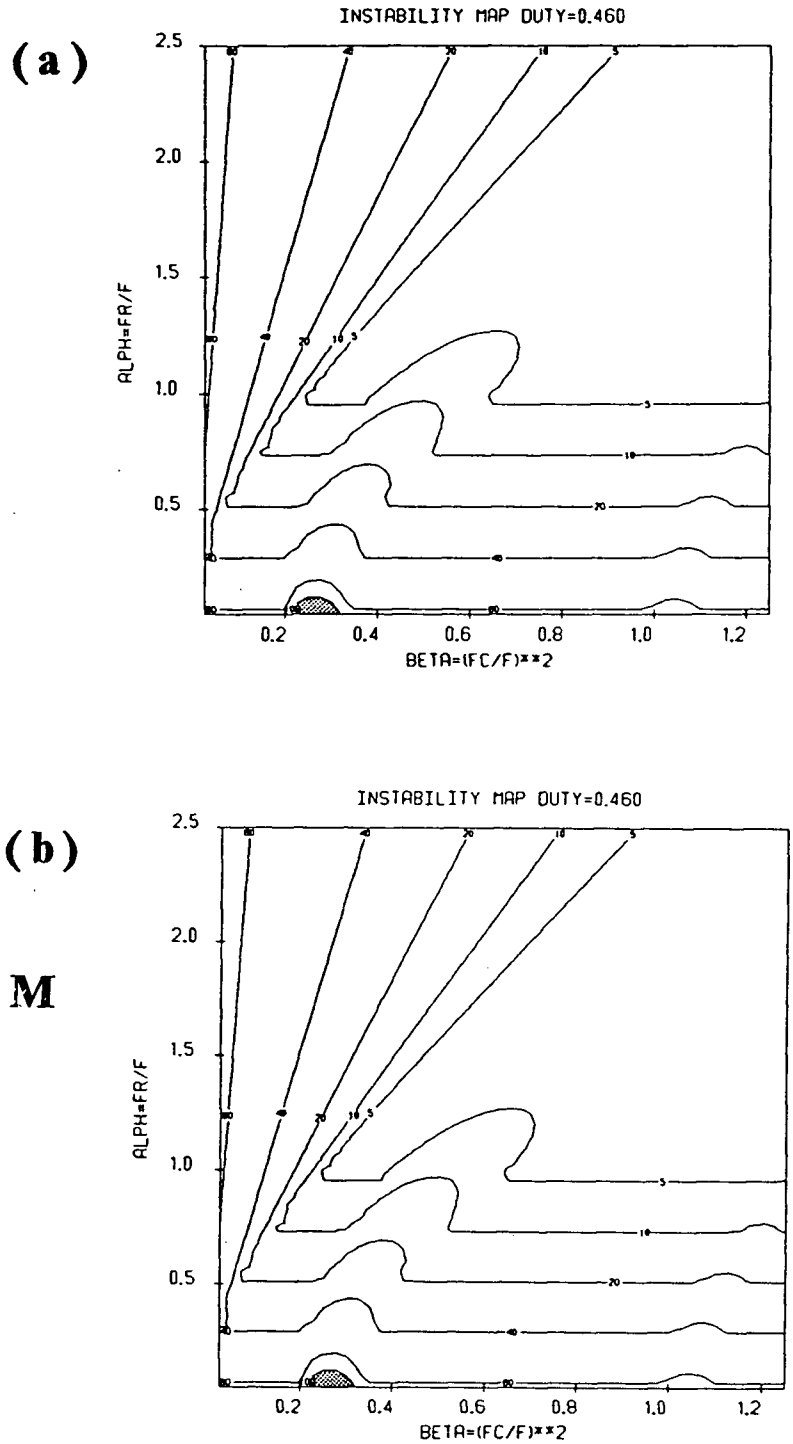

Fig.6.3 One more sample for the comparision of contours of the first multiplier, which are labeled with the amplitude multiplied by 100. Now the duty cycle $\eta = 0.46$ for (a) the gradiometer $B = 0.0$ and (b) the magnetometer. They are also the same.

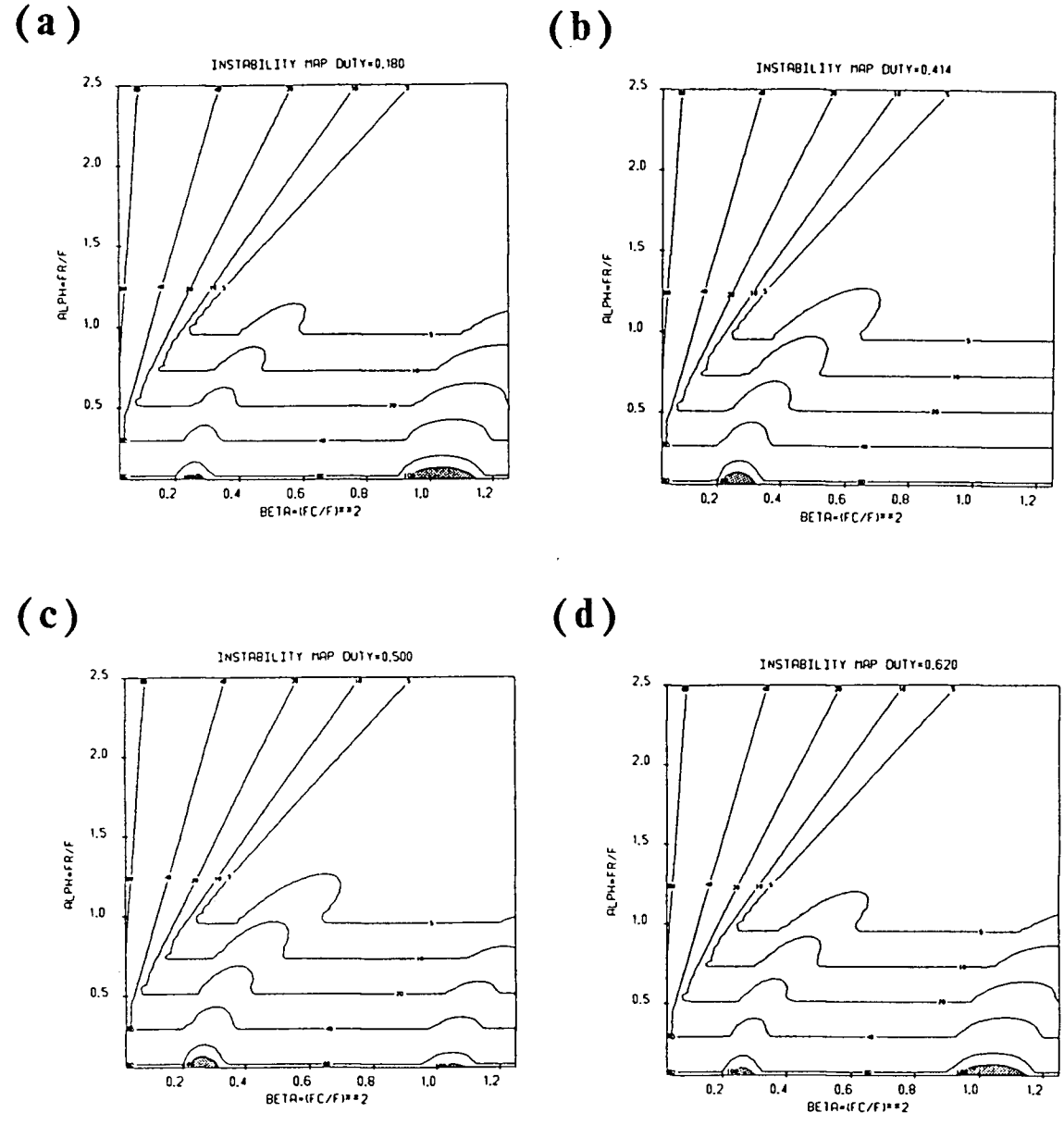

Fig.6.4 The comparision of instability maps for the gradiometer with different duty cycle: (a) $\eta = 0.18$, (b) $\eta = 0.414$, (c) $\eta = 0.50$ and (d) $\eta = 0.62$. The contours are labeled with the amplitude multiplied by 100. In (b), the unstable region near $\beta = 1$ disappears, and parts of the contours are straight.

yielding

$$\ln|\lambda| = -\left(\frac{\mathrm{tr}[\mathbf{S_j}]}{2j}\right)\frac{RT}{L_E}. \tag{6.4}$$

Equation (6.4) is useful for the design of stable fluxgate sensor systems. As I will discuss in chapter 9, the amplitudes of state variables, i.e. i, q, etc., depend on the monodromy and initial conditions, so keeping $|\lambda|$ unchanged is important for the stable operation of the fluxgate sensor in the case where temperature is varying. When we choose the operational parameters in this region, changes in C have little influence on any multiplier, λ.

Furthermore, if we proceed with expression (6.4), we can also find the way to reduce the influence of temperature on R. Assuming $R(t^\circ) = R(1 + \alpha_R t^\circ)$, then the differential temperature coefficient is

$$\frac{\partial|\lambda|}{\partial t^\circ} = -\frac{\mathrm{tr}[\mathbf{S_j}]\cdot\pi\omega_R}{2j\cdot\omega}\cdot\alpha_R\cdot|\lambda|, \tag{6.5}$$

where t° is temperature, α_R is the temperature coefficient of R.

For example, consider a fluxgate sensor loop, which includes a *shunt resistor* as load and assume the load is large compared with the resistance in the sensor winding. We assume the state variable i in the loop has the differential temperature coefficient $\sim 10^{-5}$; then we can choose the precision resistor which has the temperature coefficient $25\times 10^{-6}/degree$, also select the $\alpha = \omega_R/\omega > 0.3$ (i.e.$\lambda_M < 0.4$) and suitable C for operation at the $\lambda_M < 1$ parallel part. Of course, the final optimal parameters will be chosen with other considerations which will be discussed in the following chapters.

In the fluxgate magnetometer and gradiometer (rod) design, investigators have worked by trial and error to get stable fluxgate sensor systems and to adjust the temperature coefficient of the sensor system. These studies were very important. For example, Morris

and Pedersen's paper (1961 [6.4]) gave the experimental result that the value of shunt resistors R in gradiometers could be larger than the value in magnetometers without loss of stability. They increased the value of R to reduce the differential temperature coefficient. Now these results can be explained easily by my theory: since the $\omega_{RG} = R/2L_E$, and $\omega_{RM} = R/L_E$, the value of R for the gradiometer can be increased to twice that for a magnetometer without loss of stability.

CHAPTER 7

GENERAL SOLUTION OF THE STATE EQUATION

Thus far, we have concerned ourselves with the case of no forcing term, i.e. the homogeneous equation (3.20), which gives the stability of fluxgate sensor systems. To study the performance of fluxgate sensors in the measurement of magnetic fields or their gradient, we must deal with the state equations with a forcing term.

§7.1 Boundary condition for the existing forcing term

First of all, we should set up the boundary condition for equation (3.17) at the jumps of $\theta(t)$. There are several ways to derive the boundary condition. Appendix A-6 gives two derivations: one is based on physical principles and another uses the Delta function matching method. The results are the same, that is, the boundary condition at the jumps of $\theta(t)$ can be expressed as

$$\mathbf{x}(t_1{}^+) = \mathbf{P} \cdot \mathbf{x}(t_1{}^-) + \mathbf{u}_1, \tag{7.1}$$

$$\mathbf{x}(T^+) = \mathbf{P}^{-1} \cdot \mathbf{x}(T^-) + \mathbf{u}_2, \tag{7.2}$$

where the superscript $-$ (or $+$) refers to the moment before (or after) a jump of $\theta(t)$ and

$$\mathbf{u}_1(t) \triangleq (\mathbf{I}_{2j} - \mathbf{P}) \cdot \begin{pmatrix} \mathbf{o}_j \\ \frac{1}{L}\mathbf{S}_j \mathbf{a}_j \end{pmatrix},$$

$$\mathbf{u}_2(t) \triangleq (\mathbf{I}_{2j} - \mathbf{P}^{-1}) \cdot \begin{pmatrix} \mathbf{o}_j \\ \frac{1}{L}\mathbf{S}_j \mathbf{a}_j \end{pmatrix}.$$

Obviously, the expressions (4.48) and (4.49) are the particular cases of (7.1) and (7.2) with $\mathbf{a}_j = 0$.

§7.2 General solution with forcing term

In the derivation of the boundary matrices [cf: §4.4], I used the well known piecewise-integral method, that is, the state equation (3.20) for each piece, where $\theta(t)$ is constant and $\mathbf{A}(t)$ also is a constant matrix, can be solved from the initial value of the state variables at the beginning of each piece. At the jumps of $\theta(t)$, however, we utilize the boundary condition to continue the solution by multiplying with the boundary matrices. Using such a procedure, we can project the solution from the initial condition to any moment.

Now let us extend this procedure to the state equation (3.17) which has a forcing term. The task at hand is to determine the solution expression in each $\theta(t)$ = constant piece for equation (3.17). Recall (3.18) and (3.19), namely,

$$\mathbf{A}(t) = \begin{pmatrix} \mathbf{O_j} & \mathbf{I_j} \\ -\frac{1}{\theta LC}\mathbf{S_j} & -(\frac{\theta'}{\theta}\mathbf{I_j} + \frac{R}{\theta L}\mathbf{S_j}) \end{pmatrix}, \tag{3.18}$$

$$\mathbf{f}(t) = \frac{\theta'}{\theta\, L}\begin{pmatrix} \mathbf{o}_j \\ \mathbf{S_j}\,\mathbf{a}_j \end{pmatrix}. \tag{3.19}$$

If $\theta(t)$ is constant, $\theta'(t)$ and $\mathbf{f}(t)$ are zero. So (3.17) becomes the same as (3.20) which we already have solved in §4.4 . The solution in the $\theta = 1$ piece is expression (4.37)

$$\mathbf{x}(t) = \exp\left[(t-\tau)\mathbf{W}\right]\cdot\mathbf{x}(\tau), \tag{7.3}$$

and in the $\theta = 1/p$ piece is expression (4.40). The vector expression will be

$$\mathbf{x}(t) = \exp\left[(t-\tau)\mathbf{PW}\right] \cdot \mathbf{x}(\tau). \tag{7.4}$$

Using (7.1), (7.2) (7.3) and (7.4), we can iteratively calculate the state variables at any time. Here I give some examples:

1. The forced solution at t_1^+,

$$\mathbf{x}(t_1^+) = \mathbf{P} \cdot \exp\left[(1-\eta)T\mathbf{W}\right] \cdot \mathbf{x}(0) + \mathbf{u}_1. \tag{7.5}$$

2. The forced solution at T,

$$\begin{aligned} \mathbf{x}(T) &= \mathbf{P}^{-1} \cdot \exp\left[\eta T\mathbf{PW}\right] \cdot \mathbf{x}(t_1^+) + \mathbf{u}_2 \\ &= \mathbf{X}(T) \cdot \mathbf{x}(0) + \mathbf{P}^{-1} \cdot \exp\left[\eta T\mathbf{PW}\right] \cdot \mathbf{u}_1 + \mathbf{u}_2, \end{aligned} \tag{7.6}$$

where $\mathbf{X}(T)$ is the monodromy [cf: (4.29)].

3. The forced solution at $(T + t_1^+)$,

$$\mathbf{x}(T + t_1^+) = \mathbf{P} \cdot \exp\left[(1-\eta)T\mathbf{W}\right] \cdot \mathbf{x}(T) + \mathbf{u}_1. \tag{7.7}$$

§7.3 The initial condition

As we emphasized several times before, the solution of the state variables depends not only on the coefficients of the state equation, but also on the initial values of the state variables, i.e. the initial condition.

The assumption of an initial condition which is not realized in any real physical system may lead to an absurd conclusion. Also any assumption about the initial condition reduces generality from the mathematical point of view, which should be avoided.

During the study of the transient solution, we used the concept of the matrizant which associates an initial condition $\mathbf{X}(0) = \mathbf{I_{2j}}$. The reason is not only that it is unique and easily solved, but also according to (4.10), i.e. $\mathbf{x}(t) = \mathbf{X}(t,\tau)\cdot\mathbf{x}(\tau)$, we can calculate the state variables from the matrizant for the solution with any initial condition [cf: §4.1].

Now we study the state equation (3.17) which has a forcing term. We will also focus the *quiescent* case, i.e. $\mathbf{x}(0) = 0$ case, and the *trivial solution*, i.e. the solution under the quiescent case.

The reason is not only that the fluxgate sensor system is a causal system, i.e. a real quiescent system physically, but also if the trivial solution of the state equation with forcing term and the matrizant is known, the solution for an arbitrary initial condition can be determined. An intuitive elucidation of this fact is given in Appendix A-2.

For example, the trivial solution at T can be obtained from expression (7.6) of the previous section under the quiescent case. It is

$$\mathbf{x}_q(T) = \mathbf{P}^{-1}\cdot\exp\left[\eta T\mathbf{PW}\right]\cdot\mathbf{u}_1 + \mathbf{u}_2. \tag{7.8}$$

§7.4 Q, I waveforms for the magnetometer and the gradiometer

Using the foregoing procedure, I have plotted a variety of waveforms by computer simulation for a magnetometer and a gradiometer. Fig. 7.1 (a), (b) and (c) give Q and I waveforms which have the same operating parameters as Fig. 6.2 (a), (b) and (c), but where an external magnetic field exists and the initial condition is quiescent. Obviously, the waveforms of either Q or I are unbounded, i.e. unstable, when the operative parameters are located in the unstable region.

To demonstrate the stable waveform in detail, Fig. 7.2 (a), (b) give more examples with $\alpha = 1.0$ and $\alpha = 1.65$, respectively.

The waveforms of the gradiometer are similar. Fig. 7.3, 7.4 and 7.5 show some samples for a stable gradiometer with $\alpha = 0.4$, 1.0 and 1.62, respectively. As the unstable waveforms are similar to those of the magnetometer, I have not included them here.

Fig. 7.2 - Fig. 7.5 clearly show that when the sensor is operating in a stable region, the state variables are converging to a periodic waveform. If α is increased, not only is the magnitude of the current waveforms decreased, but they also appear more impulsive. In other words, they have more high order harmonic components.

These waveforms not only help to understand the stable operation, but also give us useful information for practical design. One result is that we should choose smaller α in the stable region, since larger α corresponds to a current with more high order harmonic components, a less useful signal. Another result is the response time of the fluxgate sensor. We can simulate the transient waveform as in Fig. 6.2 (b) for the parameters of a real design to find the response time. Alternatively, we can get the response time from the simulation for the quiescent case with a forcing term. For example, from Fig. 7.2 (a)

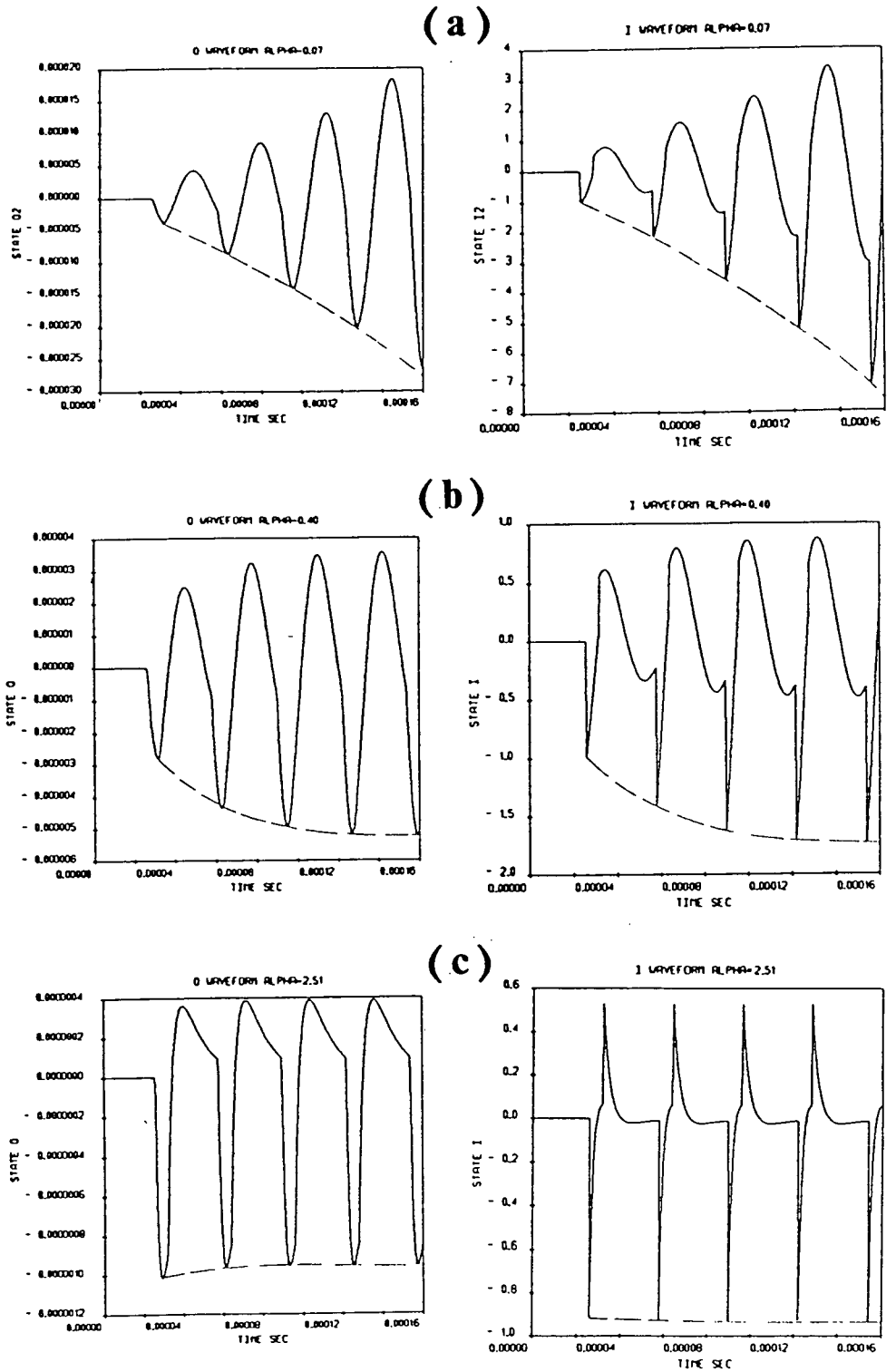

Fig. 7.1 The Q and I waveforms in the forcing case with quiescent initial condition for a magnetometer. The operative parameters are as $\beta = 0.98$ and (a) $\alpha = 0.07$ (unstable), (b) $\alpha = 0.40$ and (c) $\alpha = 2.51$ (asymptotically stable). The dashed line is the envelope of the waveform.

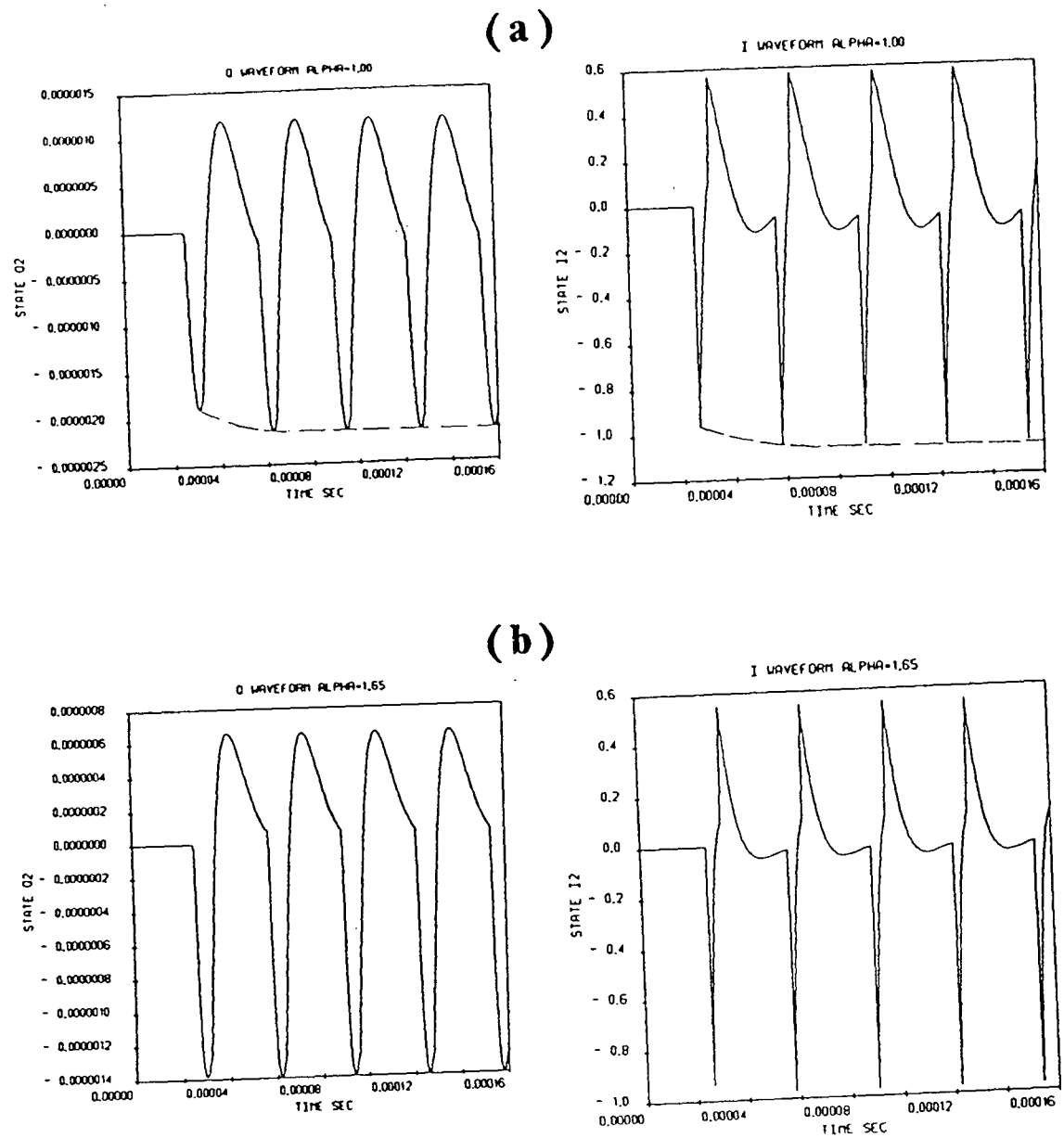

Fig. 7.2 The Q and I waveforms in the forcing case with quiescent initial condition for a magnetometer which works in stable region and has $\beta = 0.98$ and (a) $\alpha = 1.0$, (b) $\alpha = 1.65$. The dashed line is the envelope of the waveform.

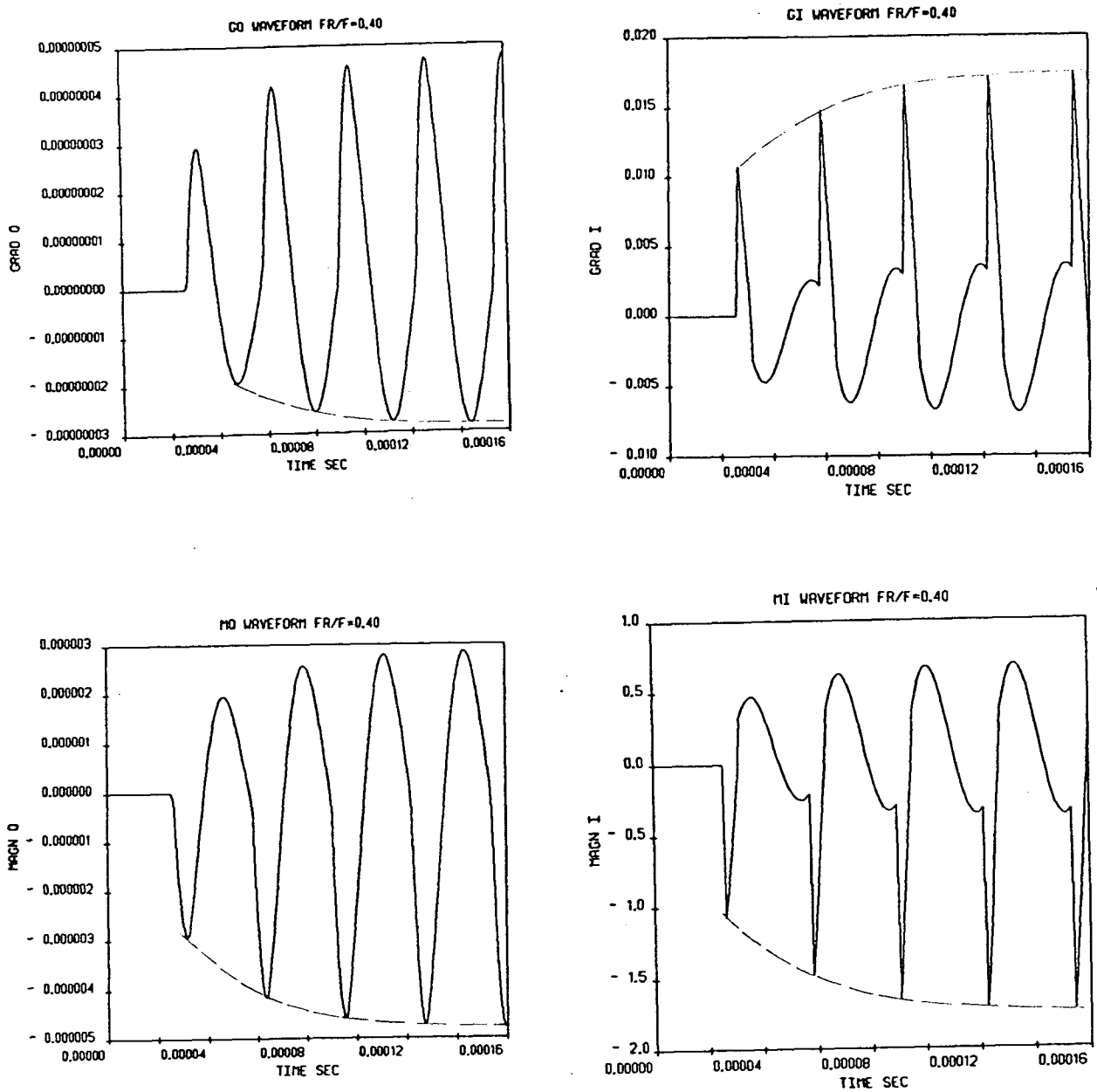

Fig. 7.3 The state variables waveforms in the forcing case with quiescent initial condition for a stable gradiometer ($\beta = 0.98$, $\alpha = 0.4$), where GQ and GI present q and i in the gradient loop; and MQ and MI present Q and I in the magnetic field loop. The dashed line is the envelope of the waveform.

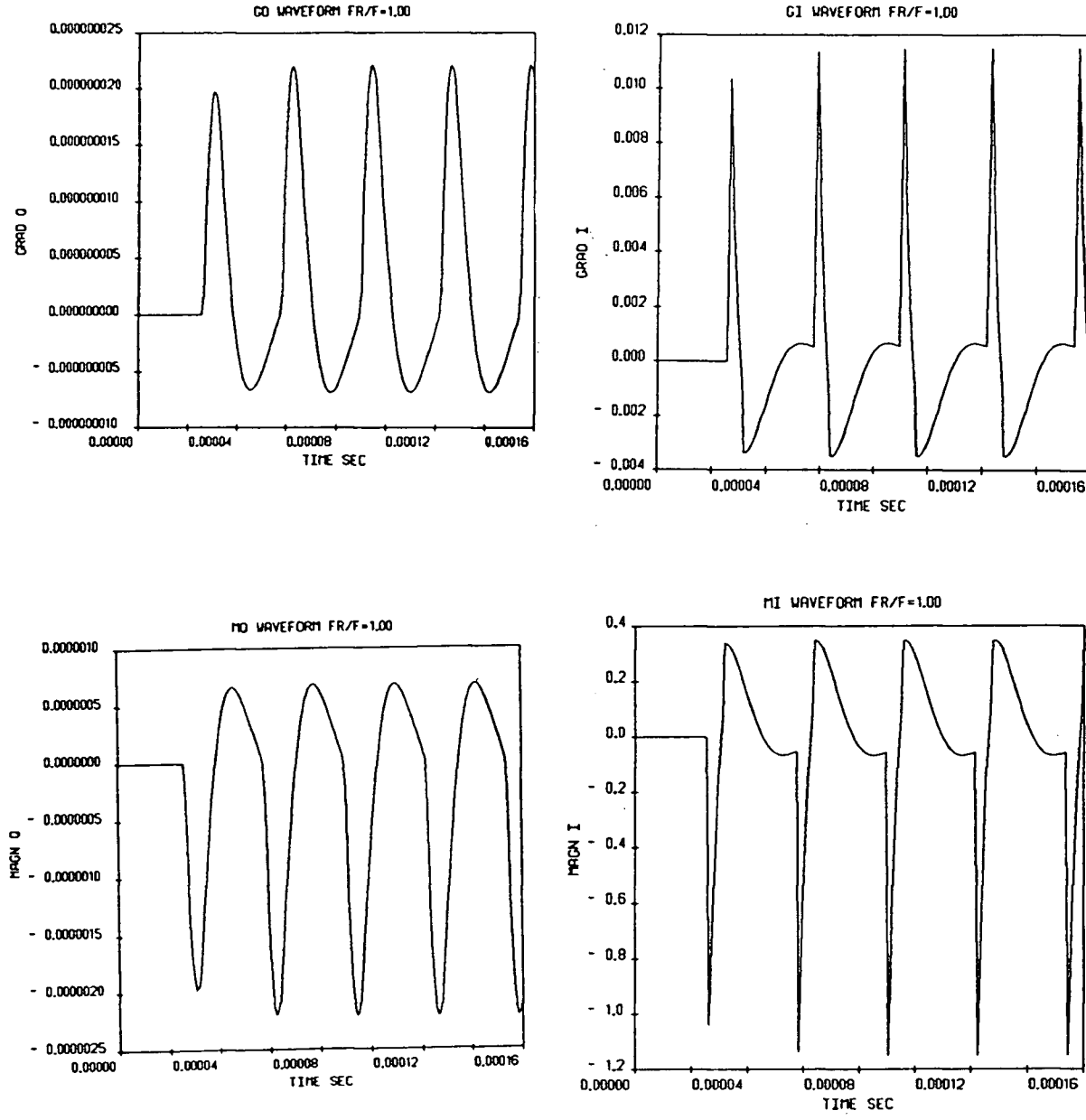

Fig. 7.4 The state variables waveforms in the forcing case with quiescent initial condition for a stable gradiometer ($\beta = 0.98$, $\alpha = 1.0$), where GQ and GI present q and i in the gradient loop; and MQ and MI present Q and I in the magnetic field loop.

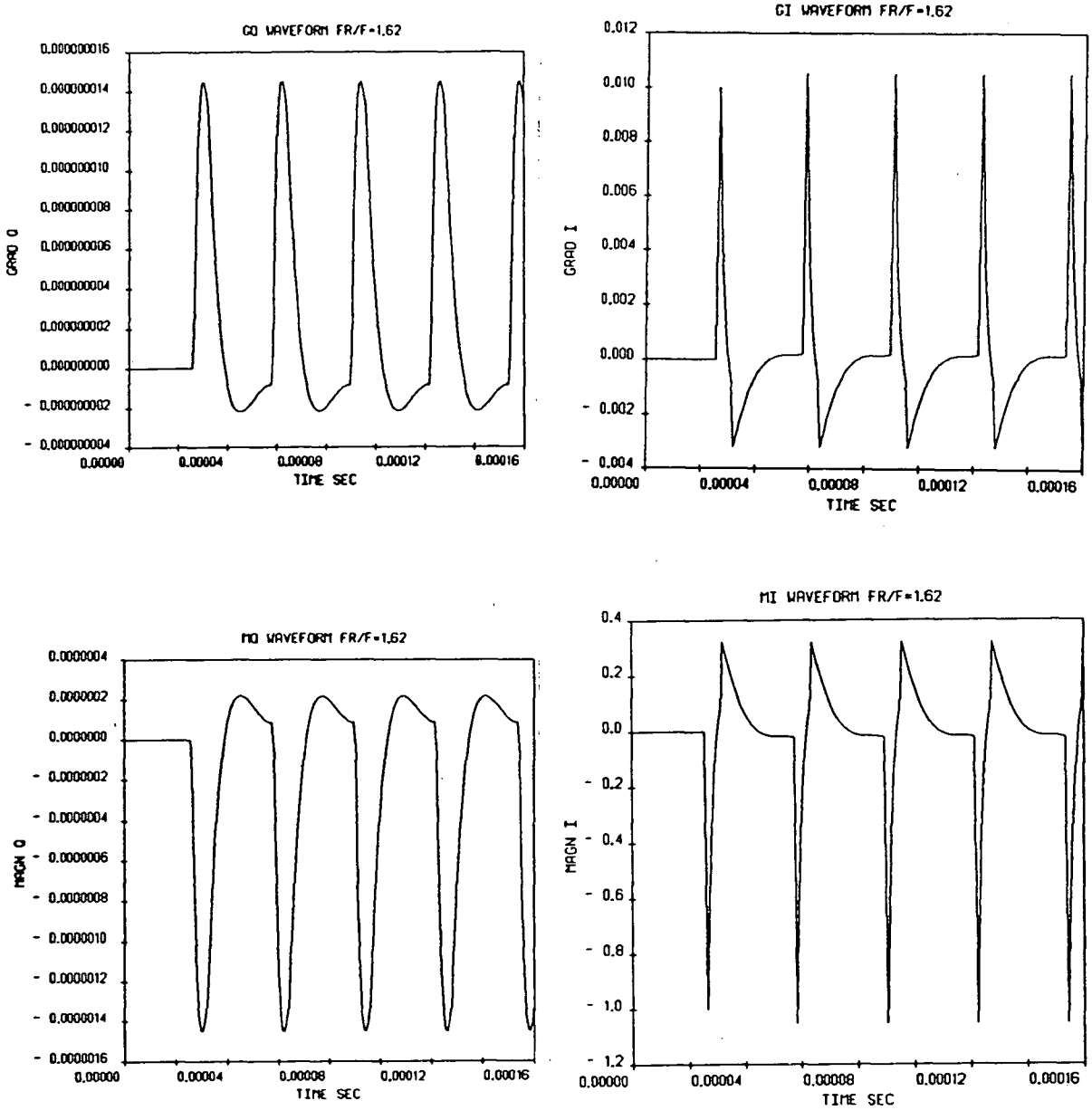

Fig. 7.5 The state variables waveforms in the forcing case with quiescent initial condition for a stable gradiometer ($\beta = 0.98$, $\alpha = 1.62$), where GQ and GI present q and i in the gradient loop; and MQ and MI present Q and I in the magnetic field loop.

and (b), we observe that if $\omega_R/\omega > 1$, the transient behaviour almost disappears after 4 periods.

CHAPTER 8

STUDY VIA PHASE SPACE

The phase space is a powerful concept for systems study, regardless of whether the system is linear or nonlinear, time-variant or time-invariant [8.1]. It not only describes both the local and global behavior of a system, but also provides an exact topological portrait of possible motions of the system under different operating conditions.

The advent of modern computer techniques has led to sketching in phase space losing fashion; that method in the past was an important tool for the study of the behaviour of many second order differential equations. In the present chapter, the reader will see that by computer simulation the various trajectories in phase space for the time-variant fluxgate state equation can be obtained quickly and that this leads to useful results.

A *phase plane* or *state plane*, i.e. second order phase space, has $x_2 = x_1'$ as ordinate, x_1 as abscissa and time as a parameter on a trajectory. A *limit cycle*, i.e. a closed trajectory, corresponds to a periodic solution.

Let us first examine the basic characteristics of the phase plane for fluxgate sensor systems.

§8.1 The equilibrium position

As we discussed before, we may assume $B = 0$ in the state equation (3.17) without loss of generality. Then $\mathbf{S_j} = \frac{1}{j} \cdot \mathbf{I_j}$ and the state equation becomes

$$\mathbf{x}' = \begin{pmatrix} \mathbf{O_j} & \mathbf{I_j} \\ -\frac{1}{jLC\theta}\mathbf{I_j} & -\left(\frac{\theta'}{\theta} + \frac{R}{jL\theta}\right)\mathbf{I_j} \end{pmatrix} \mathbf{x} + \frac{\theta'}{jL\theta} \begin{pmatrix} \mathbf{o}_j \\ \mathbf{a}_j \end{pmatrix}. \tag{8.1}$$

Thus the system with $j = 2$ can be regarded as two similar separable systems with $j = 1$ of which each could be expressed as

$$x_1{}' = x_2, \tag{8.2}$$

$$x_2{}' = -r_1(t)x_1 - r_2(t)x_2 + h_i(t), \tag{8.3}$$

where subscript i is the index of a loop and

$$r_1(t) \triangleq \frac{1}{jLC\theta}, \tag{8.4}$$

$$r_2(t) \triangleq \frac{\theta'}{\theta} + \frac{R}{jL\theta}, \tag{8.5}$$

$$h_i(t) \triangleq \frac{\theta'}{jL\theta} \cdot a_i. \tag{8.6}$$

The slope of trajectories in the phase plane is

$$\frac{dx_2}{dx_1} = \frac{x_2'}{x_1'} = \frac{-r_1(t)x_1 - r_2(t)x_2 + h_i(t)}{x_2}. \tag{8.7}$$

At the $x_1' = x_2' = 0$ point, the slope is undefined. Such a point is a *singular point* or an *equilibrium position* [8.2]. According to the theorem of Lagrange-Diric hlet [8.3], the equilibrium position corresponds to a relative minimum of potential energy.

For the state equation (3.20) without forcing term, $h_i(t) = 0$, we substitute $x_1' = x_2' = 0$ into (8.2) and (8.3), and note that if $\theta \neq 0$ everywhere, then the only equilibrium position is the one at $x_1 = x_2 = 0$ or $\mathbf{x} = 0$.

If the forcing term is non-zero, we have equations

$$x_1' = x_2 = 0, \tag{8.8}$$

$$x_2' = -r_1(t)x_1 - r_2(t)x_2 + h_i(t) = 0, \tag{8.9}$$

Substitution of (8.8) into (8.9) yields

$$x_1 = \frac{h_i(t)}{r_1(t)} = \theta' \cdot C \cdot a_i. \tag{8.10}$$

Since the fluxgate sensor system is a causal system, the starting moment $t_0 = 0^+$, $\theta(0^+) =$ constant, and $\theta'(0^+) = 0$. This means that the point $\mathbf{x} = 0$ remains as the equilibrium position.

If we use the Lagrange-Diric hlet theorem and solve the Lagrange conservation equation [cf: §**A-1** (A.1)] for fluxgate sensor systems, we will get the same result; that is, the $x_1 = x_2 = 0$ point corresponds to a relative minimum of potential energy, i.e. an equilibrium position.

The above discussion supplies more evidence to show that my choice of the initial condition as $\mathbf{x} = 0$ is reasonable.

§8.2 Trajectories without the forcing term

In the last chapter, I presented the equations (7.1)–(7.4) which can be used to iteratively calculate the state variables. By setting $\mathbf{a} = 0$ (i.e. without forcing) and using computer simulation, I can draw trajectories with different initial conditions in the phase plane for a fluxgate sensor system with $j = 1$.

1. Unstable region

Fig. 8.1 shows trajectories with operative parameters in the unstable region, where (a) has initial condition model 1 ($x_1 = 1, x_2 = 0$) and (b) has model 2 ($x_1 = 0, x_2 = 1$).

Arrows on a trajectory denote the direction of increasing time. The trajectory of (a) is diverging to equilibrium with increasing time; and obviously it is unstable. The trajectory of (b) appears to be converging with increasing time, and thus one might think this model were stable, but it is not!

If we trace the trajectory of Fig. 8.1 (b) carefully, we will find that it does not converge to the equilibrium position $\mathbf{x} = 0$, so it should be unstable.

So, if we had not plotted trajectory for a long enough time, where "enough" is difficult to determine, it would have lead to wrong conclusions. This gives us reason for caution not only for phase plane studies, but also for most computer simulations.

In fact, as I emphasized before, model 1 and model 2 constitute the $\mathbf{X}(0) = \mathbf{I}$ matrix for the calculation of the matrizant. Neither model 1 nor model 2 ever **solely** appear as a causal initial condition.

Let us move the trajectory of model 2 into the center of the trajectory of model 1. It is found that they are just different parts of the same trajectory. According to the Bendixon theorem [8.1], there is a limit cycle between the two parts, i.e. there is a periodic solution of equation (3.20) in the unstable region. But it is an unstable and unrealistic solution, because trajectories originating from inside or outside the limit cycle diverge from it. This warns us that when we calculate a periodic solution, we should also examine its stability.

2. Stable region

On the contrary, the trajectories with operative parameters in the $\lambda_M < 1$ region all converge to the equilibrium position. Fig. 8.2 gives some examples which show that they are stable. The operative parameters and initial conditions are as: (a) $\alpha = 0.40; x_1 = 1, x_2 = 0$; (b) $\alpha = 0.40; x_1 = 0, x_2 = 1$; (c) $\alpha = 1.00; x_1 = 1, x_2 = 0$; (d) $\alpha = 1.00; x_1 = 0, x_2 = 1$.

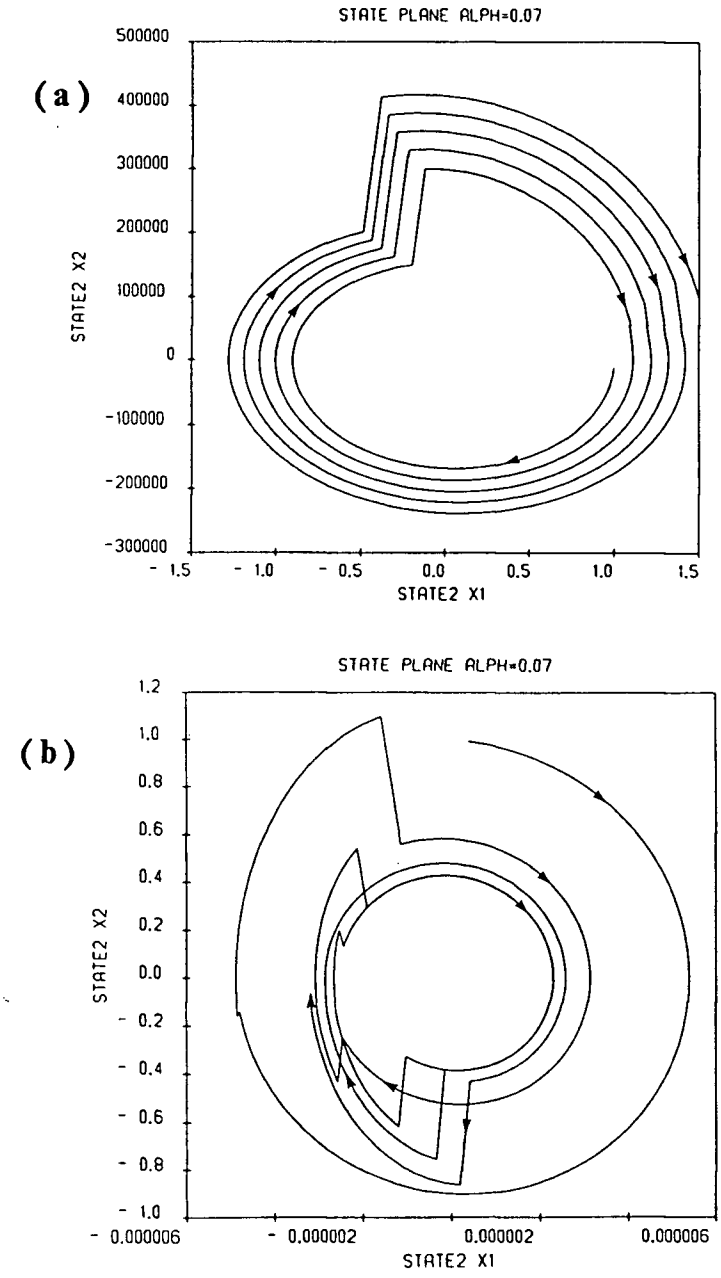

Fig. 8.1 The free trajectories with operative parameters in the unstable region, where (a) has initial condition model 1 ($x_1 = 1, x_2 = 0$) and (b) has model 2 ($x_1 = 0, x_2 = 1$). Trajectories aren't converging to equilibrium with increasing time. The arrows indicate the direction of motion of trajectory for increasing time.

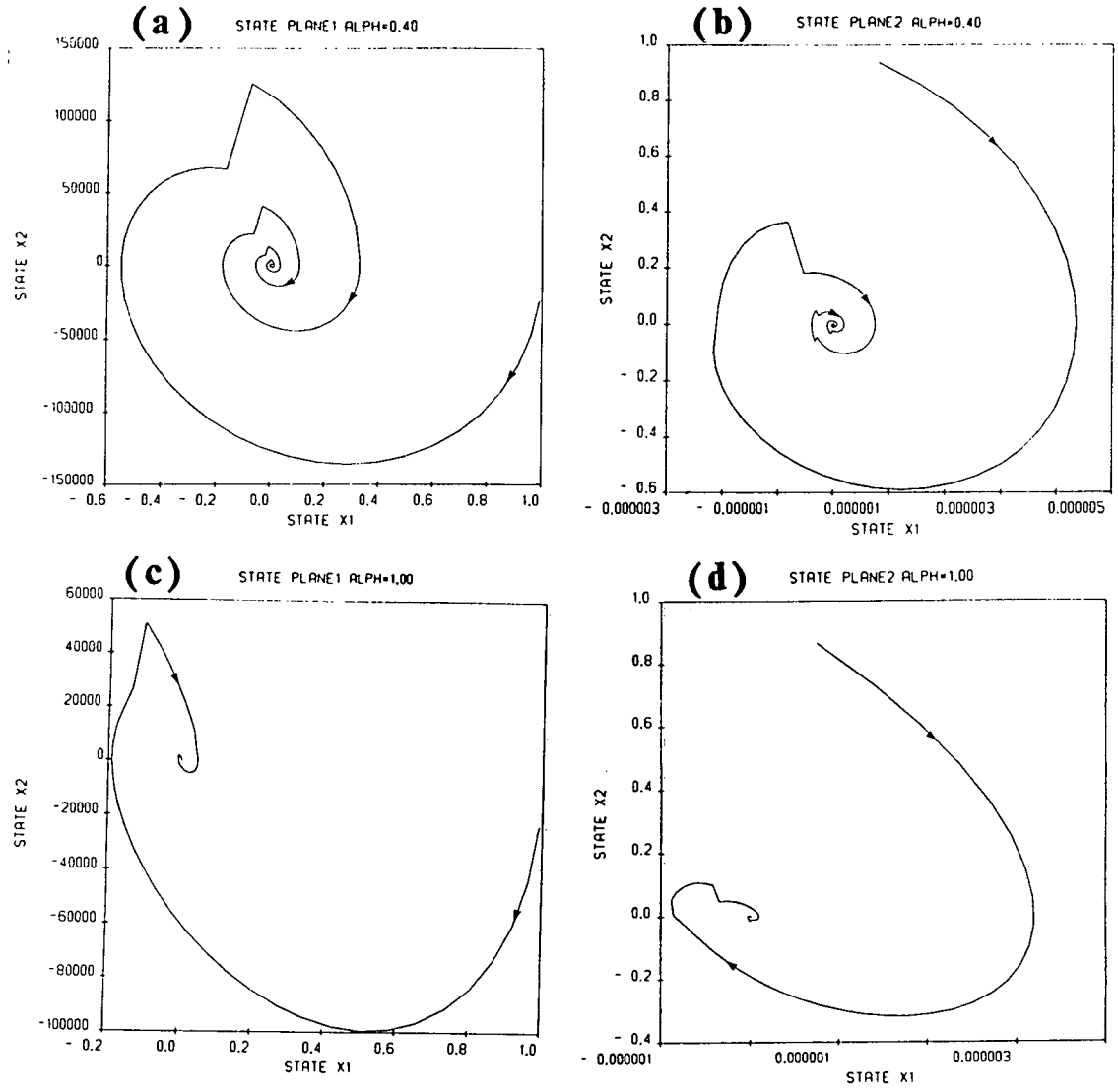

Fig. 8.2 The free trajectories with operative parameters in the $\lambda_M < 1$ region all converge to the equilibrium position. The operative parameters and initial conditions are: (a) $\alpha = 0.40; x_1 = 1, x_2 = 0$; (b) $\alpha = 0.40; x_1 = 0, x_2 = 1$; (c) $\alpha = 1.00; x_1 = 1, x_2 = 0$; (d) $\alpha = 1.00; x_1 = 0, x_2 = 1$. The arrows indicate the direction of motion of the trajectory for increasing time.

§8.3 Trajectories with the forcing term

Alternatively, here in Fig. 8.3 - Fig. 8.4 I plot trajectories for the $j = 2$ fluxgate sensor system with different operative parameters, where (a) $x_1 = q, x_3 = i$ for the gradient loop; (b) $x_2 = Q, x_4 = I$ for the magnetic field loop. They are simulated by computer using (7.1)-(7.4) and are the quiescent case, $\mathbf{x} = 0$.

Fig. 8.3 shows trajectories for the unstable region. They clearly show that with increasing time, trajectories depart from the equilibrium position. They are unstable. Thus proper initial conditions are important for the phase space study.

Fig. 8.4 gives an example where the gradiometer works with proper parameters; each trajectory converges to a limit cycle to represent the periodic current which depends on the magnitude of the forcing term (i.e. the magnetic fields). We will study the periodic solution in the next chapter.

For $j = 1$ the fluxgate sensor system has similar trajectories. Fig. 8.5 (a), (b), (c) and (d) give several examples for different operative parameters.

If the instability map on the parameter plane were a clear portrait of the stability in the parameter domain, now the present trajectories on phase plane demonstrate the stable behaviour of fluxgate sensor systems in the time domain. This means that the forgoing conclusions about stability are correct either locally, or globally.

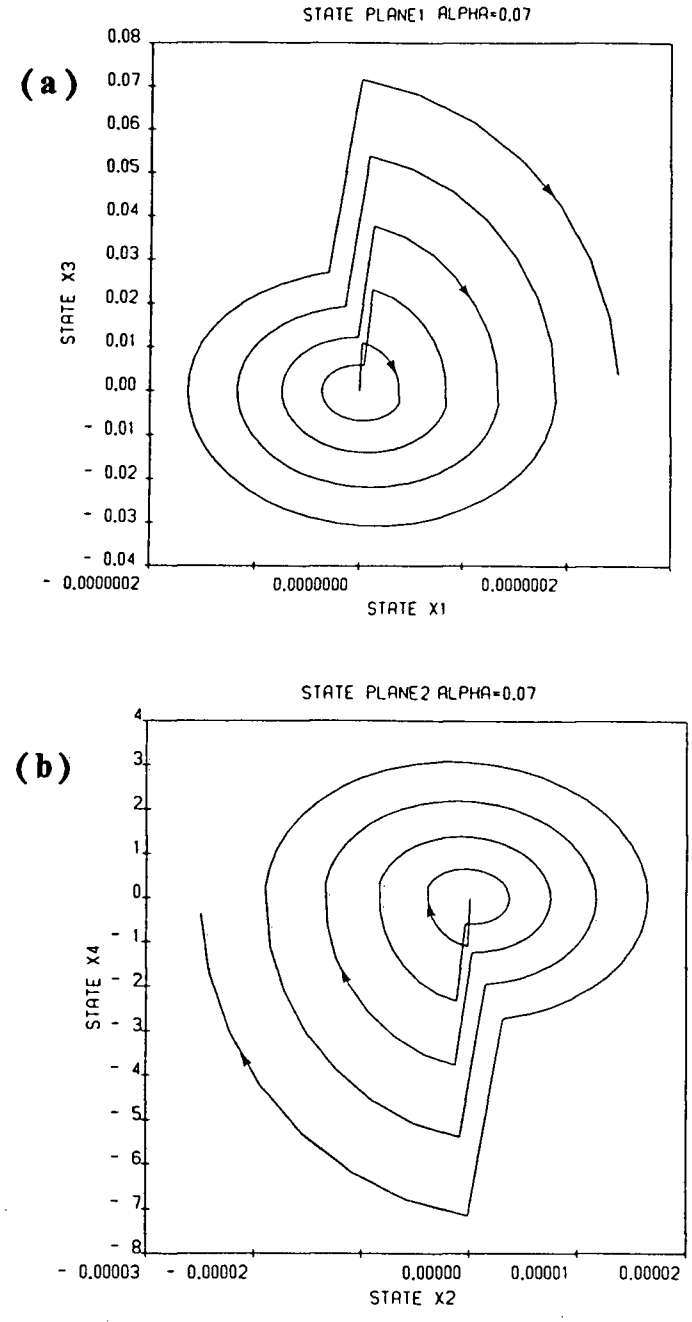

Fig. 8.3 The forcing trajectories in the unstable region for the gradiometer. (a) is for the gradient loop, i.e. $x_1 = q, x_3 = i$, and (b) is for the magnetic field loop, $x_2 = Q, x_4 = I$. The arrows indicate the direction of motion of the trajectory for increasing time.

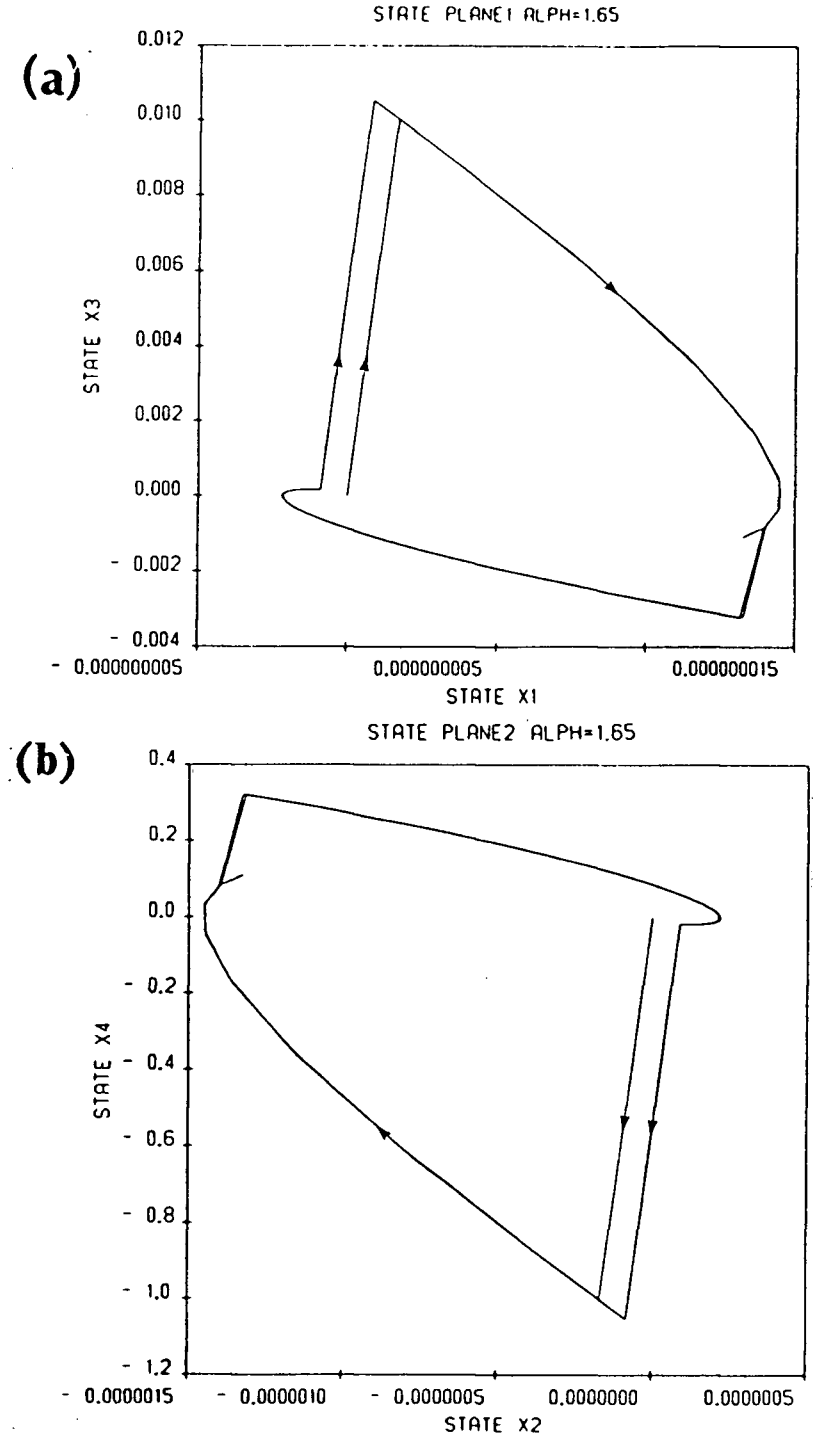

Fig. 8.4 The forcing trajectories for stable region for the gradiometer. (a) is for the gradient loop, i.e. $x_1 = q, x_3 = i$, and (b) is for the magnetic field loop, $x_2 = Q, x_4 = I$. Every trajectory converges to a limit cycle, i.e. periodic solution. The arrows indicate the direction of motion of the trajectory for increasing time.

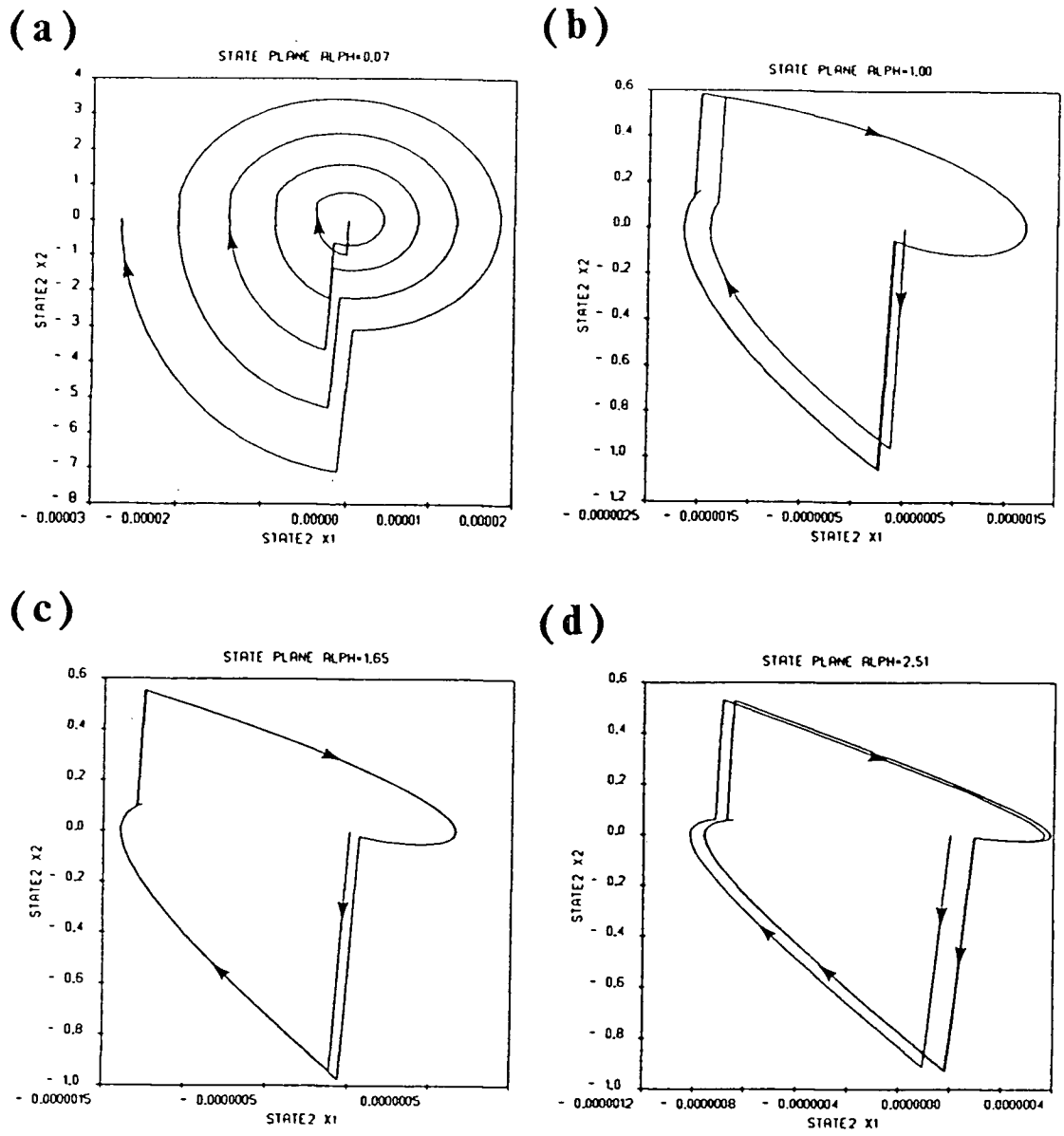

Fig. 8.5 The forcing trajectories for a magnetometer with the quiescent initial condition and different operative parameters. (a) in the unstable region, it is clearly unstable; (b), (c) and (d) are in the stable region, the trajectories converge to a limit cycle. The arrows indicate the direction of motion of the trajectory for increasing time.

CHAPTER 9

SENSITIVITY AND CHOICE OF PARAMETERS

In this chapter, the periodic solution is solved for the fluxgate sensor systems, and then the concept of sensitivity is defined and studied. The general sensitivity map and the analysis of the influence of each parameter are discussed in detail, which provides a guide for the selection of operating parameters and components for practical design.

§9.1 Periodic solution

As the last section has shown, if a fluxgate sensor system works stably in the forced case, the trajectory converges to a limit cycle, i.e. there is a periodic current flowing in the sensor loop. Now let us solve the periodic solution for the state equation (3.17) which has a forcing term.

Since the periodic solution exists, then for any $t \geq 0$ the periodic solution satisfies the relation

$$\mathbf{x}_p(t+T) = \mathbf{x}_p(t). \tag{9.1}$$

At $t = 0$, we have the periodic condition

$$\mathbf{x}_p(T) = \mathbf{x}_p(0). \tag{9.2}$$

Recall the expression of $\mathbf{x}(t)$ (7.6) for the general solution with an arbitrary initial value $\mathbf{x}(0)$

$$\mathbf{x}(T) = \mathbf{X}(T) \cdot \mathbf{x}(0) + \mathbf{P}^{-1} \cdot \exp\left[\eta T \mathbf{P} \mathbf{W}\right] \cdot \mathbf{u}_1 + \mathbf{u}_2. \tag{9.3}$$

Substitution of the periodic condition (9.2) into (9.3) yields,

$$\mathbf{x}_p(0) - \mathbf{X}(T) \cdot \mathbf{x}_p(0) = \mathbf{P}^{-1} \cdot \exp\left[\eta T \mathbf{P}\mathbf{W}\right] \cdot \mathbf{u}_1 + \mathbf{u}_2,$$

or

$$\mathbf{x}_p(0) = \left[\mathbf{I} - \mathbf{X}(T)\right]^{-1} \cdot \left(\mathbf{P}^{-1} \cdot \exp\left[\eta T \mathbf{P}\mathbf{W}\right] \cdot \mathbf{u}_1 + \mathbf{u}_2\right). \tag{9.4}$$

Applying the general solution expression (7.3) to the interval $(0, t_1^-)$ and subsitituting (9.4) in it, we obtain

$$\begin{aligned} \mathbf{x}_p(t) &= \exp\left[(t-0)\mathbf{W}\right] \cdot \mathbf{x}_p(0) \\ &= \exp\left[(t-0)\mathbf{W}\right] \left[\mathbf{I} - \mathbf{X}(T)\right]^{-1} \\ &\quad \cdot \left(\mathbf{P}^{-1} \cdot \exp\left[\eta T \mathbf{P}\mathbf{W}\right] \cdot \mathbf{u}_1 + \mathbf{u}_2\right). \end{aligned} \tag{9.5}$$

At t_1^+,

$$\begin{aligned} \mathbf{x}_p(t_1^+) &= \mathbf{P} \cdot \exp\left[(1-\eta) T \mathbf{W}\right] \left[\mathbf{I} - \mathbf{X}(T)\right]^{-1} \\ &\quad \cdot \left(\mathbf{P}^{-1} \cdot \exp\left[\eta T \mathbf{P}\mathbf{W}\right] \cdot \mathbf{u}_1 + \mathbf{u}_2\right) + \mathbf{u}_1. \end{aligned} \tag{9.6}$$

Similarly, applying (7.4) to (t_1^+, T^-), we obtain

$$\mathbf{x}_p(t) = \exp\left[(t - t_1)\mathbf{P}\mathbf{W}\right] \cdot \mathbf{x}_p(t_1^+) \tag{9.7}$$

Finally at T, we have

$$\mathbf{x}_p(T) = \mathbf{x}_p(0). \tag{9.8}$$

These equations (9.4)-(9.8) can be utilized to calculate the periodic solution for stable fluxgate sensor systems.

Fig. 9.1 (a) and (b) plot two samples of periodic solutions which were simulated by computer with equations (9.4)-(9.8) for a stable magnetometer. Comparing Fig. 9.1 to the waveforms of the general solution in Fig. 7.2, we find, as expected, that the periodic solutions have exactly the same waveform after the transient behaviour has disppeared.

Note that, the periodic solution always contains the term of $[\mathbf{I} - \mathbf{X}(T)]^{-1}$ which acts as a scale and has larger magnitude with larger monodromy. This will help us understand why a smaller ω_R/ω is associated with larger amplitude of the waveform, and is one reason why keeping $|\lambda|$ unchanged is important for the stable operation.

§9.2 Sensitivity of fluxgate sensor systems

For any measurement, the sensitivity is an important performance index. I define the *sensitivity* of a fluxgate sensor as the ratio of the second harmonic magnitude of the current in the sensor loop to the value of the external excitation. For instance, the sensitivity of the magnetometer sensor can be expressed as

$$S_m = \frac{i_{smm}}{(\mathbf{H}_1 \cdot \mathbf{K}_1)}, \tag{9.9}$$

and for the gradiometer, it is

$$S_g = \frac{i_{sgm}}{|(\mathbf{H}_2 \cdot \mathbf{K}_2) - (\mathbf{H}_1 \cdot \mathbf{K}_1)|}, \tag{9.10}$$

where $\mathbf{K}_i$ is a sensor coil constant [cf: §3.1].

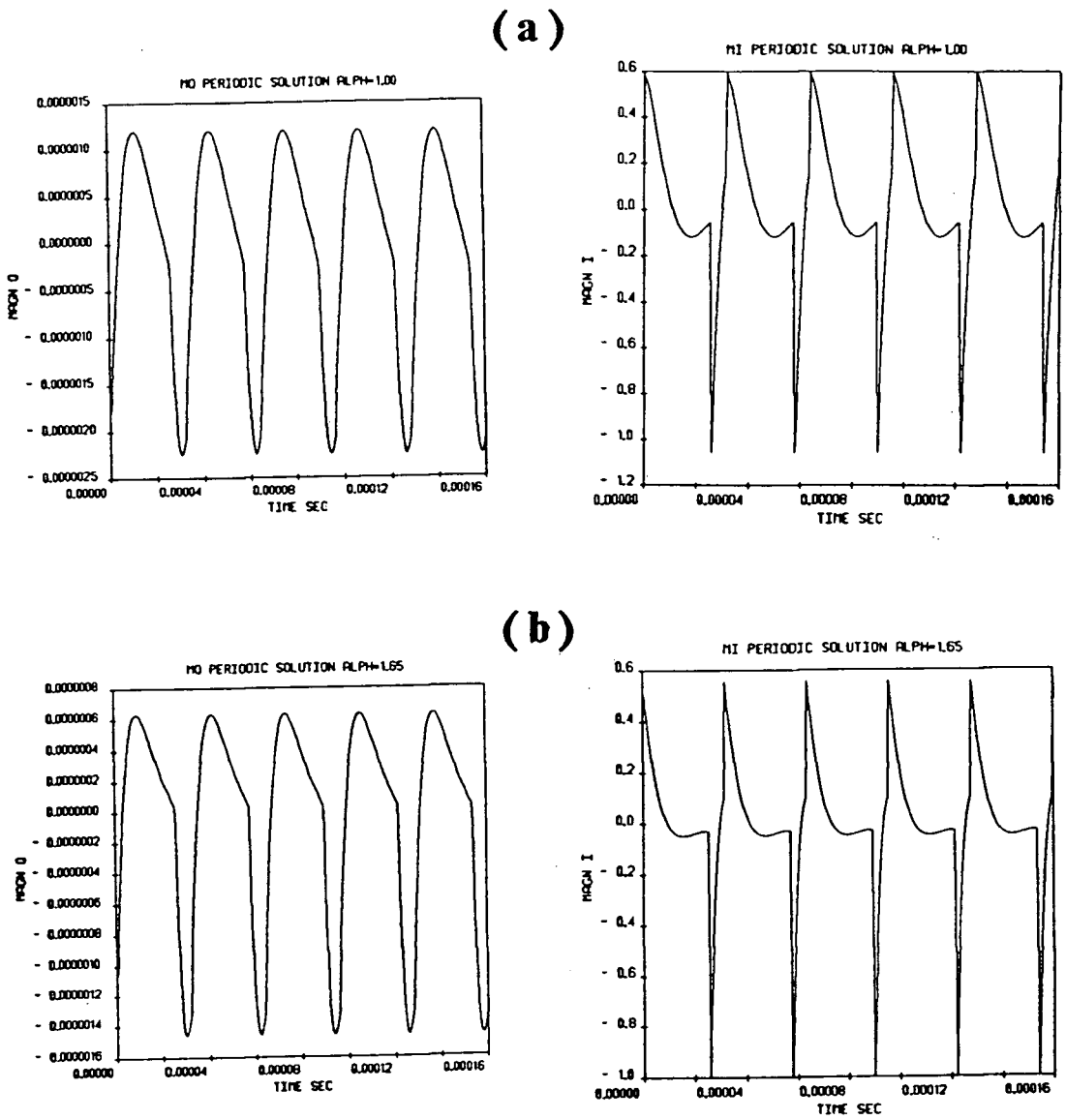

Fig. 9.1 The Q and I waveforms of the periodic solution for a stable magnetometer in the forcing case. The operating parameters are $\beta = 0.98$ and (a) $\alpha = 1.0$, (b) $\alpha = 1.65$.

The merit of this definition is that the second harmonic current is the exact signal that we would like to measure, and also the output signal of the sensor can be easily calculated from the sensitivity with the given value of the excitation (magnetic field or gradient).

§9.3 Sensitivity map on the parameter plane

Fig. 9.2 presents several sensitivity maps on the parameter plane, with different duty cycles, for a magnetometer.The contours are labeled with the sensitivity multiplied by 100. Since we are only interested in the stable region on the parameter plane, i.e. the region with the contours of multipliers parallel to the β axis, the scope of the sensitivity map is limited to $0.6 < \beta < 1.1$ as shown in Fig. 9.2.

These plots give us the impression is that the sensitivity increases rapidly with decreasing $\alpha = \omega_R/\omega$, and is not so sensitive to slight change in the capacitance, in particular, in the region where $\omega_R/\omega > 0.4$. Moreover, the top of the contour arch moves to larger values of $(\omega_C/\omega)^2$ with increasing duty cycle, i.e. the top is not fixed at $(\omega_C/\omega)^2 = 1$.

To demonstrate clearly the influence of the duty cycle η and the gate ratio p, let us examine Fig. 9.3. In Fig. 9.3 the sensitivity is plotted as a function of the duty cycle with the gate ratio p as a parameter: (a) $p = 2$ and (b) $p = 3$.

These plots show that:

1. The global maximum of sensitivity is located near duty cycle $\eta \sim 0.5$.

2. The gate ratio p is a determinant factor of sensitivity. Calculations show that the sensitivity is roughly proportional to p in the region $0.3 < \eta < 0.6$.

The ratio of sensitivity $p = 3$ to $p = 2$

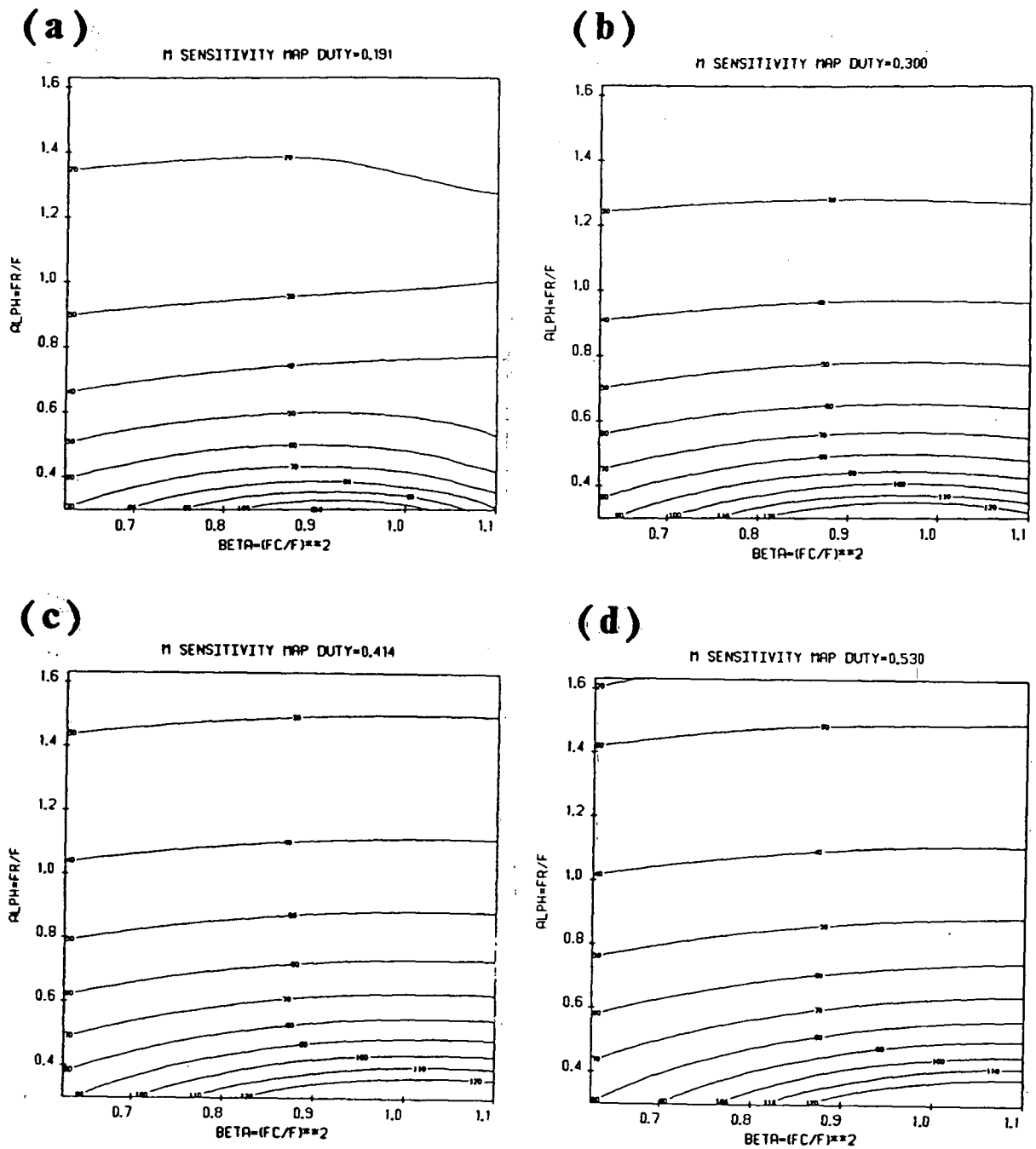

Fig. 9.2 The sensitivity maps on parameter plane with different duty cycles: (a) $\eta = 0.191$, (b) $\eta = 0.300$, (c) $\eta = 0.414$ and (d) $\eta = 0.530$. The contours are labeled with the sensitivity multiplied by 100.

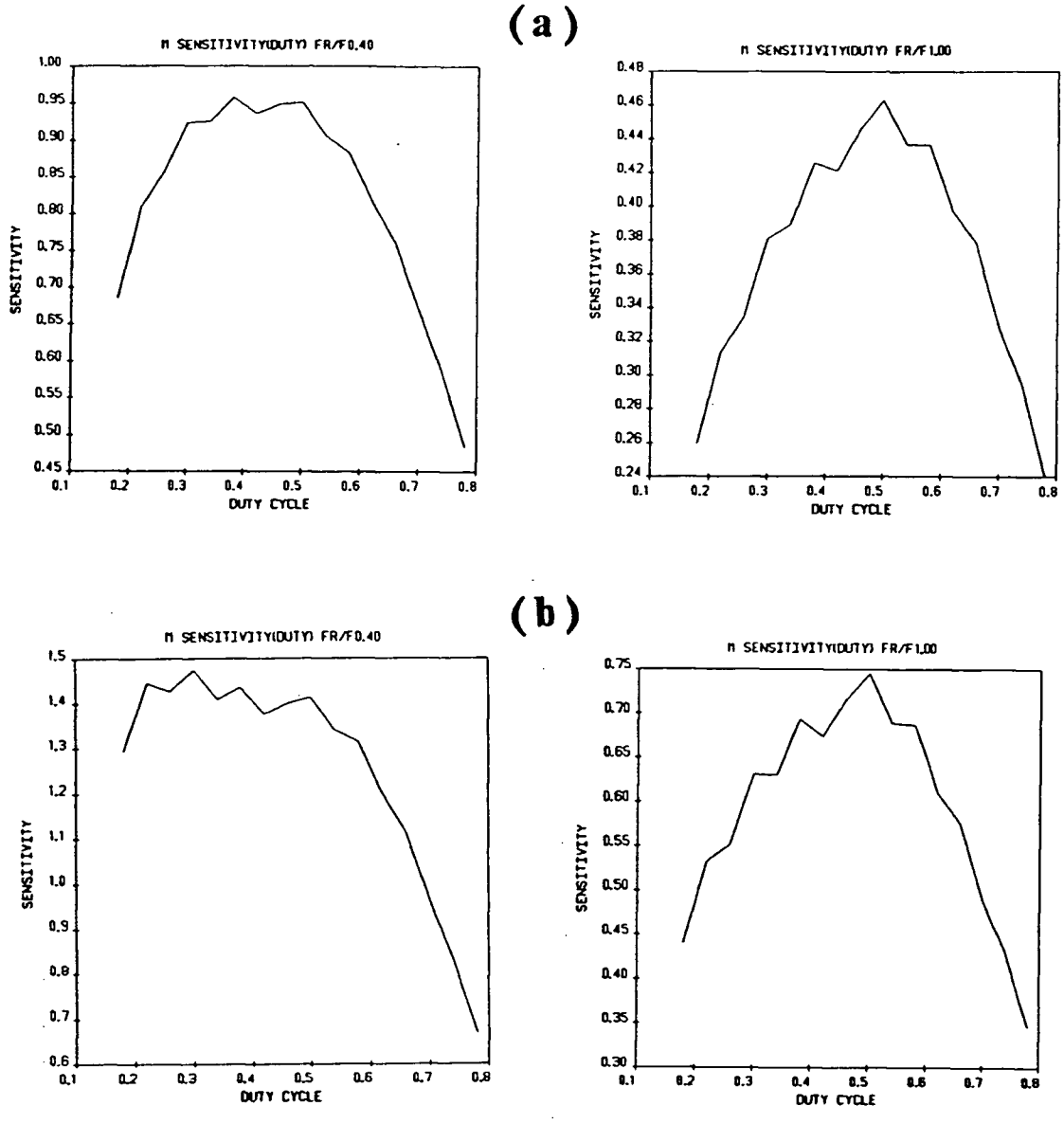

Fig. 9.3 The sensitivity as a function of duty cycle and the gate ratio p as a parameter: (a) $p = 2$, (b) $p = 3$. In the region $0.3 < \eta < 0.6$, the sensitivity is roughly proportional to p. The operating parameter $\beta = 0.98$.

$$\omega_R/\omega = 0.40, \qquad r_S = 1.49, \qquad \sigma/r_S \sim 1\%$$
$$\omega_R/\omega = 1.00, \qquad r_S = 1.60, \qquad \sigma/r_S \sim 1\%$$
$$\omega_R/\omega = 1.50, \qquad r_S = 1.60, \qquad \sigma/r_S \sim 1\%$$

where $r_S \stackrel{\triangle}{=} \text{mean}|S(p=3)/S(p=2)|$, and σ is the standard deviation.

From my laboratory tests, typical values of gate ratio are in the range of $2 < p < 3$, so the above results perhaps are typical.

In fact, the forcing term in the fluxgate state equation contains $\theta'(t)$ which, to first order, is proportional to the gate ratio p at jumps of $\theta(t)$, so the above results is just a logical extension of the linearity of the fluxgate state equation.

Thus, my sensitivity map not only is suitable for the particular value $p = 2$, but also is a general one which can be applied to calculate the sensitivity for fluxgate sensors with any value of gate ratio.

§9.4 Optimal operating parameters

The sensitivity and instability maps help us determine suitable operating parameters for the design of fluxgate sensor systems.

1. R which includes the resistance R_s of the sensor wire and the load should be chosen as small as possible from the sensitivity point of view, but with a limit $\omega_R/\omega \geq 0.3$ to guarantee the sensor against instability.

To keep the size of the fluxgate sensor small with a reasonable number of turns in a practical sensor winding, the value of R_s should remain at least in the range of a few tens of ohms. Therefore, the load cannot be chosen too small from the power transfer point of

view. In order to get high sensitivity, which is associated with small ω_R/ω, we should also choose a suitable frequency and a suitable self inductance of the sensor winding.

2. The drive frequency is half of the gate frequency $1/T$. From the sensitivity map, we see that with increasing gate frequency both ω_R/ω and $(\omega_C/\omega)^2$ are decreasing. Since ω_R/ω is nearly on exponential function of the sensitivity, and C is adjustable in most cases, it follows that to a certain degree higher frequency leads to higher sensitivity. But since every material has a limited respondent differential permeability, extremely high frequency will cause the differential permeability μ_d (then p) to decrease rapidly and eddy-currents to increase. This leads to lower sensitivity and other problems.

The above analysis coincides with the results of published experiments, for example, the measurement by Saito *et al* (1980 [9.1] p654).

3. The number N of turns in a sensor winding also is an important factor that not only determines the self-inductance of the sensor winding by expression (2.1), but also determines the sensor constant $\mathbf{K}_i$.

From the engineering practices, we know that, if $\mathbf{K}_i$ is smaller, the sensitivity is larger. Since the value of the sensor constant $\mathbf{K}_i$ is inversely proportional to the number N, large N seems be preferred. Moreover, the self inductance L of a sensor winding with a core is also proportional to N^2. Similar to discussion of frequency, larger L leads to decreasing ω_R/ω and $(\omega_C/\omega)^2$, and thus the sensitivity increases, if we keep $(\omega_C/\omega)^2$ in a suitable region by adjusting C.

But larger N leads to increasing R_s and stray capacitance which effects are harmful to sensitivity, stability and compact sensor size, particularly at high frequencies.

In engineering practice, perhaps one should possibly restrict the sensor size and available materials to choose a larger N and frequency, and then design the load to achieve a

stable sensor with the available sensitivity.

4. The duty cycle η of the gating function is an important factor for the fluxgate sensor, which depends on the drive current waveform $I_d(t)$ and other factors. If the amplitude of the drive current is large enough and the width of the current impulse is adjustable (as in most modern fluxgate systems), other factors could be ignored.

As we saw in the instability map, Fig. 6.4, that when $\eta \sim 0.414$ the unstable region (near $\beta \sim 1$) disappears and there eigenvalue contours are straight and parallel to the β axis. Now from sensitivity plots, we know that the maximum sensitivity is globally near $\eta = 0.5$. Thus my recommendation for the duty cycle is $0.3 < \eta < 0.5$.

Sometimes the dominant consideration is low-power consumption, e.g. for fluxgate sensors in satellites or on the ocean floor. Then one should choose $\eta \sim 0.20$ to save power.

5. As in the previous discussion, the gate ratio p is an important factor for sensitivity. From the definition of p and expression (2.1), we know that p depends mostly on the effective differential permeability for a given geometry. The gate ratio not only represents the characteristics of materials of core, bobbin, sensor winding ...etc., but also includes the influence of the demagnetization factor of the construction, shapes of the core and the sensor winding.

Since the gate ratio is easily measurable in any laboratory and can be compared, in particular for the ring core sensor, one can make efforts to improve this performance index.

Thus the gating function separates us from the complications of the demagnetization factor or other characteristics of materials in the fluxgate sensor theory.

Keeping in mind the present approach, I wish to concern myself with only fluxgate *sensor systems*, neither magnetometer nor gradiometer (fluxgate *instrumentation*). Real magnetometers or gradiometers always work in closed loops with a feedback transducer,

whose characteristics are obviously different from the sensor system itself. But any experienced designer knows that a deep understanding of the characteristics of an open loop is essential background for optimizing performance for a closed loop system.

CHAPTER 10

CONCLUSION

The gating function represents the fluxgate mechanism in an intuitive and forthright manner. Moreover it circumvents the complications of hysteresis and demagnetization. By testing the characteristics (duty cycle η, gate ratio p, etc.) of the gating function, we can choose an optimal drive current waveform, suitable materials and construction details for improvement of fluxgate sensor systems.

The generalized state equation derived in this approach for fluxgate sensor systems is significant because it leads to a form of formulation that is unique, straightforward and compact. The state equation is applicable to single sensors as magnetometers and as well to coupled multi-sensors as gradiometers. It can also be extended to study other fluxgate sensor systems (e.g. the second-derivative gradiometer), but the algebra becomes rapidly more cumbersome.

The calculation methods and expressions of the monodromy, the general solution and the periodic solution given in this thesis compose a complete solution set for the fluxgate state equations. They are algebraically exact and helpful for engineering practice.

The suggested method of calculating monodromy or multipliers with parameter mapping provides a unique and complete picture of the transient stability of fluxgate sensor systems. The discussion of the contours in the region where they are parallel to the β axis will help the designer to design a stable fluxgate sensor.

The general solution formulation is given for the first time in this thesis. It is implemented in the instability study in phase space. Moreover, the general solution by computer simulation can provide the response time, and other useful information for a practical sensor.

The stability of fluxgate sensor systems is completely studied in this thesis from many points of view locally and globally in the parameter domain (the parameter mapping) and the time domain (the phase space approach); for the homogeneous (free) state equation and the inhomogeneous (with forcing term) state equation; with the equilibrium and other initial position ($\mathbf{X}(0) = \mathbf{I}$). These results are fruitful for fluxgate sensor studies.

The analysis of sensitivity presented in this thesis is significant. The definition of the sensitivity involves a real signal in the fluxgate sensor, and thus it is conveniently measured and straightforwardly useful for engineering design. The general sensitivity map can provide the real signal for a fluxgate sensor with any values of parameters and force.

The major contributions of this thesis include a formulation of an integrated fluxgate theory and, more importantly, a guide for the selection of operating parameters and components for practical designs.

REFERENCES

Chapter 1

[1.1] H. Aschenbrenner and G. Goubeau, " Eine Anordnung zur registrie-rung rascher magnetischer störungen ", *Hochfrequenztechnik und Elektroakustik*, vol. 47, no 6, pp.177-181, 1936, (following the book of W. G. Geyger, 1964, cf:[1.10], pp.2).

[1.2] Hong-Jia Ding, " Fluxgate magnetometers ", *The 54 Annual International SEG meeting*, Atlanta, 1984.

[1.3] M. Kono, M. Koyanagi and S. Kokubun, " A ring-core fluxgate for spinner magnetometer ", *J. Geomag. Geoelectr.*, vol. 36, no. 4, pp.149-160, 1984.

[1.4] H. Lühr, N. Klöcker, W. Oelschlägel, B. Häusler, and M. Acuna, " The IRM fluxgate magnetometer ", *IEEE Trans. Geosci. Remote sensing*, vol. GE-23, no. 3, pp. 259-261, 1985.

[1.5] D. J. Southwood, W. A. C. Mier-jedrzejowicz, and C. T. Russell, " The fluxgate magnetometer for the AMPTE UK subsatellite ", *IEEE Trans. Geosci. Remote Sensing*, vol. GE-23, no. 3, pp. 301-304, 1985.

[1.6] The Department of Geophysics and Astronomy of UBC, *Annual Report: 1983-1984*. Vancouver: University of British Columbia, Canada, 1984, pp.19.

[1.7] T. A. Potemra, L. J. Zanett, and M. H. Acuna, " The AMPTE CCE magnetic field experiment ", *IEEE Trans. Geosci. Remote Sensing*, vol. GE-23, no. 3, pp. 246-249, 1985.

[1.8] J. F. Hermance, *The Next Generation of Magnetic Array Variometers*. SLAM Communication, Brown University, 1984.

[1.9] F. C. Williams and S. W. Nobel, " The fundamental limitations of the second harmonic type of magnetic modulator as applied to the amplification of small dc signals," in *Proc. Inst. Electrical Engrs.* (London), vol. II-97, pp.445-459,1950.

[1.10] W. A. Geyger, *Nonlinear-Magnetic Control Devices.* New York: McGraw-Hill, 1964, pp.328-378.

[1.11] D. I. Gordon, R. H. Lundsten, and R. A. Chiarodo, " Factors affecting the sensitivity of gamma-level ring core magnetometers," *IEEE Trans. Magn.*, vol. MAG-1, pp.330-377, 1965.

[1.12] S. V. Marshall, " An analytic model for the fluxgate magnetometer," *IEEE Trans. Magn.*, vol. MAG-3, pp.459-463, 1967.

[1.13] F. Primdahl, " The fluxgate mechanism," *Danish Meteorological Institute, geophysical papers,* vol. R-11, 1969.

[1.14] J. R. Burger, " The theoretical output of a ring core fluxgate sensor," *IEEE Trans. Magn.*, vol. MAG-8, pp.791-796, 1972.

[1.15] Yi-Zhong Qiu, " The engineering calculation of fluxgate magnetometers," *Journal of Shanghai Chiao-Tung University,* no.1, pp.93-113, 1978.

[1.16] Yi-Zhong Qiu, " On coordination of the second harmonic fluxgate magnetometer effected by a load," *Journal of Shanghai Chiao-Tung University,* no.1, pp.1-22, 1979.

[1.17] U. M. Zolotova, " Demagnetization factor of toroidal tape cores ", Translated from *Avtomatika i Telemekhanika*, no. 1, pp.155-163, 1977.

[1.18] P. H. Serson and W. L. W. Hannaford, " A portable electrical magnetometer," *Canadian J. Technology,* vol. 34, pp.232-243, 1956.

[1.19] R. D. Russell, B. B. Narod and F. Kollar, " Characteristics of the capacitively loaded flux gate sensor, " *IEEE Trans. Magn.*, vol. MAG-19, pp.126-130, 1983.

[1.20] B. B. Narod and R. D. Russell, " Steady-state characteristics of the capacitively loaded flux gate sensor ", *IEEE Trans. Magn.*, vol. MAG-20, pp592-597, 1984.

[1.21] A. H. Nayfeh and D. T. Mook, *Nonlinear Oscillations*, New York: Wiley, 1979, pp.273-284.

[1.22] V. A. Yakubovich and V. M. Starzhinskii, *Linear Differential Equations with Periodic Coefficients*. New York: John Wiley and Sons, 1975, ch.2, pp.88-98.

Chapter 2

[2.1] see [1.19].

[2.2] see [1.20].

[2.3] B. B. Narod, J. R. Bennest, J. O. Strom-Olsen, F. Nezil, and R. A. Dunlap, " An evaluation of the noise performance of Fe, Co, Si, B amorphous alloys in ring-core fluxgate magnetometers ", accepted for publication, *Canadian J. of Physics*, November 1985.

[2.4] see [1.18].

Chapter 3

[3.1] see [1.6].

[3.2] see [1.19].

Chapter 4

[4.1] see [1.22].

[4.2] V. M. Starzinski, " Survey of works on conditions of stability of the trivial solution of a system of linear differential equations with periodic coefficients ", *Trans. Am. Math. Soc., series 2*, vol. 1, pp.189-239, 1955.

[4.3] C. S. Hsu, " Application of the theory of impulsive parametric excitation and new treatments of general parametric excitation problems ", *J. Appl. Mechanics*, vol. 40, pp.78- 86, 1973.

[4.4] C. S. Hsu, " On approximating a general linear periodic system, " *J. Math. Analy. Appl.*, vol.45, pp.234-251, 1974.

Chapter 5

[5.1] D. D. Siljak, *Nonlinear Systems: The Parameter Analysis and Design.* New York: John Wiley and Sons, 1975, ch.3, pp.107-151.

[5.2] see [1.22].

[5.3] see [4.2].

Chapter 6

[6.1] see [1.19].

[6.2] see [1.20].

[6.3] see [1.18].

[6.4] R. M. Morris and B. O. Pedersen, " Design of a second harmonic flux gate magnetic field gradiometer, " *Rev. Scientific Instrum.*, vol.32, no. 4, pp.444-448, 1961.

Chapter 7

Chapter 8

[8.1] see [5.1].

[8.2] D. P. Atherton, *Stability of Nonlinear System.* New York: Chichester: Research Studies Press, 1981, §2.5, pp.24-29.

[8.3] N. Rouche and J. Mawhin, *Ordinary Differential Equations: Stability and Perodic Solutions.* Boston: Pitman Advanced Publishing Prog., 1980, §1, pp.1-4.

Chapter 9

[9.1] T. Saito, T. Sakurai, K. Yumoto, T. Tamura, M. Seto, T. Haysaka and I. Aoyama, " Magnetometers for geophysical use Part 2, test of twelve kinds of ring core ", *J. Geomag. Geoelectr.*, vol. 32, pp.649-659, 1980.

APPENDIX A

§A-1 Derivation of gradiometer equation

Following Russell's expression [A.1] for the fluxgate magnetometer sensor, we can express the kinetic energy $\mathcal{T}$, the potential energy $\mathcal{V}$, and the dissipative part $\mathcal{D}$ for the configuration of the gradiometer in Fig. 3.1 as follows:

$$\begin{aligned}\mathcal{T} = &\frac{1}{2}l_1\theta q'^2 + \frac{1}{2}l_2\theta q'^2 + \frac{1}{2}L_1\theta Q'^2 + \frac{1}{2}L_2\theta Q'^2 + M_1\theta q'Q' - M_2\theta q'Q' \\ &+ (\mathbf{H}_1\cdot\mathbf{K}_1)L_1\theta Q' + (\mathbf{H}_2\cdot\mathbf{K}_2)L_2\theta Q' + (\mathbf{H}_1\cdot\mathbf{k}_1)l_1\theta q' - (\mathbf{H}_2\cdot\mathbf{k}_2)l_2\theta q' \\ \mathcal{V} = &\frac{1}{2}\frac{q^2}{C} + \frac{1}{2}\frac{Q^2}{C} \\ \mathcal{D} = &\frac{1}{2}rq'^2 + \frac{1}{2}RQ'^2,\end{aligned}$$

where the definitions and the meanings of symbols are referred to §3.1. Using the Lagrange conservation equation, i.e.

$$\frac{d}{dt}\left(\frac{\partial(\mathcal{T}-\mathcal{V})}{\partial x'}\right) - \frac{\partial(\mathcal{T}-\mathcal{V})}{\partial x} + \frac{\partial\mathcal{D}}{\partial x'} = 0, \tag{A.1}$$

yields the following equations *

$$2l\left(\theta q'\right)' + (M_1 - M_2)\left(\theta Q'\right)' + \frac{q}{C} + rq' = a_1\theta', \tag{3.1}$$

$$2L\left(\theta Q'\right)' + (M_1 - M_2)\left(\theta q'\right)' + \frac{Q}{C} + RQ' = a_2\theta', \tag{3.2}$$

* The set of equations (3.1) and (3.2) is just an adaptation of a set derived by Dr. Russell on January 31, 1984 for a gradiometer.

Q.E.D

§A-2 The expression of the forced solution

If $\mathbf{X}(t,\tau)$ represents the matrizant for the state equation (3.20) which started at time τ, the solution of the state equation (3.17) with a forcing term can be expressed as the following (cf: [A.2]):

$$\mathbf{x}(t) = \mathbf{X}(t,\tau)\cdot\mathbf{x}(\tau) + \int_{\tau}^{t}\mathbf{X}(t,s)\cdot\mathbf{f}(s)\,ds, \tag{A.2}$$

where $\mathbf{x}(\tau)$ is the initial value of the state variables, s is a dummy variable of integration.

When $\mathbf{f}(t) = 0$, (A.2) becomes equation (4.10), namely,

$$\mathbf{x}(t) = \mathbf{X}(t,\tau)\cdot\mathbf{x}(\tau). \tag{A.3}$$

Consider the quiescent case $\mathbf{x}(\tau) = 0$. The forced trivial solution is

$$\mathbf{x}_q(t) = \int_{\tau}^{t}\mathbf{X}(t,s)\cdot\mathbf{f}(s)\,ds. \tag{A.4}$$

If we know $\mathbf{x}_q(t)$, then the general solution of (3.17) for any initial value can be calculated from the expression

$$\mathbf{x}(t) = \mathbf{X}(t,\tau)\cdot\mathbf{x}(\tau). + \mathbf{x}_q(t). \tag{A.5}$$

Q.E.D

§A-3 Expressions for the average self inductance L_E

The expression (4.15) or (4.16) for the average self inductance L_E is for the gating function as shown in Fig. 2.4 or Fig. 2.5, respectively.

We assume that without loss of generality the gating function has linear falling or rising edges; also assume that each edge takes an equal time interval Δ. Then the gating function and the appropriate integral along the falling edge can be expressed as

$$\frac{1}{\theta(t)} = \frac{p\Delta}{p\Delta - (p-1)\,t}, \tag{A.6}$$

$$\int_0^{\Delta} \frac{dt}{\theta(t)} = \frac{p\Delta}{(p-1)} \ln p. \tag{A.7}$$

Consequently, expression (4.14) becomes

$$\begin{aligned} \frac{1}{L_E} &\triangleq \frac{1}{T}\int_0^T \frac{ds}{\theta(s)\,L} \\ &= \frac{1}{T}\left(\frac{(1-\eta)T - 2\Delta}{L} + \frac{\eta T p}{L} + \frac{2p\Delta}{(p-1)L}\ln p\right). \end{aligned}$$

Thus, for the Fig. 2.4 case

$$L_E = \frac{L}{1 + (p-1)\,\eta - \frac{2\Delta}{T} + \frac{2\Delta p}{(p-1)T}\ln p}, \tag{4.15}$$

If $\Delta/T \to 0$, i.e. the case in Fig. 2.5, then

$$L_E = \frac{L}{1 + (p-1)\,\eta}. \tag{4.16}$$

Q.E.D

§A-4 Calculation of the monodromy

The expressions (4.29) and (4.30) for the monodromy are for the gating function as shown in Fig. 2.5. First, I state two theorems for a matrix function.

Theorem A·1: If p is positive and real, then

$$\exp\begin{pmatrix} \mathbf{O_j} & \mathbf{O_j} \\ \mathbf{O_j} & \ln p\mathbf{I_j} \end{pmatrix} = \begin{pmatrix} \mathbf{I_j} & \mathbf{O_j} \\ \mathbf{O_j} & p\mathbf{I_j} \end{pmatrix} \triangleq \mathbf{P}. \tag{A.8}$$

Proof: According to the definition of the exponential function of a matrix, we have

$$\begin{aligned} \exp\begin{pmatrix} \mathbf{O_j} & \mathbf{O_j} \\ \mathbf{O_j} & \ln p\mathbf{I_j} \end{pmatrix} &= \mathbf{I_{2j}} + \begin{pmatrix} \mathbf{O_j} & \mathbf{O_j} \\ \mathbf{O_j} & \ln p\mathbf{I_j} \end{pmatrix} + \frac{1}{2!}\cdot\begin{pmatrix} \mathbf{O_j} & \mathbf{O_j} \\ \mathbf{O_j} & \ln p\mathbf{I_j} \end{pmatrix}^2 + \ldots \\ &= \begin{pmatrix} \mathbf{I_j} & \mathbf{O_j} \\ \mathbf{O_j} & \left[1 + \ln p + \frac{1}{2!}\cdot \ln p^2 + \ldots\right]\cdot \mathbf{I_j} \end{pmatrix} \\ &= \begin{pmatrix} \mathbf{I_j} & \mathbf{O_j} \\ \mathbf{O_j} & p\mathbf{I_j} \end{pmatrix} \triangleq \mathbf{P}. \end{aligned}$$

Q.E.D

Theorem A·2: If the $n \times n$ square matrix $\mathbf{A}$ has an inverse, then for an $n \times n$ square matrix $\mathbf{B}$, one has

$$\mathbf{A}^{-1}\exp\left[\mathbf{B}\right]\cdot\mathbf{A} = \exp\left[\mathbf{A}^{-1}\cdot\mathbf{B}\cdot\mathbf{A}\right]. \tag{A.9}$$

Proof: Using the definition of the matrix exponential function, we have

$$\begin{aligned}\mathbf{A}^{-1}\exp[\mathbf{B}]\cdot\mathbf{A} &= \mathbf{A}^{-1}\cdot\mathbf{I}\cdot\mathbf{A}+\mathbf{A}^{-1}\cdot\mathbf{B}\cdot\mathbf{A}+\frac{1}{2!}\mathbf{A}^{-1}\cdot\mathbf{B}^{2}\cdot\mathbf{A}+\ldots \\ &= \mathbf{I}+\mathbf{A}^{-1}\cdot\mathbf{B}\cdot\mathbf{A}+\frac{1}{2!}\left(\mathbf{A}^{-1}\cdot\mathbf{B}\cdot\mathbf{A}\right)\left(\mathbf{A}^{-1}\cdot\mathbf{B}\cdot\mathbf{A}\right)+\ldots \\ &= \exp\left[\mathbf{A}^{-1}\cdot\mathbf{B}\cdot\mathbf{A}\right].\end{aligned}$$

Q.E.D

Now let us return to the derivation of the monodromy. Consider one period of the gating function to be divided into m intervals, when each interval corresponds to the falling or rising edge time Δ in the gating function [cf: Fig. A.1]. In m intervals, m_1 of which are during $\theta(t)=1$; m_s during $\theta(t)=1/p$; $m_f=1$ for the falling edge, i.e. $\theta(t)$ from 1 to $1/p$ in (t_1,t_2); and $m_r=1$ for the rising edge, i.e. $\theta(t)$ from $1/p$ to 1 in (t_3,T).

Let us examine the constant matrix $\mathbf{C_n}$ in Hsu's method for each interval of time.

In (t_0,t_1), each constant matrix is the same and has the form as

$$\begin{aligned}\mathbf{C_{n1}} &\triangleq \frac{1}{\Delta}\int_{t_{n1-1}}^{t_{n1}}\mathbf{A}(s)\,ds \\ &= \frac{1}{\Delta}\begin{pmatrix}\mathbf{O_j} & \mathbf{I_j}\\ -\frac{1}{LC}\mathbf{S_j} & -\frac{R}{L}\mathbf{S_j}\end{pmatrix} \\ &= \frac{1}{\Delta}\mathbf{W}, \qquad (A.10)\end{aligned}$$

where we define $\mathbf{W}$ as the *loop matrix*,

$$\mathbf{W}\triangleq\begin{pmatrix}\mathbf{O_j} & \mathbf{I_j}\\ -\frac{1}{LC}\mathbf{S_j} & -\frac{R}{L}\mathbf{S_j}\end{pmatrix}. \qquad (A.11)$$

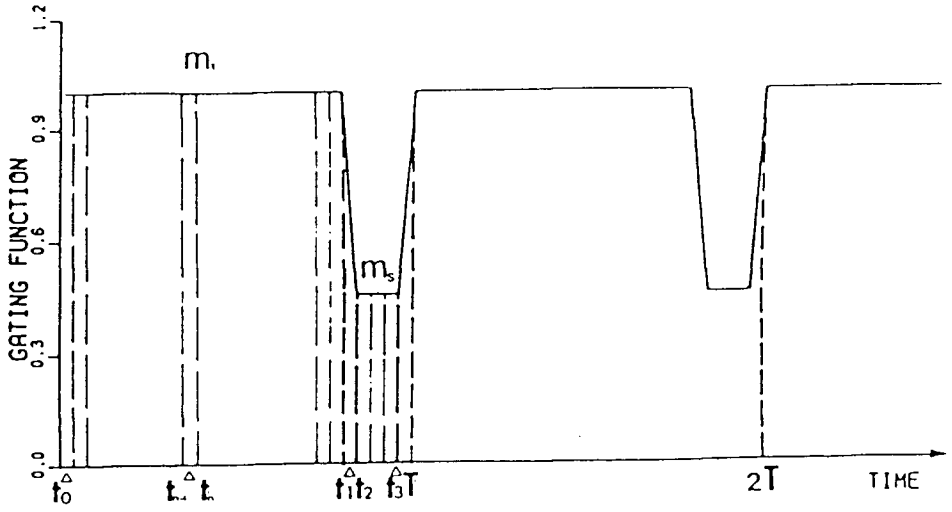

Fig. A.1 To calculate the monodromy, one period of the gating function was divided into m intervals (each is Δ). In the m intervals, m_1 of which are during $\theta(t) = 1$; m_s during $\theta(t) = 1/p$; $m_f = 1$ for the falling edge; and $m_r = 1$ for the rising edge.

Similarly, during t_2 to t_3, each constant matrix also is the same and has the form

$$\begin{aligned}\mathbf{C_{n2}} &\triangleq \frac{1}{\Delta}\int_{t_{n2-1}}^{t_{n2}} \mathbf{A}(s)\,ds \\ &= \frac{1}{\Delta}\begin{pmatrix} \mathbf{O_j} & \mathbf{I_j} \\ -\frac{p}{LC}\mathbf{S_j} & -\frac{Rp}{L}\mathbf{S_j} \end{pmatrix} \\ &= \frac{1}{\Delta}\mathbf{PW}, \end{aligned} \tag{A.12}$$

where $\mathbf{P}$ is the *boundary matrix*

$$\mathbf{P} \triangleq \begin{pmatrix} \mathbf{I_j} & \mathbf{O_j} \\ \mathbf{O_j} & p\mathbf{I_j} \end{pmatrix}. \tag{A.13}$$

For the interval (t_1, t_2), where $t_2 - t_1 = \Delta$, we can use (A.7) to get the following expression

$$\begin{aligned}\mathbf{C_f} &\triangleq \frac{1}{\Delta}\int_{t_1}^{t_2} \mathbf{A}(s)\,ds \\ &= \frac{T}{\Delta}\begin{pmatrix} \mathbf{O_j} & \frac{\Delta}{T}\mathbf{I_j} \\ -\left[\frac{C_p\Delta}{LCT}\right]\mathbf{S_j} & \frac{\ln p}{T}\mathbf{I_j} - \left[\frac{C_pR\Delta}{LT}\right]\mathbf{S_j} \end{pmatrix}, \end{aligned} \tag{A.14}$$

where $C_p \triangleq [p/(p-1)]\ln p$ is a constant. For the interval (t_3, T), we have similar expression

$$\begin{aligned}\mathbf{C_r} &\triangleq \frac{1}{\Delta}\int_{t_3}^{T} \mathbf{A}(s)\,ds \\ &= \frac{T}{\Delta}\begin{pmatrix} \mathbf{O_j} & \frac{\Delta}{T}\mathbf{I_j} \\ -\left[\frac{C_p\Delta}{LCT}\right]\mathbf{S_j} & \frac{-\ln p}{T}\mathbf{I_j} - \left[\frac{C_pR\Delta}{LT}\right]\mathbf{S_j} \end{pmatrix}, \end{aligned} \tag{A.15}$$

Substitute (A.10)-(A.15) into (4.27), we obtain

$$\mathbf{H}(m) = \exp(\Delta \mathbf{C_r}) \prod_{i=1}^{m_r} \exp(\Delta \mathbf{P W}) \exp(\Delta \mathbf{C_f}) \prod_{i=1}^{m_1} \exp(\Delta \mathbf{W}). \tag{A.16}$$

When $\lim \Delta / T \rightarrow 0$, the gating function is as shown in Fig. 2.5 and the terms of (A.16) become as follows:

$$\lim_{\Delta/T \rightarrow 0} \exp(\Delta \mathbf{C_f}) = \exp \begin{pmatrix} \mathbf{O_j} & \mathbf{O_j} \\ \mathbf{O_j} & \ln p\mathbf{I_j} \end{pmatrix},$$

$$\lim_{\Delta/T \rightarrow 0} \exp(\Delta \mathbf{C_r}) = \exp \begin{pmatrix} \mathbf{O_j} & \mathbf{O_j} \\ \mathbf{O_j} & -\ln p\mathbf{I_j} \end{pmatrix},$$

$$\lim_{\Delta/T \rightarrow 0} \prod_{i=1}^{m_1} \exp(\Delta \mathbf{W}) = \exp \left[\mathbf{W} \cdot \lim_{\Delta/T \rightarrow 0} \sum_{1}^{m_1} \Delta \right]$$

$$= \exp[(1-\eta) T \mathbf{W}],$$

$$\lim_{\Delta/T \rightarrow 0} \prod_{i=1}^{m_r} \exp(\Delta \mathbf{P W}) = \exp[\eta T \mathbf{P W}].$$

Using the theorem A-1 and substituting the result into (A.16), we obtain

$$\mathbf{X}(T) = \lim_{\Delta/T \rightarrow 0} \mathbf{H}(m)$$

$$= \mathbf{P}^{-1} \cdot \exp[\eta T \mathbf{P W}] \cdot \mathbf{P} \cdot \exp[(1-\eta) T \mathbf{W}]. \tag{4.29}$$

Note the theorem A-2, we get the monodromy as

$$\mathbf{X}(T) = \exp[\eta T \mathbf{W P}] \exp[(1-\eta) T \mathbf{W}]. \tag{4.30}$$

Q.E.D

§A-5 Characteristic equation of U for gradiometers

To derive the characteristic equation (5.20) of U for gradiometers, we substitute (5.21) into (5.7), then

$$\mathbf{U} = \begin{pmatrix} \mathbf{O_2} & \mathbf{I_2} \\ -2\omega_{CG}{}^2\mathbf{S_2} & -2\omega_{RG}\mathbf{S_2} \end{pmatrix}. \tag{A.17}$$

Thus, the characteristic equation of U becomes

$$\det\left[s\mathbf{I_4} - \mathbf{U}\right] = \det\begin{pmatrix} s\mathbf{I_2} & -\mathbf{I_2} \\ 2\omega_{CG}{}^2\mathbf{S_2} & 2\omega_{RG}\mathbf{S_2} \end{pmatrix}. \tag{A.18}$$

Proceeding (A.18) with the determinant reduction of the Laplace expansion theorem, after some manipulations we obtain

$$s^4 + \left(\frac{8}{4-B^2}\omega_{RG}\right)s^3 + \left(\frac{4}{4-B^2}\omega_{RG}^2 + \frac{8}{4-B^2}\omega_{CG}^2\right)s^2 + \left(\frac{8}{4-B^2}\omega_{RG}\omega_{CG}^2\right)s + \frac{4}{4-B^2}\omega_{CG}^4 = 0, \tag{5.20}$$

Q.E.D

§A-6 Boundary condition for the gradiometer

Method 1: *

* This derivation is an extension of the method, which was given by Dr. Russell in the lecture GP422 on February 23, 1984, for magnetometers.

Recalling (3.1), (3.2)

$$2l\left(\theta q'\right)' + b\left(\theta Q'\right)' + \frac{q}{C} + rq' = a_1\theta', \tag{3.1}$$

$$2L\left(\theta Q'\right)' + b\left(\theta q'\right)' + \frac{Q}{C} + RQ' = a_2\theta', \tag{3.2}$$

and combining together the terms which contained $\theta(t)$, we obtain

$$\left[\theta\left(2lq' + bQ' - a_1\right)\right]' + \frac{q}{C} + rq' = 0, \tag{A.19}$$

$$\left[\theta\left(bq' + 2LQ' - a_2\right)\right]' + \frac{Q}{C} + RQ' = 0. \tag{A.20}$$

Consequently,

$$\left(\theta\left[\mathbf{D}\mathbf{q}' - \mathbf{a}_2\right]\right)' + \frac{1}{C}\mathbf{q} + \begin{pmatrix} r & 0 \\ 0 & R \end{pmatrix}\mathbf{q}' = 0. \tag{A.21}$$

For the notations of $\mathbf{D}$, $\mathbf{q}$, $\mathbf{a}_2$ please refer to §3.1.

Energy conservation requires that $\mathbf{q}$ and $\mathbf{q}'$ are finite quantities. Thus the first term on the left side of (A.21) should be finite too. It implies that $\theta[\mathbf{D}\mathbf{q}' - \mathbf{a}_2]$ is a continuous function. This can be expressed by

$$\theta^-\left[\mathbf{D}\begin{pmatrix} i^- \\ I^- \end{pmatrix} - \mathbf{a}_2\right] = \theta^+\left[\mathbf{D}\begin{pmatrix} i^+ \\ I^+ \end{pmatrix} - \mathbf{a}_2\right], \tag{A.22}$$

where the superscript $-$ or $+$ refers to the value at the moment before or after a jump of $\theta(t)$; and $i = q', I = Q'$.

For example, at t_1 [cf: Fig. 2.5] the falling jump: $\theta^- = 1, \theta^+ = 1/p$, then

$$p\cdot\left[\mathbf{D}\begin{pmatrix} i^- \\ I^- \end{pmatrix} - \mathbf{a}_2\right] = \mathbf{D}\begin{pmatrix} i^+ \\ I^+ \end{pmatrix} - \mathbf{a}_2. \tag{A.23}$$

Since $\mathbf{D}$ is nonsingular, we obtain

$$p \cdot \begin{pmatrix} i^- \\ I^- \end{pmatrix} - (p-1) \cdot \mathbf{D}^{-1} \cdot \mathbf{a}_2 = \begin{pmatrix} i^+ \\ I^+ \end{pmatrix}. \tag{A.24}$$

Consequently, as $q' = i, Q' = I$ are finite, we know that the charges q, Q are continuous functions. Then we have the state variable form as

$$\mathbf{x}^+ = \begin{pmatrix} q^+ \\ Q^+ \\ i^+ \\ I^+ \end{pmatrix} = \begin{pmatrix} \mathbf{I_2} & \mathbf{O_2} \\ \mathbf{O_2} & p\mathbf{I_2} \end{pmatrix} \begin{pmatrix} q^- \\ Q^- \\ i^- \\ I^- \end{pmatrix} - (p-1) \cdot \begin{pmatrix} \mathbf{o}_2 \\ \mathbf{D}^{-1} \cdot \mathbf{a}_2 \end{pmatrix}. \tag{A.25}$$

or

$$\mathbf{x}^+ = \mathbf{P}\mathbf{x}^- + \mathbf{u}_1, \tag{A.26}$$

where $\mathbf{P}$ is the boundary matrix and

$$\begin{aligned} \mathbf{u}_1 &\triangleq -(p-1) \begin{pmatrix} \mathbf{o}_2 \\ \mathbf{D}^{-1} \cdot \mathbf{a}_2 \end{pmatrix} \\ &= (\mathbf{I} - \mathbf{P}) \begin{pmatrix} \mathbf{o}_2 \\ \mathbf{D}^{-1} \cdot \mathbf{a}_2 \end{pmatrix}. \end{aligned} \tag{A.27}$$

Proceeding similarly, at T we have

$$\mathbf{x}^+ = \mathbf{P}^{-1}\mathbf{x}^- + \mathbf{u}_2, \tag{A.28}$$

and

$$\mathbf{u}_2 \triangleq -\left(\frac{1-p}{p}\right) \begin{pmatrix} \mathbf{o}_2 \\ \mathbf{D}^{-1} \cdot \mathbf{a}_2 \end{pmatrix}$$

$$= (\mathbf{I} - \mathbf{P}^{-1}) \begin{pmatrix} \mathbf{o}_2 \\ \mathbf{D}^{-1} \cdot \mathbf{a}_2 \end{pmatrix}. \tag{A.29}$$

If $2l = 2L$, $\mathbf{D}^{-1} = \mathbf{S_2}/L$. It is easily verified that the expressions (A.26) and (A.28) are true for magnetometers, but the subscripts must change from 2 to 1 in (A.27) and (A.29), because the order of the system now is $j = 1$.

Method 2 (Delta function matching method) : *

Let us examine the equations (3.1), (3.2) and $\theta(t)$ in Fig. 2.5. Since each jump of $\theta(t)$ can be represented by the Heaviside function, $\theta'(t)$ in the right side of (3.1) and (3.2) should be the Impulse function or an assemblage of Delta functions. For Delta function matching, the highest order differential q'', Q'' of the left side must match the right side, i.e. q'' or Q'' should be an Impulse function or Delta function too.

Thus, $q' = i, Q' = I$ should be Heaviside functions at jumps of $\theta(t)$. In other words, i, I are the same kind of piece-wise continuous function as $\theta(t)$. Consequently, q and Q are ordinary continuous functions at the jumps of $\theta(t)$.

Thus, at the moment t_m of the $\theta(t)$ jump, we have

$$q^- = q^+, \tag{A.30}$$

$$Q^- = Q^+. \tag{A.31}$$

We arrange equations (3.1) and (3.2) in the form

$$(\theta\,[\mathbf{D}\mathbf{q}' - \mathbf{a}_2])' = -\frac{1}{C}\mathbf{q} - \begin{pmatrix} r & 0 \\ 0 & R \end{pmatrix} \mathbf{q}'. \tag{A.32}$$

---

* The Delta function matching method was introduced to me by Dr. G. Bluman for the magnetometers' equation on April 16, 1985.

Integrating (A.32) in the interval (t_m^-, t_m^+), we have

$$\theta\left[\mathbf{D}\mathbf{q}' - \mathbf{a}_2\right]\Big|_{t_m^-}^{t_m^+} = -\frac{1}{C}\int \mathbf{q}\,dt\Big|_{t_m^-}^{t_m^+} - \begin{pmatrix} r & 0 \\ 0 & R \end{pmatrix}\mathbf{q}\Big|_{t_m^-}^{t_m^+}. \tag{A.33}$$

Since $q, Q, \int q dt, \int Q dt$ are continuous, the right side of (A.33) is equal to zero. Then we get as a result the same expression (A.22), namely,

$$\theta^-\left[\mathbf{D}\begin{pmatrix} i^- \\ I^- \end{pmatrix} - \mathbf{a}_2\right] = \theta^+\left[\mathbf{D}\begin{pmatrix} i^+ \\ I^+ \end{pmatrix} - \mathbf{a}_2\right]. \tag{A.22}$$

Preceeding as before, we can get boundary conditions the same as (7.1) and (7.2)

$$\mathbf{X}(t_1{}^+) = \mathbf{P}\cdot\mathbf{X}(t_1{}^-) + \mathbf{u}_1, \tag{7.1}$$

$$\mathbf{X}(T^+) = \mathbf{P}^{-1}\cdot\mathbf{X}(T^-) + \mathbf{u}_2. \tag{7.2}$$

Q.E.D

Reference

[A.1] see [1.19]

[A.2] H. D'Angelo, *Linear Time-Varying Systems: Analysis and Synthesis*. Boston: Allyn and Bacon, 1970, ch.3, pp.53-88.

APPENDIX B

§B-1 Some theorems

1. Floquet-Lyapunov theorem [B.1 pp.90].

Consider a system which can be expressed by a differential equation with T-periodic coefficients in the form

$$\mathbf{x}'(t) = \mathbf{A}(t) \cdot \mathbf{x}(t), \tag{B.1}$$

then the matrizant $\mathbf{X}(t)$ of the system may be expressed in the following form,

$$\mathbf{X}(t) = \mathbf{V}(t) \exp(t\mathbf{K}), \tag{B.2}$$

where $\mathbf{V}(t)$ is a T-periodic matrix function, nonsingular for all t, continuous with an integrable piecewise-continuous derivative, and such that $\mathbf{V}(0) = \mathbf{I}$; and $\mathbf{K}$ is a constant matrix.

2. Liouville-Jacobi Formula [B.1 pp.74].

The Liouville-Jacobi formula states that for any fundamental solution $\mathbf{\Phi}(t)$ of (B.1), the following relation is true

$$\det[\mathbf{\Phi}(t)] = \det[\mathbf{\Phi}(\tau)] \exp\left[\int_{\tau}^{t} \mathrm{tr}[\mathbf{A}(s)]\, ds\right], \tag{B.3}$$

where τ is the starting moment.

3. Bendixon Theorem [B.2 pp.586].

If a half-trajectory remains in a closed, bounded domain D without approaching an equilibrium position, then the trajectory either is a closed trajectory or approaches a closed trajectory. When D is a ring-shaped domain and which is bounded by two closed curves C_1 and C_2, it is sufficient for the existence of at least one limit cycle that (a) trajectories enter (leave) D through every point of C_1 and C_2; (b) there are no equilibrium positions either in D or on C_1 and C_2.

References

[B.1] V. A. Yakubovich and V. M. Starzhinskii, *Linear Differential Equations with Periodic Coefficients.* New York: John Wiley and Sons, 1975, ch.2.

[B.2] D. D. Siljak, *Nonlinear Systems: The Parameter Analysis and Design.* New York: John Wiley and Sons, 1975, ch.3.

§B-2 Notation list

a_1	the forcing term in the gradient loop	16
a_2	the forcing term in the magnetic field loop	16
$\mathbf{a}_1$	the forcing term for the magnetometers	19
$\mathbf{a}_2$	the forcing term for the gradiometers	17
$\mathbf{A}(t)$	the time-variant coefficient matrix in the state equations	18
b	the difference between mutual inductances	16
B	the ratio of the difference between mutual inductances to the self-inductance	18
C	the serial capacitance in sensor loops	14
C_p	a constant $C_p = \ln p \cdot p/(p-1)$	95
$\mathbf{C}_n$	constant matrix, replaces $\mathbf{A}(t)$ in the $n-$th interval	27
d_{rc}	the diameter of the ring core (m)	9
$\mathbf{D}$	a symmetric, nonsingular constant matrix	16
$\mathbf{f}(t)$	the time-variant forcing term in the state equation	18
h_i	a scalar function, represents the force in the phase space approach	62
H	the magnetic field, exerts on the sensor axis	7
H_G	the gate threshold	9
$\mathbf{H}_i(t)$	the magnetic field where the $i-$th sensor is located	14
$\mathbf{H}(m)$	the growth matrix in Hsu's method	27
i	the current in the sensor loop; in particular, in the gradient loop	17
i_{sgm}	the magnitude of the second harmonic current for gradiometers	73
i_{smm}	the magnitude of the second harmonic current for magnetometers	73
I	the current in the magnetic field loop for gradiometers	17
$I_d(t)$	the drive current in the drive winding	7
I_{dt}	the threshold of the drive current at which $L(I_d)$ reduced to $10\%(L-L_0)+L_0$	9
$\mathbf{I}_n$	the $n \times n$ unit matrix	17
j	the order of the fluxgate sensor system	19
k, K	the sensor constants	16
K_{Fe}	a constant determined by the geometry of the core and the winding	7
$\mathbf{K}$	a constant matrix in the matrizant	21
l_i, L_i	the self-inductances of sensor windings without drive current	14
L	the original value of the self-inductance for a sensor winding	9
$L(H)$	the self-inductance as a function of the exterting H on the core	7
$L(I_d)$	the self-inductance as a function of the drive current I_d	7
$L(t)$	the time-variant self-inductance of a sensor winding	12
L_0	the self-inductance of a sensor winding without any core	7

L_E	the average self-inductance of a sensor winding	24
N	the turn number of a sensor winding	7
N_c	the turn number of the drive winding in a ring core	9
M_i	the mutual inductance between two sensor windings with the same $i-$th core	14
$\mathbf{o}_n$	the zero $n-$vector	18
$\mathbf{O_n}$	the $n \times n$ zero matrix	18
p	the gate ratio of the gating function	9
$\mathbf{P}, \mathbf{P}^{-1}$	the boundary matrices	28
q, Q	the charges on the capacitors C	16
$\mathbf{q}$	the charge vector	16
$\mathbf{Q}$	a constant matrix associated with the monotromy and Λ matrix	22
r, R	the combined resistances of R_s and the load	14
$r_i(t)$	the scalar coefficient function in the phase space approach	62
r_s	the ratio of sensitivities of $p = 3$ to $p = 2$	78
R_s	the resistance of a sensor winding	78
s	the roots of the characteristic equation	37
S_g	the sensitivity for gradiometers	73
S_m	the sensitivity for magnetometers	73
$\mathbf{S_2}$	a symmetric constant matrix for gradiometers	18
t	the time variable	9
t°	the temperature in degrees	49
t_1^-	the time before the falling jump of the gating function	31
t_1^+	the time after the falling jump of the gating function	32
t_m	the time when the gating function has a jump	100
T	the gate period which is equal to the half drive period	9
T_1^-	the time before the rising jump of the gating function	32
T_1^+	the time after the rising jump of the gating function	32
$\mathbf{u}_1$	the force vector at the falling jump	50
$\mathbf{u}_2$	the force vector at the rising jump	50
$\mathbf{U}$	the system matrix, i.e. the mean value of $\mathbf{A}(t)$ over a period	36
$\mathbf{V}(t)$	the periodic part of the matrizant	21
$\mathbf{W}$	the loop matrix	28
x_i	the state variables	17
$\mathbf{x}$	the state variable vector	17
$\mathbf{x}_p(t)$	the periodic solution of the force state equation	71
$\mathbf{x}_q$	the trivial solution, i.e. the solution for the quiescent case	53
$\mathbf{x}(\tau)$	the initial value of the state vector started at τ	23
$\mathbf{X}(t)$	the matrizant of a state equation	21
$\mathbf{X}(t, \tau)$	the matrizant indicating the initial time at τ	23
$\mathbf{X}(T)$	the monodromy, i.e. the value of a matrizant over a period	21
$\mathbf{y}$	the vector variable in the Lyapunov reducible transform	35

$\mathbf{Z}(t)$	a fundamental solution with the initial condition $\mathbf{Q}^{-1}$	22
α	the adjustable ordinate parameter in the parameter plane	39
α_R	the temperature coefficient of R	48
β	the adjustable abscissa parameter in the parameter plane	39
Δ	the falling or rising edge times of the gating function	9
ς	the relative damping coefficient	38
η	the duty cycle of the gating function	9
$\theta(t)$	the gating function	9
$\lambda_{1i}, \lambda_{2i}$	the eigenvalues of $\mathbf{W}$, $\mathbf{WP}$, respectively	29
λ_i	the multipliers, i.e. eigenvalues of the monodromy	41
λ_{ki}	the characteristic exponents, i.e. eigenvalues of $\mathbf{K}$	36
λ_M	the amplitude of first multiplier	41
λ_{ui}	eigenvalues of the system matrix $\mathbf{U}$	37
$\mathbf{\Lambda}$	the diagonal matrix containing multipliers	22
μ_d	the effective differential permeability	7
$\mu_d(H)$	the effective differential permeability as a function of H	7
$\mathbf{\Phi}(t)$	a fundamental solution of the state equation	24
ω	the gate angular frequency	25
ω_C	the LC angular frequency	40
ω_n	the undamping natural frequency	38
ω_R	the RL angular frequency	25